ISBN 978-82-471-2924-1 (printed ver.)
ISBN 978-82-471-2925-8 (electronic ver.)
ISSN 1503-8181

Petra Rüther
Doctoral Thesis

Doctoral theses at NTNU, 2011:187

Petra Rüther

# Wood Weathering from a Service Life Perspective

NTNU
Norwegian University of
Science and Technology

Thesis for the degree of
philosophiae doctor

Faculty for Engineering Science and Technology
Department for Civil and Transport Engineering

NTNU
Norwegian University of
Science and Technology

Doctoral theses at NTNU, 2011:187

NTNU

Petra Rüther

# Wood Weathering from a Service Life Perspective

Thesis for the degree of philosophiae doctor

Trondheim, June 2011

Norwegian University of
Science and Technology
Faculty for Engineering Science and Technology
Department for Civil and Transport Engineering

NTNU
Norwegian University of
Science and Technology

**NTNU**
Norwegian University of Science and Technology

Thesis for the degree of philosophiae doctor

Faculty for Engineering Science and Technology
Department for Civil and Transport Engineering

©Petra Rüther

ISBN 978-82-471-2924-1 (printed ver.)
ISBN 978-82-471-2925-8 (electronic ver.)
ISSN 1503-8181

Doctoral Theses at NTNU, 2011:187

Printed by Tapir Uttrykk

*Small strokes fell big oaks*

# Abstract

Untreated wooden cladding has a long tradition and has in recent years become a both economically and environmentally beneficial solution in miscellaneous modern building applications. Untreated wood in cladding and similar applications represents a building part that changes its appearance rather dramatically without compromising its technical functionality. The aesthetic service life is often the decisive criterion for these applications. This thesis comprises a study on the weathering of untreated, i.e. unpainted wood. Following the service life prediction methodology suggested in the ISO 15686 standard, wood was weathered both outdoors and in two laboratory weathering apparatuses. Climate data for the test site were assessed including temperature, wind-driven rain and solar radiation. The performance of non-structural wood components in exterior above-ground applications is often closely related to the aesthetics of the wooden component in question. Hence, a method for color determination of large samples was developed, and the topic of human color perception is discussed briefly. It was found that the colonization by mold growth fungi contributes significantly to its surface appearance. Differences between materials and exposure directions were investigated. The topic of limit-state for aesthetic service life is discussed and a possible assessment method for such applications is presented. No simple dose-response relationship between solar radiation and wind-driven rain, and color response of the material could be established. Acceleration factors for the conducted laboratory weathering tests are discussed. Furthermore, color changes by outdoor versus laboratory weathering were evaluated. It was found that the conducted laboratory weathering cycles could not recreate the visual appearance of an outdoor weathered surface. In summary, the suggested bottom-up approach of the service life prediction methodology is not easily adaptive for wood in this application.

# Preface

I commenced this study back in 2003, which was founded by NTNU and supervised by Per Jostein Hovde at the Department of Civil and Transport Engineering, whose support and understanding is acknowledged. Along the way I found my co-supervisor Bjørn Petter Jelle at SINTEF Byggforsk. His constant professional support and always objective and strongly scientific view on things is deeply acknowledged. Also, I would like to thank Ole Aunrønning for helping with the analysis of the wooden samples, Egil Rognvik at SINTEF for access to data collected within the *Klima 2000* project, and the rest of my colleagues at SINTEF Byggforsk for inviting me to their legendary Norwegian parties and providing a pleasant working environment throughout these years.

After some longer breaks due to unforseen duplication processes and the following dynamics, name it Theo and Fridtjof, I was offered the opportunity to finish the work on my thesis. I would like to express my deepest gratitude for making this possible to Marit Støre Valen and Berit Time. My fellow PhD student up on the *bookshelf*, Kathinka Leikanger Friquin, thanks for moral support and fellowship these years. I would also like to thank my friends in Norway for many joyful hours besides research.

Thanks to my dear old friends in Germany. Despite geographical hindrances, getting together with you still is and will hopefully always be heartwarming. Thanks to my parents for always backing up my decisions and helping in any possible way. My parents, sister, sisters- and parents-in-law, thank you for child caring, house holding, moving, renovating, and helping out in difficult and busy times. Theo and Fridtjof, my little sons, thanks for adding new dimensions to my life every day. Last, but most certainly not least, I would like to thank you Nils for your encouragement, love and support, and if nothing else patience. *Ich verneige mich in Dankbarkeit.*

# Contents

# 1. Introduction

*"Sustainable development which implies meeting the needs of the present without compromising the ability of future generations to meet their own needs, should become a central guiding principle of the United Nations, governments and private institutions, organizations and enterprizes."*

United Nations, Our Common Future [1]

Sustainable construction or sustainability in the building sector is an important part of the concept of sustainable development. Relative to its economy, the construction and operation of the built environment has a disproportionate impact on the natural environment. Although it represents only about 11% of the gross national product in the European Union it is responsible for up to 40% of all manmade waste, and consumes up to 40% of all produced energy for its manufacturing, construction and operation [2]. Additionally, extensive amounts of raw materials, green space, and water are exploited. At the same time, it engages a large amount of human resources directly or indirectly: construction workers, designers, governmental institutions, maintenance companies, to name just a few of the actors. Despite its important role with regard to sustainable development, the problem seems to be approached in a rather diffident way. The sustainability of the construction sector is dependent on a fundamental shift in the way in which resources are used, from non-renewables to renewables, from high amounts of waste to high levels of reuse and recycling, and from solutions based on lowest first costs to those based on whole life cycle costs [3].

In light of the immense challenges associated with climate change, growing interest in sustainable development has led to subordinate documents such as the *Construction Products Directive* by the EU commission [4], stipulating essential requirements to be fulfilled during an economically reasonable working life: 1) mechanical strength and stability, 2) safety in

the case of fire, 3) hygiene, health and the environment, 4) safety in use, 5) protection against noise, and 6) energy economy and heat retention. The working life is defined as 'the period of time during which the performance of a product will be maintained at a level that enables a properly designed and executed work to fulfil the essential requirements, i.e. the essential characteristics of a product meet or exceed minimum acceptable values without incurring major costs for repair or replacement [5]. The first part of the ISO 15686 series was published in 2000. These standards incorporates service life prediction procedures, life-cycle costing, environmental impacts, performance evaluation, and the assessment of service life data of buildings and constructed assets [6].

The overall performance of a product or building assembly depends on the requirements that need to be fulfilled. Thus, different working lives can be defined: on the basis of risk management, on the basis of its function, economical or social requirements. The end of the functional working life often marks the end of the working life of a component. In other cases components or materials are replaced because of obsolescence, e.g. changes in style or fashion require new materials, although the function of the component still remains intact. Hence, working life is not necessarily connected to durability.

In the process of enhancing service life[1] prediction models data of e.g. the prevailing exposure environment and the influence of different material parameters are required. Ideally, alterations of material properties depend on certain parameters of the exposure environment. Both the characterization and understanding of degradation processes, and the analysis of the exposure environment are crucial to definition, modeling, and application of service life prediction models in the future. The development of degradation models based on damage functions or dose-response relationships is preferable.

Service life prediction methodologies adapted from ISO 15686-2 have been applied in this study. As a case study, untreated (not painted) wooden cladding has been chosen. Untreated wooden cladding, or more generally, non-structural wood in above-ground applications, has experienced a renaissance in modern architecture lately. Wooden cladding is used

[1]This term is used in the ISO 15686 series; the definition is consistent to *working life*

Figure 1.1.: Wooden shingle cladding at *Chesa Futura* by Norman Foster in St.Moritz, Switzerland, photo Claudio Castellacci

in many different applications; single family houses, office buildings, and industrial buildings. The use of wood in both interior and exterior applications has a long tradition. In the light of current challenges with respect to carbon dioxide emissions and climate change, the application of wood as a natural renewable resource is highly contemporary. Additionally, low (maintenance) costs, easy accessability and relatively simple processing contribute to the increasing popularity of wood. From a service life perspective, untreated wooden cladding is an example of a building component that degrades over time without loosing its functionality. The main function of the cladding is the protecting of wind barrier and insulation layer in a wall from rain and solar radiation. However, alterations in appearance due to color changes, changes in surface structure, and biological surface growth change the aesthetics of a wooden cladding significantly. Much appreciated among many architects but also controversially discussed, the aesthetics of untreated wood has so far been subject to only

a few scientific publications.

Surface alterations of untreated wood caused by climatic strains appear rapidly and are rather dramatic. Those changes are termed *weathering* and describe a strictly superficial phenomenon, which is not to be confused with decay. Weathering is caused by several climatic agents, mainly solar radiation and moisture. Alterations caused by weathering are more of an aesthetic that of a technical nature. Therefore, weathering affects solely the aesthetic service life of an untreated wooden component. It is assumed that the changes depend to a certain extend on the dosage of certain environmental agents.

An investigation of color changes due to weathering by means of color measurement is conducted in this study. Several different wood materials, four different wood species and three types of treated wood materials, are used to assess differences in the development of color depending on wood species and exposure conditions. Wood exposed vertically facing different directions shows differences in how color changes develop, caused by different dosages of climatic strains and their interaction. Therefore, this study investigates the quantitative dependency of solar radiation and wind driven rain dosage on color changes of wood.

Service life prediction methodologies suggest accelerated weathering tests to determine service life and investigate degradation mechanisms and durability. Such accelerated weathering tests are widely used in material testing, for example in coating technology or in applications for the automotive industry. However, accelerated test methods are delicate since acceleration might lead to changes in material properties that do not occur in real-life applications. In this study, several accelerated weathering tests are performed to evaluate and assess natural and accelerated weathering. Different accelerated weathering cycles are compared with respect to their suitability to simulate natural weathering. The issue of suitability of accelerated weathering for this specific application is discussed.

# 2. Service Life

*"Buildings, the most significant components of the built environment, are complex systems that are perhaps the most significant embodiment of human culture, often lasting over time measured in centuries. Architecture can be a form of high art, and great buildings receive much the same attention and adoration as sculpture and painting. Their designers are revered and criticized in much the same manner as artists. This character of buildings as more than mere industrial products differentiates them from most other artifacts. Their ecology and metabolism is marked by a long lifetime, with large quantities of resources expended in their erection and significant resources consumed over their operational lives."*

(Kibert et al. *Construction ecology* [7]).

Service life is defined as the 'period of time after installation during which a building or its parts meets or exceeds the performance requirements' [6], which is similar to the term *working life* in the EOTA documents [8]. The estimated service life is defined as 'the service life that a building or parts of a building would be expected to have in a set of specific in-use conditions, calculated by adjusting the reference in-use conditions in terms of materials, design, environment, use, and maintenance'. A recent work on the state-of-art of service life prediction for non-structural building components was published by the National Research Council Canada [9]. A common way of illustrating the many processes and factors involved in service life planning is shown in Figure 2.1.

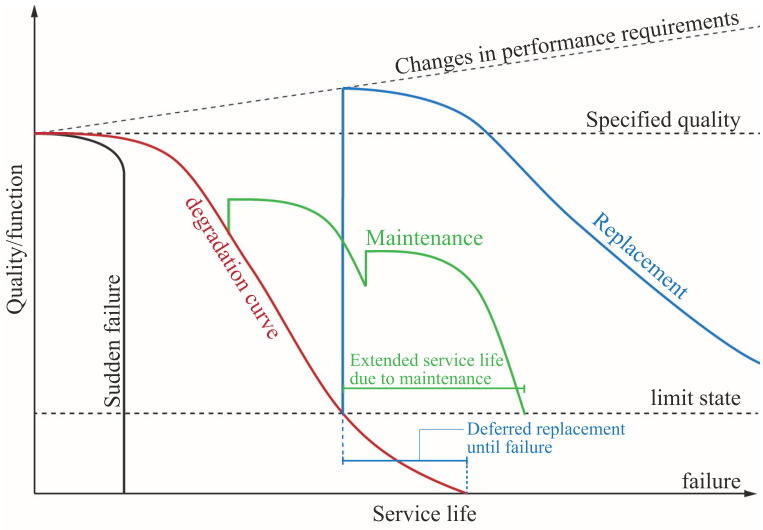


Figure 2.1.: Processes and factors in service life planning and design (adapted from [10]).

## 2.1. Methodology

The intention of the methodologies suggested in the ISO 15686 series is to provide tools for service life prediction (SLP) procedures. Manufacturers, who wish to provide data on performance of their products, technical approval organizations, and product standards draft and development work are the main target audience. A simplified version of the service life prediction (SLP) methodology presented in ISO 15686-2 is shown in Figure 2.2. *Definition* includes user needs and the building context, as well as the type and range of agents, performance requirements and material characterization. The identification of degradation agents and effects, the choice of performance characteristics and evaluation techniques is outlined in *Preparation*. The aim of *Pretesting* is to verify the correct choice of mechanisms and loads for the material or component in question. *Exposure and evaluation* is the heart of the procedure, where both *Short-term exposure* either by short in-use condition tests or accelerated exposure tests and *Long-term exposure* is conducted and assessed. *Long-term exposure* can involve field exposure, inspection of buildings, experimental buildings,

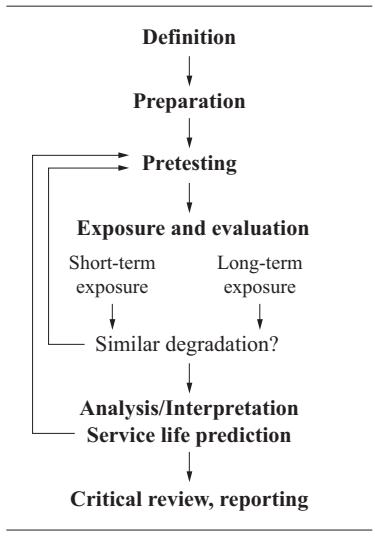


Figure 2.2.: Systematic methodology for Service Life Prediction (SLP) of building components (adapted from [6]).

and in-use exposure. After the verification of similar degradation for both short-term and long-term exposure, the *Analysis* and *Interpretation* of the gathered data results in a performance-over-time or dose-response relation that can be used to establish *Service life prediction* models. Finally, a *Critical review* of data and procedure is required.

## 2.2. Factor method

The so called factor method as presented in ISO 15686 [6] was designed to account for different agents and conditions that are likely to affect service life. Seven factor categories are introduced, *A*) Inherent performance level, *B*) Design level, *C*) Work execution level, *D*) Indoor environment, *E*) Outdoor environment, *F*) Usage conditions, and *G*) Maintenance level.

Taking into account the relevant factors for the specific application in question the *reference service life* ($t_{RSL}$) of a material or component is

decreased or increased, resulting in the *estimated service life ($t_{ESL}$)*[6]:

$$t_{ESL} = t_{RSL} \cdot \phi_A \cdot \phi_B \cdot \phi_C \cdot \phi_D \cdot \phi_E \cdot \phi_F \cdot \phi_G \tag{2.1}$$

As both the reference service life and the factors are usually not a single value, but a distribution, the estimated service life will also be a distribution. An recent work about the factor method was carried out by Listerud [11], and an extensive work about the factor method and its usability was carried out by Marteinsson [12].

## 2.3. Limit state

*Limit state* characterizes the point where a building component is not able to fulfill the performance requirements any more, hence, the end of service life. The methodology is truly adapted from structural engineering, where the limit state design refers to the application of statistics to define the safety requirements for a structure. [13] states three classes of limit state: *1*) Structural limit state, *2*) Durability limit state, and *3*) Usability limit state . The structural limit state causing failure and collapse of a building or structure is the most crucial one with respect to safety. However, durability and usability limit states are probably economically more relevant. Aikivuori [14] studied the reasons for the initiation of repair projects and found out that only 17% were initiated due to deterioration. *Subjective feature of decision maker* was reported to be the reason for refurbishment in 44% of the cases, followed by *change in use* (26%), *deterioration* (17%), *optimization of economical factors* (9%), and finally *change of circumstances* (4%). Hence, 70% of the projects were initiated due to a usability limit state. This is often termed *Obsolescence*, the loss of ability of an item to perform satisfactory due to changes in performance requirements [6]. Kesik et al. [10] use the term *differential service life* to point out the different limit states.

## 2.4. Environmental characterization

The mapping, modeling and characterization of the environment is an important issue in the light of service life planning and prediction. Service life of building materials and components exposed to the outdoor environment is technically but also economically important. Högberg [15] investigated to what extend weather data can be transformed to a microclimatic level in order for use in the design of durable buildings. The study provides an overview over existing transformation models and investigates their suitability for building design questions. It was found that, e.g. the surrounding of the building in question and architectural detailing of building parts have a major role in the actual microclimatic load. Haagenrud [16] presents an overview over various projects on the topic, including dose-response relationships, and the effects of different environmental agents on degradation processes of different materials. The determination of relevant degradation processes for a material in question implies the understanding and characterization of the relevant climatic agents. In the field of polymer degradation the characterization of weather loads is an important topic [17].

## 2.5. Dose-response relationship

Assumably, the changes in any material property are related to the dosage of the relevant degradation factors, a so called dose-response relation or function. Dose-response relations can be helpful to e.g. assess the risk of wood decay. Scheffer [18] developed a map for the U.S. where the risk of fungal decay is presented depending on precipitation and temperature level. Lisø [19] adapted this methodology to establish a map for decay risk in Norway. Further, a guide to design solutions for timber design for Australia, taking into account various degradation mechanisms and climatic conditions was established [20]. See also 6.4.

# 3. Weathering of wood

Changes that occur during outdoor exposure above ground are termed weathering[1]. It occurs on all surfaces and building parts exposed to climatic strains. Both the actual environmental factors and the effects of weathering vary for different materials. Weathering of wood involves color changes, loss of surface fibres, roughening and cracking of the surface, and changes in chemical composition. Weathering is not to be confused with decay caused by fungi that are capable of destroying wooden cells causing significant weakening of the wooden structure. The effects of weathering are strongly superficial. Wood is a polymeric material, solar radiation, especially the UV has a major role in the initiation of the weathering process. An overview over wood color and color changes caused by different climatic strains, chemicals and microorganisms is given by Hon and Minemura [21]. Sell and Leukenes [22] and Wälchli [23] investigated the climatic and biological strains on wood exposed to the outdoors. They state that durability and serviceability are usually not impaired by the chemical and mechanical aging processes. They assumed radiation, precipitation and air movements to be the main climatic strains involved in wood weathering. Mold growth on different untreated and painted wooden surfaces was investigated by Kühne et al. [24]. Feist and Mraz [25] compared erosion rates for outdoor and accelerated weathered softwoods and found that wood density correlates strongly with erosion rates. Sell [26] discussed the role of wood density in the erosion of wood during weathering, and Sell and Leukenes investigated 20 untreated wood species that were exposed outdoor for one year. They found relatively equal surface greying for all 20 materials by visual inspection. Evans et al. [27] conclude that surface checking is increased due to photodegradation by ultraviolet and visible light. Hon and Chang [28] investigated the surface degradation of wood

[1] weathering is also referred to as *aging*

Figure 3.1.: Wooden shingles, facade detail from Eidsborg stave church, built in the $13^{\text{th}}$ century.

by ultraviolet light and found that UV light cannot penetrate deeper than 80 $\mu m$ of a wood surface. Pandey studied the effect of photoirradiation on the surface chemistry of wood [29, 30]. Fúto investigated the influence of temperature on the degradation of wood [31, 32]. He concluded that increased temperatures lead to accelerated evaporation of degradation products and thereby greying of the wooden surface. Arnold [33] investigated wood weathering in the laboratory. The study involved two different light sources and water spray. They found that the timing of the weathering cycles plays a major role on the development of weathering stresses. In two recent studies Oltean et al. [34] investigated color changes of sixteen wood species exposed to simulated indoor sunlight and Schnabel et al. [35] conducted a study on color changes of naturally weathered wood. He states that by using a locally weighted regression method it could be possible to compare different weathering locations and wood species.

## 3.1. Wood structure and chemistry

On a macroscopic level, wood species can be distinguished into softwoods and hardwoods, characterized by the types of cells and their distribution. Softwoods consist mainly of so called tracheids, elongate cells which can be several millimeters long. About 95% of these cells are oriented along the longitudinal axis of the standing tree. This cellular distribution contributes significantly to the anisotropy present in wood. Hardwoods contain additional cell types, e.g. vessels, short, wide cells built for water conduction. In both softwoods and hardwoods, the tree trunk is typically divided into two zones, that often also can be distinguished by color: sapwood and heartwood. The active part, in which cells are still alive and active, is referred to as sapwood. Heartwood is the often darker-colored part found in the inner part of the trunk. However, for some wood species, e.g. ash, aspen and beach, heartwood and sapwood are not easily distinguished. Heartwood functions as a long-term storage of biochemicals collectively known as extractives, e.g. oils, gums and resins. Due to these toxic compounds stored in the cells and its lower water permeability, heartwood has a greater natural durability than sapwood. However, strength properties remain unaffected [36, 37]. Due to seasonal differences in the climatic conditions in temperate regions, the growth season is limited to the spring and summer months. In the beginning of the growth season, earlywood cells are formed, characterized by thin cell walls, while later in the growth season cells with thicker walls are formed (see Figure 3.2). On a macroscopic level, these differences in cellular structure are perceived as annual rings. Wood is a polymeric material. It consists of cellulose, hemicellulose, lignin, and a minor portion of extractives. Figure 3.2 shows the structure of a wood cell wall. The chemical components are distributed differently in the different layers of the cell wall. The majority of cells in soft wood are tracheids. Figure 3.3 shows the main parts of a wood cell,the lumen, a void space, the primary use is for water conduction, and the cell wall, which again consists of three main regions: the middle lamella, the primary cell wall, and the secondary wall. The adhesion to the surrounding cells is provided by the middle lamella. The primary cell wall is characterized by random orientation of the cellulose microfibrils. The secondary cell wall again is composed of three layers; the outer $S_1$

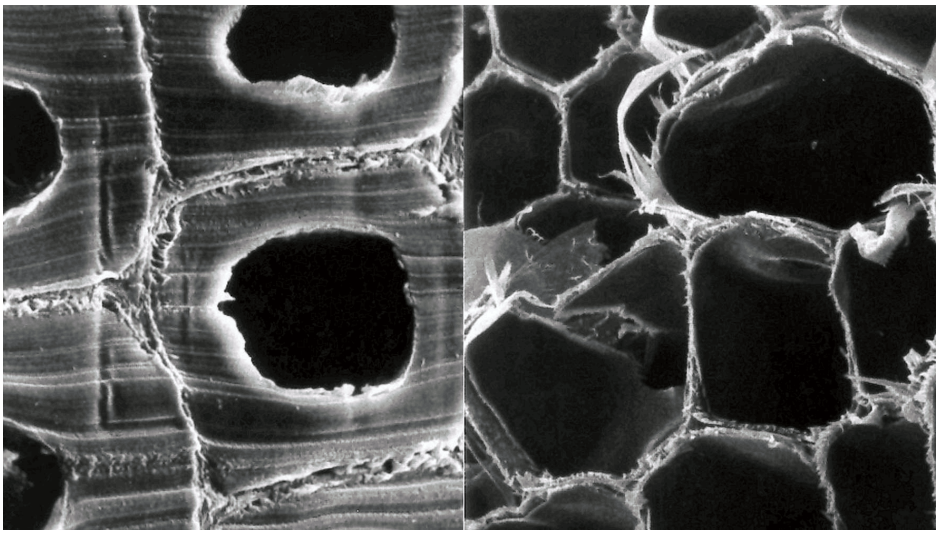

Figure 3.2.: Latewood (left) and earlywood (right) [38]

Table 3.1.: Chemical composition of wood (adapted from [39])

| Component | Mass | | Polymeric state | Function |
|---|---|---|---|---|
| | Softwood [%] | Hardwood [%] | | |
| Cellulose | 42±2 | 45±2 | crystalline, highly oriented, large linear molecule | 'fibre' |
| Hemicelluloses | 27±2 | 30±5 | semicrystalline, smaller molecule | 'matrix' |
| Lignin | 28±3 | 20±4 | amorphous, large 3D molecule | 'matrix' |
| Extractives | 3±2 | 5±4 | principally compounds soluble in organic solvents | extraneous |

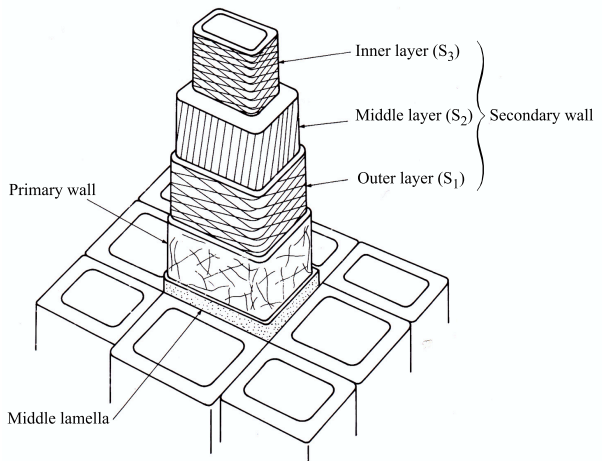


Figure 3.3.: Simplified structure of the cell wall, adapted from [39]

layer, the middle $S_2$ layer, and the inner $S_3$ layer. They vary in microfibril angle, thickness and lignin content. The $S_2$ layer is the thickest and thereby most important to wood properties on a macroscopic level. The distribution of the chemical constituents in the cell wall has a major role in the weathering behavior of wood. Cellulose is mostly found in the secondary cell wall, while the middle lamella and primary cell wall contain much of the lignin and very little cellulose [40, 41].

## 3.2. Environmental agents

**Solar radiation** In order to cleave chemical bonds in the molecular structure of a material, radiation has to to be absorbed by a chemical constituent. Carbon-hydrogen single bonds, carbon-oxygen, and carbon-carbon bonds are the predominant bonds in wood. Several of the chemical bonds found in lignin fall within the UV radiation range (295-400 nm). However, color changes of wood by light are a superficial phenomenon, the penetration depth is reported to be about 75 $\mu m$ for UV light and around 200 $\mu m$ for visible light [41, 40, 28].

**Water** The major role of water in the weathering of wood is washing out solubles from the surface [42]. Water vapor contributes to the swelling of wood, opening up inaccessible regions of the cell structure [40]. Dimensional changes caused by wetting and drying result in surface stresses that cause cracking of the wooden surface.

**Temperature** Higher temperatures favor chemical reactions, also photodegradation of wood [31, 32]. However, it is unlikely that heat alone causes degradation of wood. However, repeated freezing and thawing has been reported to cause physical deterioration [43]. Furthermore, elevated temperatures contribute significantly to increased reaction rates of chemical reactions, see 6.5.

**Microorganisms** Due to the presence of oxygen, sunlight and moisture, mold fungi colonize wooden surfaces [44, 22], as presented in Figure 3.4. Mold fungi are not to be confused with decay, a process where wood-destroying fungi break down the macroscopic structure of wood. Decay is a great danger to the integrity of a wooden structure. Conditions that favor decay are high moisture content over a long period of time connected with temperature [45]. Surface molds are not capable of utilizing the chemical components of wood as nutrient, they use non-polymeric substances in wood, carbohydrates, simple sugars, and starch [37, 46]. Sell and Leukenes [47] compared outdoor and accelerated weathering of wood and found that the missing colonization by mold fungi has a major role in the appearance of weathered wood.

## 3.3. Effects of weathering

Changes in surface properties and alterations in appearance are the foremost consequences of weathering. The process of weathering is initiated by solar radiation, mostly the UV part. Chemical bonds are destroyed, soluble fractions are washed out and microorganisms colonize the surface.

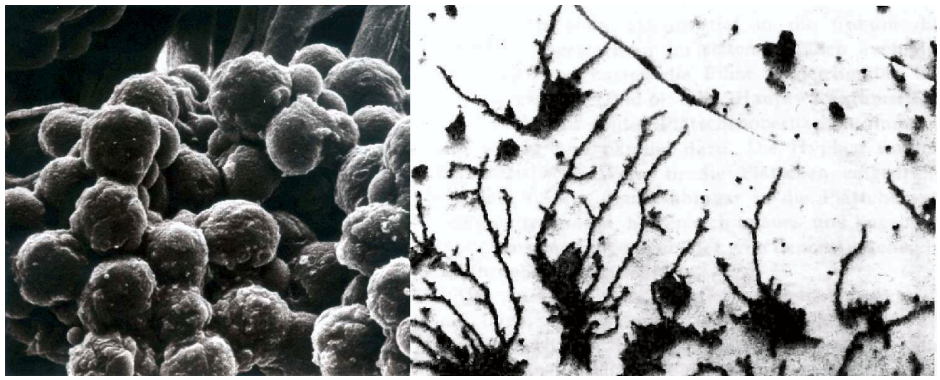

Figure 3.4.: Fungal growth on wood surfaces (left [38], right [22])

### 3.3.1. Microscopic changes

The chemical reactions behind wood weathering are not fully understood and subject to ongoing research. Questions around wavelength dependency, the influence of the presence of water, and temperature dependency are still not answered [48]. However, the UV part of solar radiation is known to be responsible for the initiation of a chemical reaction that in its course leads to the photodegradation of wood. The middle lamella, rich in lignin, is eroded first. Depending on the species and thereby density, the erosion rate is reported to be 6-12 mm per century [49, 41, 48, 22, 23, 50].

### 3.3.2. Macroscopic changes

Changes in appearance are the most noticeable feature of wood weathering. Photodegraded lignin is washed out by water, leaving a surface rich in cellulose fibres. Stresses due to shrinking and swelling cause surface checks and cracks and the surface gets rougher. Thinner earlywood cell walls are more rapidly eroded that thicker latewood cell walls, contributing to the roughening of the surface. Also the overall density of the material influences on the erosion rate [49]. Figure 3.5 shows a weathered wooden surface; note the ridges of less eroded late wood and the loose (eventually black) fibres that remain loosely attached to the surface. In past studies,

Figure 3.5.: Weathered wooden surface, Røros, Norway

erosion rate or weight loss was chosen as evaluation criterion. Arnold et al. [51, 33] measured erosion rates after artificial weathering. They found that the presence of water was essential to the simulation of natural weathering. Derbyshire et al. conducted an extensive study on the photodegradation of wood, using tensile strength as evaluation criterion. They found that also visible light contributes to the photodegradation of wood and that also cellulose is degraded when wood is exposed to the full solar radiation spectrum. Furhter, they showed that degradation was temperature dependent and determined the activation energy to be 5.9 to 24.8 kJ/mol depending on the prevailing chemical reaction [52, 53, 54, 55].

### 3.3.3. Color and color changes

Only a small portion of the electromagnetic spectrum can be recognized by the human eye; it responds to wavelengths between about 390 and 750 nm. UV light at wavelengths below 390 nm and infrared light above 750 nm is not recognized. Hence, the color of an object is actually the reflection of light. If all light is reflected, the objects' color is recognized as white. In contrast, if all light is absorbed, the object's color is recognized as black.

The description of color by numeric values is based on the trichromatic quality, which means that any color is a mixture of three colors. The mechanical determination of color is based on the measurement of spectral

reflectance.

The visible portion of the electromagnetic spectrum absorbed by wood determines its color. Different wood species are composed differently, and surface characteristics vary from sample to sample. Hence, the perception of wood color varies. The irradiation direction will influence on color perception, as well as moisture content, and surface roughness [21].

Color changes caused by weathering involve darkening and fading of the wooden surface, depending on the wood species in question. Hon and Minemura [21] present various studies on the discoloration of wood by light. The discoloration process induced by light is by and by overlayed by the colonization by mold growth. The weathered wooden surface appears grey, where much of the appearance is contributed by mold fungi [47].

## 3.4. Accelerated weathering

Accelerated weathering describes a process, where one or several of the environmental agents are accelerated. Acceleration can imply a more rapid repetition (time compression) and/or an increase in dosage of a weathering agent. For example, solar radiation dosage can be increased significantly by tilting a vertical surface towards the sun, e.g. by 45°(see also Section 4.2. Figure 3.7 shows an old Norwegian stave church, the wooden shingles are regularly treated with tar. The variation in color shadings of the wooden shingles develop due to different exposure conditions, e.g. tilted surfaces and shading by roof overhang. In the automotive industry, the application of polymeric materials is very common and their error-free performance is often crucial both from a safety and an economical point of view. The question of e.g. the color stability of automotive coatings is subject of extensive research. Climate characterization and the development of advanced equipment and procedures for accelerated testing has been the focus of this research fields for many years [57, 58, 59]. The general principles of accelerated material testing might be applied to other applications as well. Figure 3.6 shows the methodology of material testing. In general, two methods are commonly combined under the expression *accelerated weathering*, mostly applied in laboratory testing:

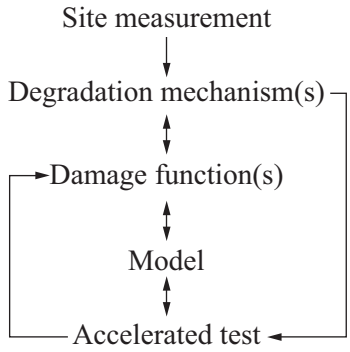


Figure 3.6.: Critical components of test design (adapted from [56])

*1*) Time compression, and *2*) Acceleration . *Time compression* is defined as a line-up of strains observed in a real application, a reproduction of the outdoor environment omitting periods where the climatic strains are known to be under a critical level, e.g. at night. *Acceleration* means increasing the quantity of a climatic strain over the level of a real-time application. Acceleration may involve all agents, radiation, temperature, and water. The calculation of acceleration factors to compare accelerated weathering to natural weathering are useful in order to relate accelerated weathering to a desired service life of a product.

The repeatability and reproducibility of weathering tests is a widely discussed topic. Repeatability is defined as *'the closeness of agreement between independent results obtained with the same method on identical test material, under the same conditions (same operator, same apparatus, same laboratory and after short intervals of time).* Reproducibility is defined as *'the closeness of agreement between independent results obtained with the same method on identical test material but under different conditions (different operators, different apparatus, different laboratories and/or after different intervals of time)'* [60]. It has been shown that neither repeatability nor reproducibility of outdoor weathering tests (in this case polymeric materials) is granted [61].

Since UV radiation is responsible for the initiation of degradation processes, the spectral distribution of light sources used for accelerated weath-

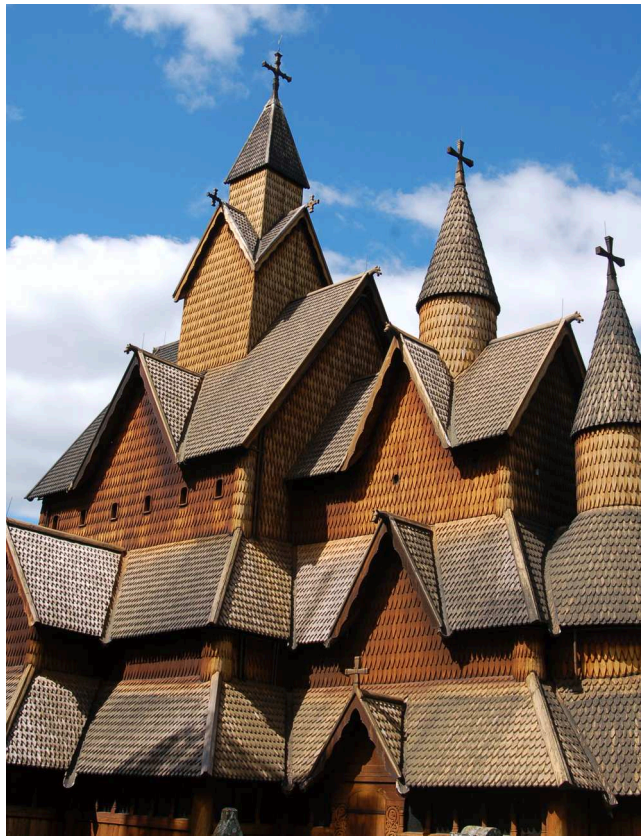

Figure 3.7.: Wooden shingle cladding at Heddal stave church, Notodden, Norway.

ering is important. A spectral distribution close to that of natural sunlight is desirable, different light sources can cause effects that cannot be compared to those of natural sunlight [62, 30].

# 4. Climate for Weathering

## 4.1. Outdoor test site

The outdoor test site is located at Voll in Trondheim, Norway (longitude 10°27'16" N, latitude 63°24'39"E, elevation above sea level 120 m). The test site that comprises several test assemblies is owned by the *Norwegian University of Science and Technology (NTNU)* and *SINTEF Building and Infrastructure*. A meteorological station owned by *The Norwegian Meteorological Institute (DNMI)* is located at the same site. A range of climatic data is logged at the test site, e.g. temperature, relative humidity, precipitation, wind speed and direction, air pressure, global radiation, and longwave radiation. Additionally, various parameters are measured on a test building on the same site, e.g. wind driven rain, both free and at walls, temperatures, and time-of-wetness (see [63] for a detailed description of the measured parameters).

Climatic data measured at site was classified according to the Köppen-Geiger climatic classification system. Monthly average temperature and accumulated monthly precipitation serve as input to the classification system. Climates are divided into five main types: *A*) equatorial, *B*) arid, *C*) warm temperate, and *D*) polar climates. Subtypes for each main climate classify more specific. Kottek et al. [64] presented an updated world map of the Köppen-Geiger climate classification based on temperature and precipitation data for a period from 1951 to 2000. According to this map the Voll test sites' climate is classified to be *Dfc*, snow climate, fully humid, with cool summer and cold winter. Using climatic data measured at the test site as input to the Köppen-Geiger classification system returns the results presented in table 4.1.

Table 4.2 gives an overview of the climatic conditions at the test site during

Table 4.1.: Köppen-Geiger climatic classification of Voll test site for exposure period

| Year | Class | Description | Criterion main class |
|---|---|---|---|
| NP | Dfc | Snow climates, fully humid, with cool summer and cold winter | $T_{min}$ = -3.3 ℃ |
| 2005 | Csb | Warm temperate climate, with dry and warm summer | $T_{min}$ = -1.2 ℃ |
| 2006 | Cfb | Warm temperate climate, fully humid, with warm summer | $T_{min}$ = -0.7 ℃ |
| 2007 | Dfc | Snow climates, fully humid, with cool summer and cold winter | $T_{min}$ = -4.0 ℃ |
| 2008 | Cfb | Warm temperate climate, fully humid, with warm summer | $T_{min}$ = -0.6 ℃ |

the exposure period and the current normal period (NP). Temperature, precipitation, and solar radiation on a horizontal plane are measured by *DNMI* on site. The current normal period ranges from 1961 until 1990 and is obtained from the Risvollan weather station close by the Voll test site. The primary wind direction is 202.5 degrees from north, equivalent with SSW.

## 4.2. Solar radiation

Radiation is one of the foremost degradation agents. Solar radiation intensity is measured in $W/m^2$, also referred to as irradiance, an instantaneous measurement of radiation. Integrated over a certain unit of time, usually an hour or a day, it is referred to as irradiation, measured in $Ws/(m^2)$ or $J/m^2$. The shorter wavelength the higher intensity of radiation, i.e. UV radiation is much more intense than infrared radiation. The sun emits a fairly constant[1] amount of radiation, called the solar constant $G_{sc}$=1366 $W/(m^2)$. This corresponds to the total solar radiation measured outside the earths' atmosphere, at air mass 0 (for a more detailed description of terms and definitions see Appendix B). Solar radiation on

[1]The solar constant does not remain constant over longer periods of time. However, for engineering purposes the variations due to sun-earth geometry overrule these.

Table 4.2.: Temperature, precipitation, and solar radiation on a horizontal plane measured by *DNMI* at the Voll test site (Trondheim) during exposure period.

| | | Jan | Feb | Mar | Apr | May | June | July | Aug | Sep | Oct | Nov | Dec | Av. | Total |
|---|---|---|---|---|---|---|---|---|---|---|---|---|---|---|---|
| Temp.[°C] | NP | -3.3 | -2.7 | 0.1 | 3.6 | 8.7 | 12.0 | 13.2 | 12.7 | 9.0 | 5.6 | 0.3 | -2.0 | 4.7 | |
| | 2005 | 1.6 | -1.2 | 0.1 | 5.6 | 7.2 | 11.1 | 15.8 | 12.9 | 10.5 | 7.7 | 4.0 | -0.8 | 6.2 | |
| | 2006 | 0.2 | -0.7 | -4.1 | 4.5 | 9.3 | 12.4 | 15.8 | 17.3 | 12.7 | 6.7 | 4.2 | 4.5 | 6.9 | |
| | 2007 | -0.5 | -4.0 | 3.5 | 4.7 | 8.2 | 14.1 | 15.7 | 13.3 | 8.6 | 6.0 | 1.0 | 0.2 | 5.9 | |
| | 2008 | 0.6 | 1.3 | 0.5 | 5.6 | 9.3 | 13 | 16.1 | 13.7 | 10.4 | 6.5 | 2.2 | -0.6 | 6.6 | |
| Precip. [mm] | NP | 76 | 59 | 59 | 49 | 46 | 63 | 81 | 76 | 110 | 103 | 78 | 90 | 74.1 | 890 |
| | 2005 | 116.4 | 59.6 | 22.6 | 32.1 | 45.2 | 73.4 | 20.6 | 116.8 | 105 | 41 | 66.0 | 124.9 | 68.7 | 632 |
| | 2006 | 94 | 126.3 | 49 | 28.9 | 45.9 | 37.1 | 54 | 40 | 69.3 | 98.3 | 74.4 | 99.4 | 68.1 | 816 |
| | 2007 | 138.2 | 59 | 51 | 81.6 | 49.3 | 18.1 | 128.1 | 104.9 | 115.1 | 97.16 | 199.6 | 30 | 89.3 | 1072 |
| | 2008 | 62.3 | 107.3 | 61.2 | 22.1 | 33.9 | 53.9 | 38.4 | 57.5 | 52.1 | 69.4 | 123.9 | 31.1 | 59.4 | 713 |
| Solar radiation [kWh/m$^2$] | 2005 | 2.96 | 18.29 | 55.84 | 108.50 | 122.25 | 121.76 | 140.90 | 87.31 | 52.826 | 28.52 | 5.58 | 1.45 | 62.18 | 746.19 |
| | 2006 | 2.98 | 14.60 | 63.06 | 109.42 | 139.01 | 129.41 | 147.45 | 119.69 | 54.60 | 24.40 | 5.95 | 1.32 | 67.88 | 811.88 |
| | 2007 | 3.01 | 20.74 | 55.12 | 74.88 | 111.57 | 161.03 | 132.50 | 93.40 | 51.34 | 23.50 | 5.10 | 1.71 | 61.16 | 710.40 |
| | 2008 | 2.82 | 14.06 | 61.33 | 101.06 | 133.71 | 143.02 | 155.26 | 113.43 | 68.53 | 23.16 | 6.04 | 1.81 | 68.65 | 824.22 |

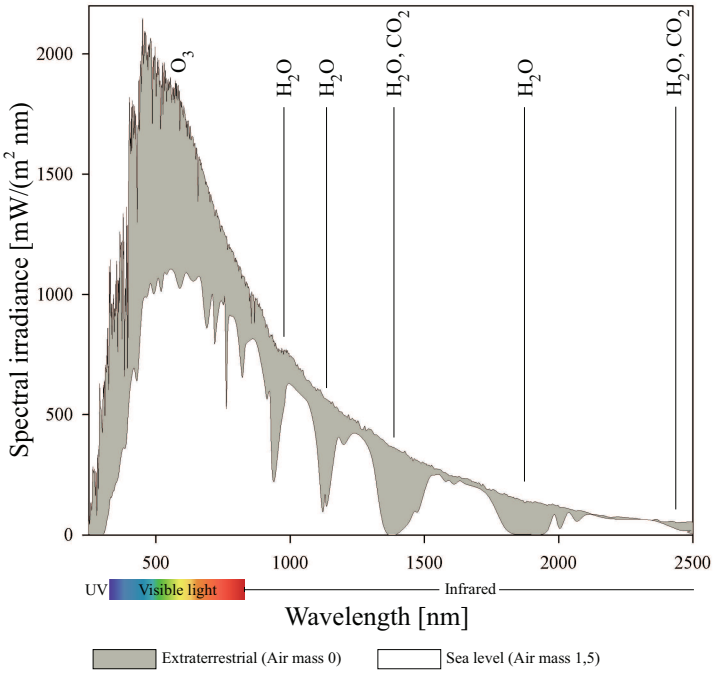


Figure 4.1.: Spectral distribution of solar irradiance for air mass 0 (extraterrestrial) and air mass 1.5 (Sea level), adapted from *NASA*

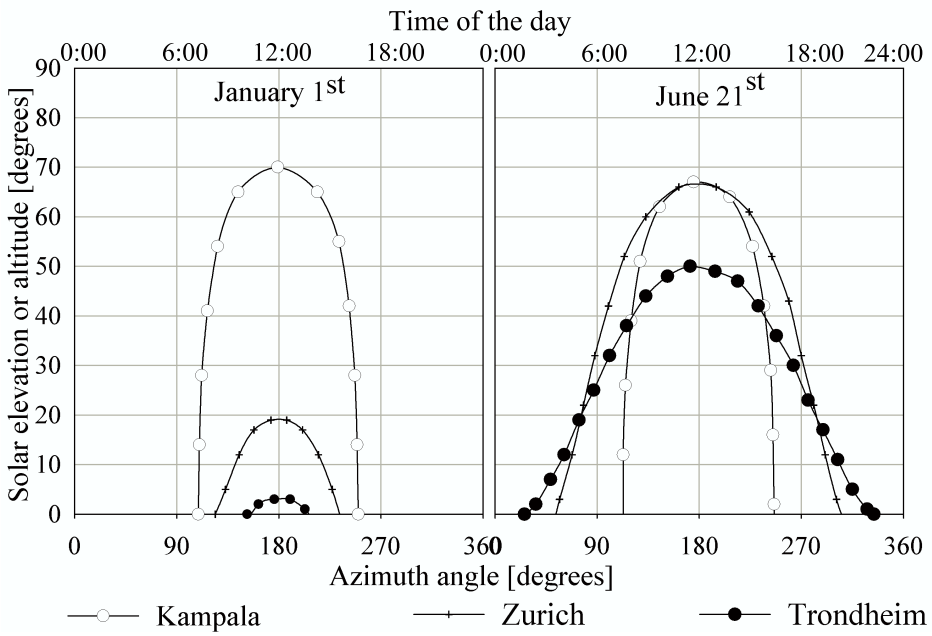


Figure 4.2.: Sunpath (solar azimuth angle and solar altitude angle) for January and June for cities on various latitudes.

a surface is usually referred to as *global radiation* or *total solar radiation* as it refers to the sum of *direct* and *diffuse* radiation. Direct radiation is solar radiation received from the sun without having been scattered by the atmosphere[2]. Diffuse radiation has been scattered by the atmosphere [66]. How much radiation an object on the earths' surface receives, depends on atmospheric effects, sun-earth geometry, and object geometry.

### 4.2.1. Atmospheric effects

Scattering by air molecules, water, and dust, and atmospheric absorption by ozone, water and carbon dioxide have a major role in how much radiation is received at the earths' surface. Scattering is caused by the

[2]It is also referred to as *beam* radiation [65]

interaction of radiation with particles. The number of particles and their size relative to the wavelength of the radiation affect the extend of scattering, e.g. air molecules, water, and dust. Absorption of radiation in the atmosphere is largely due to ozone in bands in the ultraviolet and to water and carbon dioxide in bands in the infrared. Figure 4.1 shows solar radiation spectra for extraterrestrial (air mass = 0) and scattered radiation (air mass = 1.5) together with the bandwidths of the main absorbers, e.g. ozone. Much of the UV radiation is absorbed by gaseous absorbers in the higher and lower atmosphere.

### 4.2.2. Sun-earth geometry

The position of a location on the earths' surface in relation to the sun (see Figure 4.5) has a major role for solar radiation intensity, both on a daily but also on a seasonal basis. The earths' axis' tilt of 23.44° causes seasonal climatic differences. These differences increase with increasing latitude; close to the equator, there are almost no seasonal variations to be found, solar radiation values are fairly constant throughout the year. Figure 4.2 shows the position of the sun for locations of different latitude for *a*) January 21st and *b*) June 21st. Kampala, the capital of Uganda (0°18'0"N, 32°32'0"E), altitude 1155 m, Zurich, Switzerland (47°22'44"N,8°32'28" E), altitude 408 m, and Trondheim (10°27'16" N, 63°24'39"E), altitude 3 m. In Kampala, both sunshine duration and solar elevation are fairly similar in January and June, whereas the cities on the European continent experience both significantly shorter days and lower solar elevation during the winter time. The altitude of a location can increase the effects caused by sun-earth geometry. Figure 4.3 illustrates this effect. Kampala, with a total of 77 kWh/m$^2$ shows the expected low variations in radiation values, while all European locations show the same seasonal pattern. As an example radiation values for the Matterhorn in Zermatt , one of the highest mountains in Europe, is plotted. A comparison of values for Zurich with an altitude 414 m and the Matterhorn with an altitude 4478 m illustrates the influence of the altitude of a location; while Zurich has a total accumulated irradiation of 39 kWh/m$^2$, the Matterhorn has a total of 60 kWh/m$^2$. Trondheim with its far north location has a total of 29 kWh/m$^2$.

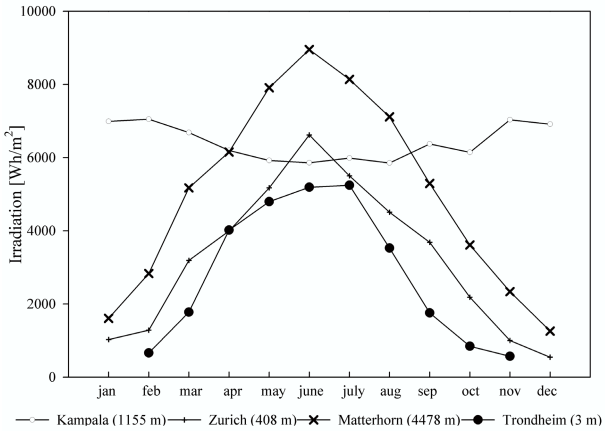


Figure 4.3.: Accumulated monthly solar irradiation for 2005 for various locations

### 4.2.3. Object geometry

Solar radiation values vary significantly with exposure direction and inclination. Figure 4.4 illustrates the path of the sun during the first six months of the year in Trondheim. The sun reaches its highest elevation on June 21st, 12 am. It is evident that inclined surfaces exposed to different directions receive varying radiation doses due to seasonal differences.

Solar radiation is typically measured on horizontal surfaces. A pyranometer is commonly used for solar irradiance measurements. Global radiation (direct and diffuse fractions) measured ranges from approximately 300nm to 2800 nm, covering the whole solar radiation spectrum. A direct deduction of values for inclined surfaces is not possible and its calculation is a rather complex task. Irradiation on an inclined surface comprises direct, diffuse, and reflected radiation. The angular distribution of the diffuse component and the estimation of the reflected part are crucial to the calculation. Simplified models, e.g. the assumption that all radiation is direct, lead to a substantial overestimation of irradiation values for inclined surfaces [65]. The direct fraction on an exposed surface stands

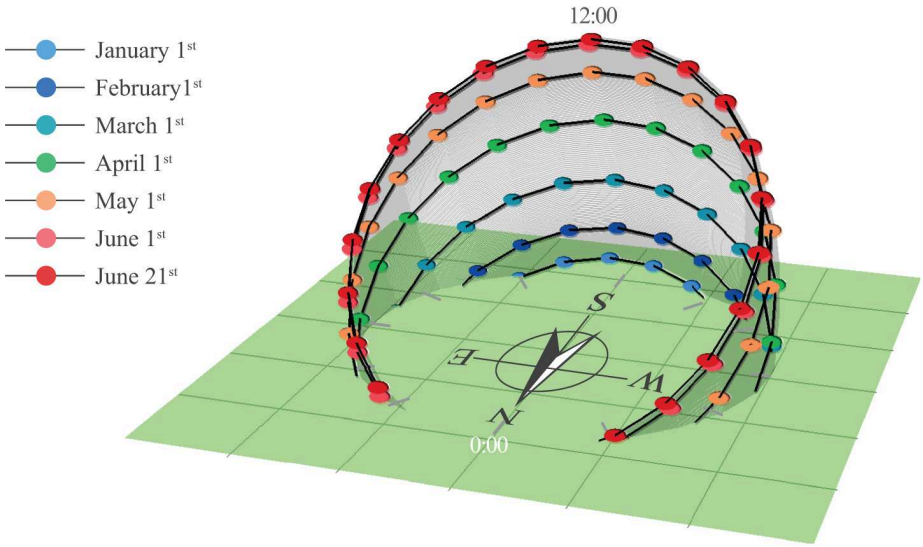


Figure 4.4.: Sunpath (solar azimuth angle and solar altitude angle) from January to June for Trondheim.

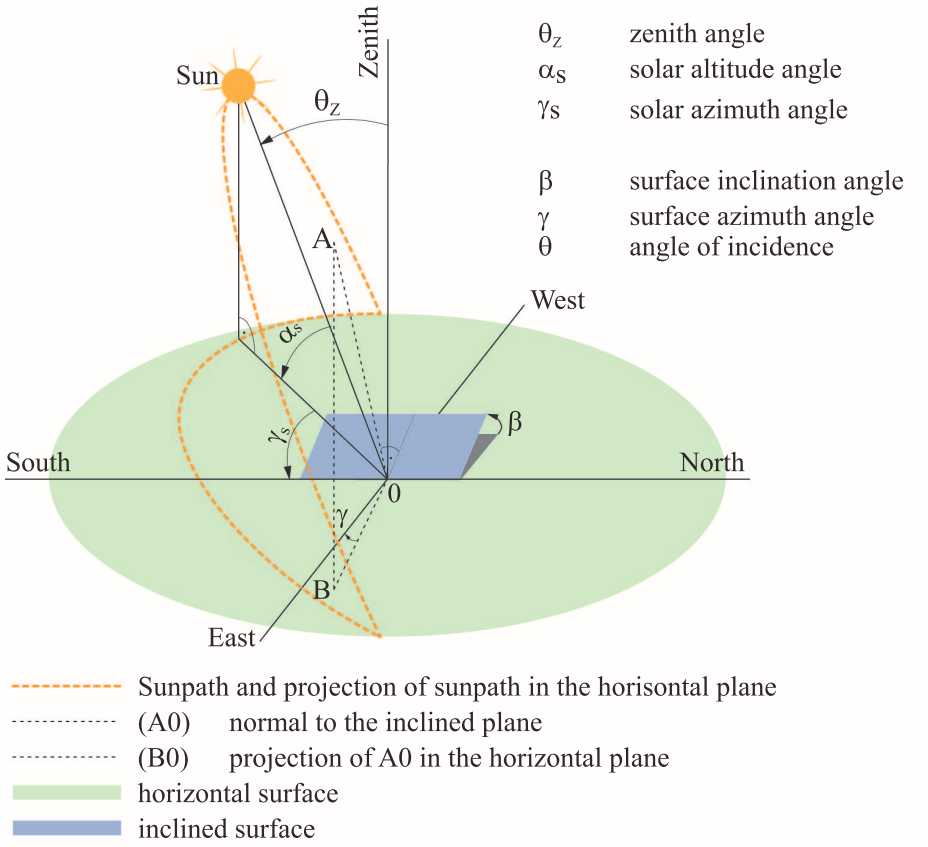


Figure 4.5.: Definitions and terminology for sun-earth geometry for horizontal and inclined surfaces, adapted from [66], [65]

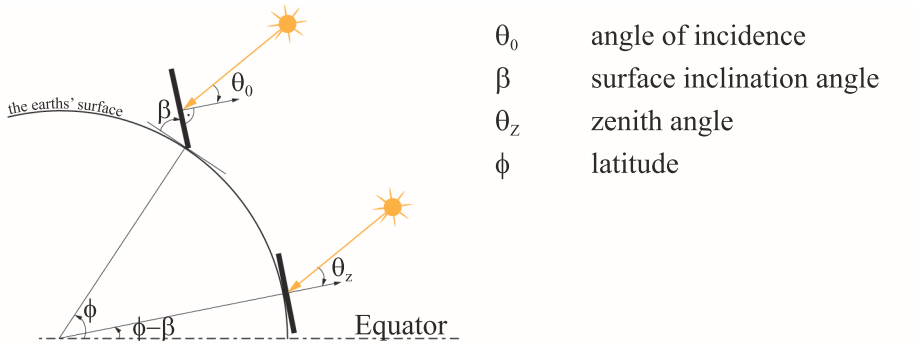


Figure 4.6.: Inclined surfaces facing the equator, relation between latitude, inclination and angle of incidence (adapted from [66])

for the major part of the solar radiation received by an inclined surface. Hence, the inclination angle $\beta$ has a major role. Figure 4.6 illustrates how angle of incidence $\Theta$, latitude $\Phi$, and inclination angle $\beta$ are connected. The greater the latitude, the less solar radiation is received for a horizontal surface. Hence, for the purpose of accelerated weathering, the inclination angle should correspond to the latitude angle to maximize solar radiation impact.

### 4.2.4. Solar radiation database

Solar radiation data for inclined surfaces for this study were obtained from *SoDa.SoDa-Services for Professionals in Solar Energy and Radiation* that provides access to databases on e.g. solar radiation, comprises a system *(SoDa IS)* that builds links to other resources that are located in various countries. A detailed description of the database can be found in [67] and [68]. A comparison of solar radiation data measured on site and data obtained from *SoDa* showed good correlation. Figure 4.7 illustrates the differences between the exposure directions from this study; north, south, east, west, and south facing rack (see Section 5.2.1 for a more detailed description. Additionally, the graph contains values for irradiation on a horizontal surface for both *SoDa* and values measured on site. To emphasis variation in climatic strains for different exposure directions,

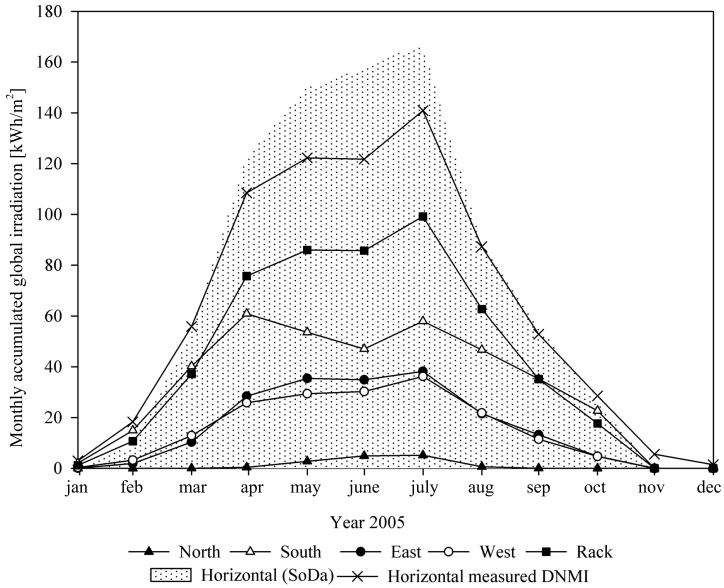


Figure 4.7.: Monthly accumulated irradiation for 2005 for different exposure directions compared with measured and modeled values for a horizontal surface for Trondheim.

Table 4.3 presents solar radiation and wind driven rain data for vertical surfaces (inclination 90°), and south facing rack (inclination 30° above the horizontal plane). Solar radiation load on a wall facing north is, for instance, only 27.7 % of that on a horizontal surface, while solar radiation on a south facing surface with an inclination of 30°above the ground is 107 % of that on a horizontal surface.

## 4.3. Wind driven rain

Wind driven rain data used in this study are measured by *SINTEF Building and Infrastructure* at another test building on the same site. A more detailed description of those measurements and its test set up can be found in [69]. Wind driven rain varies significantly with exposure direc-

Table 4.3.: Solar radiation and wind driven rain on inclined (vertical) surfaces at Voll test site (Trondheim), accumulated over exposure period, February 2005 to August 2008.

| | Horizontal | North | South | East | West | Rack |
|---|---|---|---|---|---|---|
| Solar radiation [kWh/m$^2$][a] | 3557 | 986 | 2745 | 2060 | 2111 | 3805 |
| Percentage solar radiation [b] [%] | 100 | 27.7 | 77.2 | 57.9 | 59.4 | 107.0 |
| Wind driven rain [l/m$^2$][c] | (2998)[d] | 74 | 315 | 18 | 482 | -[e] |
| Percentage of precipitation [%] | 100 | 2.5 | 10.5 | 0.6 | 16.1 | -[e] |

[a] Data acquired from *SoDa* [b] compared to horizontal plane

[c] Data measured by *SINTEF Building and Infrastructure*

[d] Precipitation measured by *DNMI* [e] no data available

tion. Table 4.3 presents wind driven rain data for the test site, Figure 4.8 illustrates the directionality of the two climatic parameters wind driven rain and solar radiation.

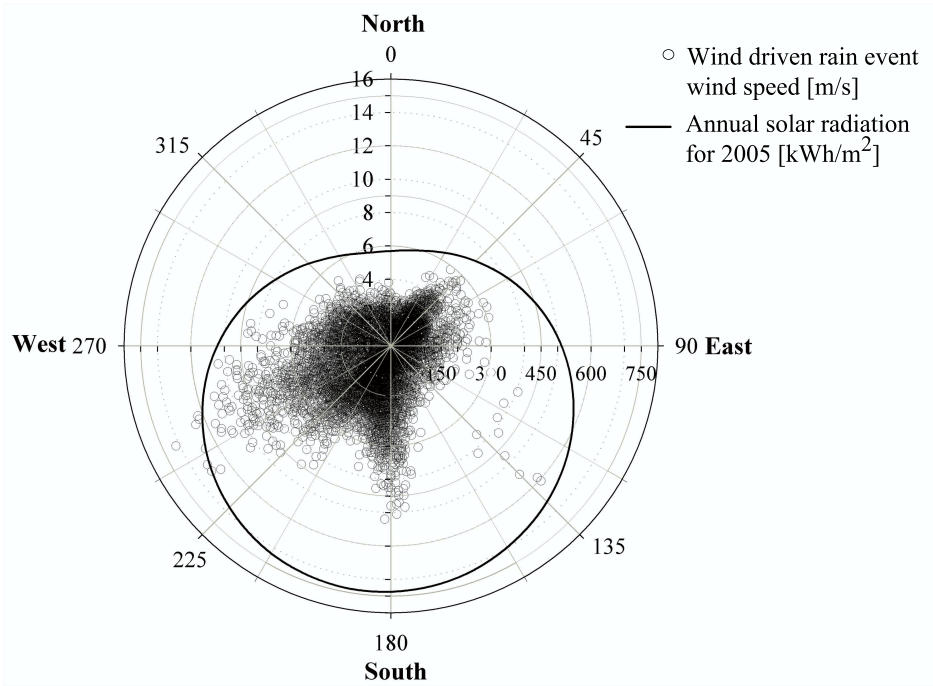


Figure 4.8.: Wind driven rain events (wind direction and speed [m/s]) for exposure period and annual solar radiation [kWh/m$^2$] on vertical surfaces for 2005 for Trondheim. Data from [63].

# 5. Experimental Setup

## 5.1. Materials and sampling

Test specimens consist of a total of nine different wood materials, five untreated wood species and four materials that are treated by means of different impregnation of modification techniques. Local wood species, typically used in facades were chosen for this study. The edges of the materials are not rounded, except material 1, which is a ready shaped cladding board from the manufacturer. Surfaces are either rough sawn or planed. Table 5.1 presents the materials used in this study, together with average mass densities and its standard deviation, surface quality, and initial average color values. The test specimens are approximately 150 mm in width. Different lengths are used for different exposures, 500 mm length for outdoors and in the rotating climate chamber (RCC), and 200 mm for exposure in the ATLAS solar simulation chamber (ASS), see section 5.2.2. Thicknesses vary between 17 mm and 22 mm. Samples are conditioned in a climate chamber at 20 °C and 60% RH until equilibrium moisture content prior to exposure and prior to examination.

## 5.2. Weathering methods

### 5.2.1. Outdoor exposure

Test specimens were exposed vertically on the walls of the test building[1] facing north, south, east and west. Nine samples of each species are exposed on the east and west side of the building, whereof respectively six are

[1] see 4.1 for details

Table 5.1.: Materials, oven-dried densities, average initial color values, and durability class for all materials used.

| No. | Material | Density | Std. dev. | Initial color values | | | Durability class[g] |
|---|---|---|---|---|---|---|---|
| | | | | L* | a* | b* | |
| | | [kg/m$^3$] | [kg/m$^3$][a] | [-] | [-] | [-] | |
| 1 | Norway Spruce[b] (*Picea abies (L.) H.* Karst.) | 411.7 | 11.07 | 80.6 | 6.0 | 24.5 | 4 |
| 2 | Norway Spruce (*Picea abies (L.) H.* Karst.) | 456.6 | 52.19 | 79.2 | 6.1 | 24.2 | 4 |
| 3 | Scots Pine heartwood (*Pinus silvestris* L.) | 478.5 | 49.29 | 73.1 | 11.3 | 31.0 | 3-4 |
| 4 | Aspen (*Popolus tremula* L.) | 493.8 | 24.61 | 79.3 | 5.0 | 23.8 | 3.8[h] |
| 5 | Larch (*Larix decidua* Mill.) | 492.8 | 18.14 | 56.2 | 12.6 | 31.9 | 1-2 |
| 6 | Kebony Furu[c] (*Pinus silvestris L.*) | 542.1 | 41.97 | 23.3 | 5.9 | 18.5 | 1-2 |
| 7 | Kebony SYP [d] (*Pinus taeda*) | 731.1 | 53.34 | 27.7 | 4.0 | 16.0 | 1-2 |
| 8 | Scots Pine, royal impreg.[e] (*Pinus silvestris L.*) | 432.9 | 57.19 | 48.2 | 1.3 | 35.2 | - |
| 9 | Scots Pine, pressure treated[f] (*Pinus silvestris* L.) | 496.5 | 33.01 | 34.0 | 5.2 | 24.5 | - |

[a] derived from several samples per material.

[b] Ruptimal® surface, mechanically roughened surface. [c] Scots Pine, untreated heartwood (0-100 %) and sapwood treated with furfuryl alcohol. [d] Southern yellow pine, sapwood, treated with furfuryl alcohol. [e] as no. 9, add. impregnation with colored linseed oil.

[f] class AB, corresponds to use in hazard class 3 according to NS EN 335-1 [70].

[g] according to NS-EN 350-2 [71]. [h] according to [72].

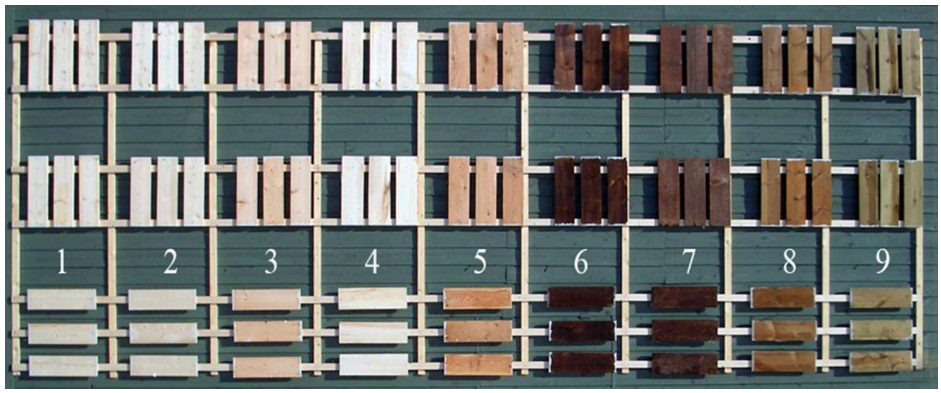


Figure 5.1.: Photo of the test setup at the Voll test site,Trondheim. West facing wall, February 2005, numbers refer to material numbers from Table 5.1.

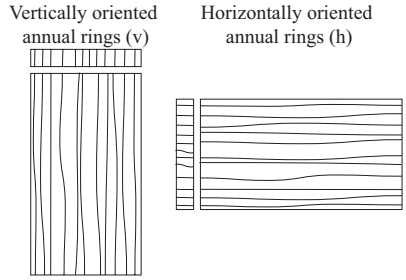


Figure 5.2.: Illustrations of vertically and horizontally oriented annual rings

mounted with vertically oriented annual rings and two with horizontally oriented ones (see Figure 5.1). Two samples are mounted on the north and four on the south side, whereof respectively half with horizontally oriented annual rings. Additionally, two samples of each material were exposed on a rack at the test site facing south with an angle of 30 ° from the ground. Samples were exposed at the test site from February 2005 to August 2008, altogether more than three years (1322 days).

Table 5.2.: Overview over test conditions for laboratory weathering for the ASS (Run 1-4) and the rotating climate chamber (RCC).

| Run | Exp.time [days] | Light [hours] per 24 hrs | Irrad. [kWh/m$^2$] | Water [hours] per 24 hrs | Water [l/(m$^2$h)] per 24 hrs | Temp.[a] [°C] | RH[a] [%] |
|---|---|---|---|---|---|---|---|
| 1 | 112 | 20 | 1200 | 4 | 102 | 63 | 50 |
| 2 | 26 | 5 x 4h | 1200 | 1 x 4h | 102 | 63 | 50 |
| 3 | 10 | 5 x 4h | 1200 | 1 x 4h | 102 | 22 | 50 |
| 4 | 42 | 5 x 4h | 600 | 1 x 4h | 102 | 63 | 50 |
| RCC | 888 | 6 x 1h | 257 [c]<br>15.4 [d] | 6 x 50 min | 15 | 63 | - |

[a] during solar radiation [c] calculated solar radiation [d] measured UV radiation

## 5.2.2. Laboratory exposure

Artificial weathering tests were performed in two apparatuses: An *ATLAS SC 600 MHG* solar simulation chamber (ASS) and a rotating climate chamber (RCC). The ASS can be programmed according to the users requirements, while the RCC runs in a fixed cycle that is defined in NT Build 495 [73]. The ASS is equipped with a 2500 W metal halide global lamp, wavelengths ranging from 280 nm to 3000 nm. Figure 5.3 presents spectral distributions for the lamp used in the ASS compared to sunlight. The radiation intensity is 1200 W/m$^2$ at the sample surface 55 cm from the light source glass cover. The other test parameters that may be custom set are temperature (+15°C to +80°C ± 0.5°C), relative humidity (10 % to 80 % RH ± 5 % RH) and water spray (e.g. 1.7 l/(m$^2$min)). The effective testing area is 0.76 m x 0.78 m. Samples are exposed on a horizontal grillage that allows water to run off.

The rotating climate chamber (RCC) is designed based on specifications in NT Build 495 [73], see also [74]. The apparatus consists of a rectangular rotating central unit where test specimens might be mounted on four sides, each capable of carrying a vertically mounted test specimen of maximum 1.5 m x 2.5 m (width x height). The central unit rotates stepwise 90° every hour, which thus passes the test specimens into four different exposure environments: *1*) UV and IR radiation (for UVA 14 W/m$^2$ and UVB 1.4 W/m$^2$) at a black panel temperature of 63 °C ± 5 °C), *2*) water spray (15 ± 2 l/(m$^2$ h)), *3*) frost (-20 °C ± 5 °C), and *4*) laboratory cli-

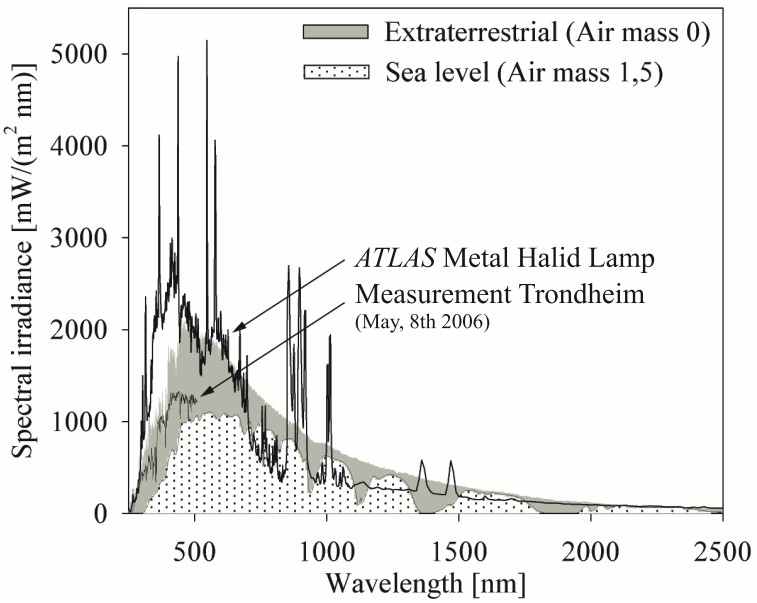


Figure 5.3.: Spectral distribution for solar radiation, ASS Metal Halid lamp, and a measurement taken by the Department of Physics at NTNU(data from NASA, ATLAS, and NTNU)

mate (defrosting of test specimens). Four different test cycles were run in the ASS, one in the RCC. Table A.10 presents test specifications for the different runs for the artificial laboratory weathering tests. Run 1, which is used in other studies [33], consists of 20 hours of solar radiation at a temperature of 63 ℃ and 50 % RH, followed by 4 hours of water spray. Run 2 applies the same total strains per 24 hours, but split into four minor parts, i.e. 5 hours of sunlight are followed by 1 hour of water spray. Run 3 is based on run 2, except that the temperature during solar radiation exposure is reduced from 63 ℃ to 22 ℃. Run 4 is also based on run 2, with the difference that radiation is reduced by applying a physical UV-filter (metal grid) that absorbs 50 % of the total radiation. Throughout the radiation period the relative humidity is set to 50 %, temperature during the water spray period is set to 10 ℃, which applies to all runs.

## 5.3. Evaluation methods

As stated in Chapter 1 the limit state of a building part or material is often not related to its technical, but to its aesthetic appearance. Therefore, changes in appearance of weathered wood surfaces were determined by color measurements. Thereby, usually descriptive and subjective evaluation of color changes are transformed into numerical values.

### 5.3.1. Color measurement

Color models can be used to quantify color and color changes. Most of them are based on a standard developed by the *International Commission on Illumination (CIE)* [75, 76]. They attempt to describe color according to human color perception. These color models use numerical values to represent the visible spectrum of color. The color model determines the relationship between values, and the color space defines the absolute meaning of those values as colors. The *CIELab* model describes color in terms of its lightness component L* and two chromatic components, a* (green-red) and b* (blue-yellow). Together, those three components form a three-dimensional color space. L*, the lightness component ranges from 0 (black) to 100 (white), representing the achromatic axis of greys. a* and b* range from -128 to 127(see Figure 5.4). Color differences can be calculated by determining the Euclidean distance between two colors as [77, 78, 79]

$$\Delta E^* = \sqrt{(\Delta L^*)^2 + (\Delta a^*)^2 + (\Delta b^*)^2} \tag{5.1}$$

By summing up $\Delta E^*$ for all analyzed points in time, the course of the color changes can be taken into account:

$$\sum_{i-1,i}^{n} = \Delta E^*_{0,1} + \Delta E^*_{1,2} + ... + \Delta E^*_{n-1,n} \tag{5.2}$$

Chroma C* is defined as the Euclidean distance between a color and its achromatic point of the same lightness:

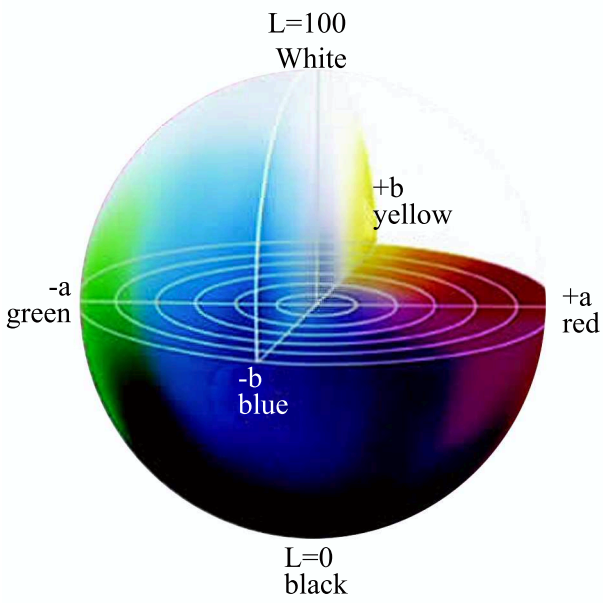


Figure 5.4.: Graphic interpretation of the CIE L*a*b* color space. (Adapted from www.rehab.research.va.gov)

$$C^* = \sqrt{a^{*2} + b^{*2}} \tag{5.3}$$

Chroma differences can be calculated as

$$\Delta C^*_{1,2} = C^*_2 - C^*_1 = \sqrt{a^{*2}_2 + b^{*2}_2} - \sqrt{a^{*2}_1 + b^{*2}_1} \tag{5.4}$$

Hue H* is referred to as the shade of color, i.e. red, green, blue, and yellow. Difference in hue can be calculated as

$$\Delta H^* = \sqrt{\Delta E^{*2} - \Delta L^{*2} - \Delta C^{*2}} \tag{5.5}$$

To determine the color development of the outdoor exposed samples, test specimens were demounted periodically, altogether thirteen times during the exposure period from February 2005 to August 2008. After conditioning in a standard climate (20 °C, 60 % RH) until equilibrium moisture content, samples were scanned using an *EPSON Perfection 2580 Photo*. Samples tested in the laboratory were assessed at the same point of the weathering cycle. Color values were obtained using *Matlab*® corrected by means of a color profile obtained by a scanner target according to ISO 12641 [80, 81]. Average color values and their standard deviation for each sample were determined. In addition, to determine the overall changes of the surface color, the distribution of color changes represented by the standard deviation were also obtained. This provides a time effective sample handling; many samples can be processed in a reasonable amount of time. Furthermore, irregularities inherent in wood surfaces can be evened out by applying this method. Additional color measurements using a colorimeter *Datacolor Mercury 3000* showed that the scanning method produced reliable results. Color determination by image processing could also be adaptable to color measurements in-situ. By placing a reference color next to the area in question, color values might be corrected accordingly and determined by image processing.

### 5.3.2. Mold growth

As stated in Section 3.2, surface mold growth contributes significantly to the appearance of a weathered wood surface. They might be identified with the naked eye as little black spots, see Figures 6.8 and 6.11. At the end of the exposure time, samples of fungal organisms on the sample surfaces were collected with a tape lift. The samples were evaluated by means of an evaluation scale ranging from 1 (no growth) to 4 (rich growth).

# 6. Results and Discussion

## 6.1. Outdoor exposure

Figure 6.1 shows the scanned and color corrected images of Scots Pine heartwood (Material 3) during the course of outdoor exposure. Exposure time in days is indicated on top. Each row contains samples from one exposure direction, from top to bottom north, south, east, west, and south facing rack. A complete set of images and graphs of all nine materials may be found in Appendix A.

### 6.1.1. Material

Comparing color changes for the different materials shows that they might be divided into two groups: untreated wood species (Materials 1-5) and treated wood (Materials 6-9). Color changes of untreated wood species follow a certain model:

1. increase in chroma at the beginning of the exposure (first evaluation after approximately two months), characterized by an increase in both a* and b* values, which is common to all exposure directions, and simultaneous darkening, characterized by a decrease in L* values.
2. bleaching and greying, characterized by an increase in L*, a* and b* values.

*Grey* is characterized by the absence of chroma, a* and b* value being zero. a* values for untreated materials at the end of the exposure period vary from -1.15 to 5.68, b* values from 6.10 to 10.34 (average for all exposed samples). This implies a significant loss in chroma for all untreated wood species, though an overall positive b* value shows a rest of yellow in the

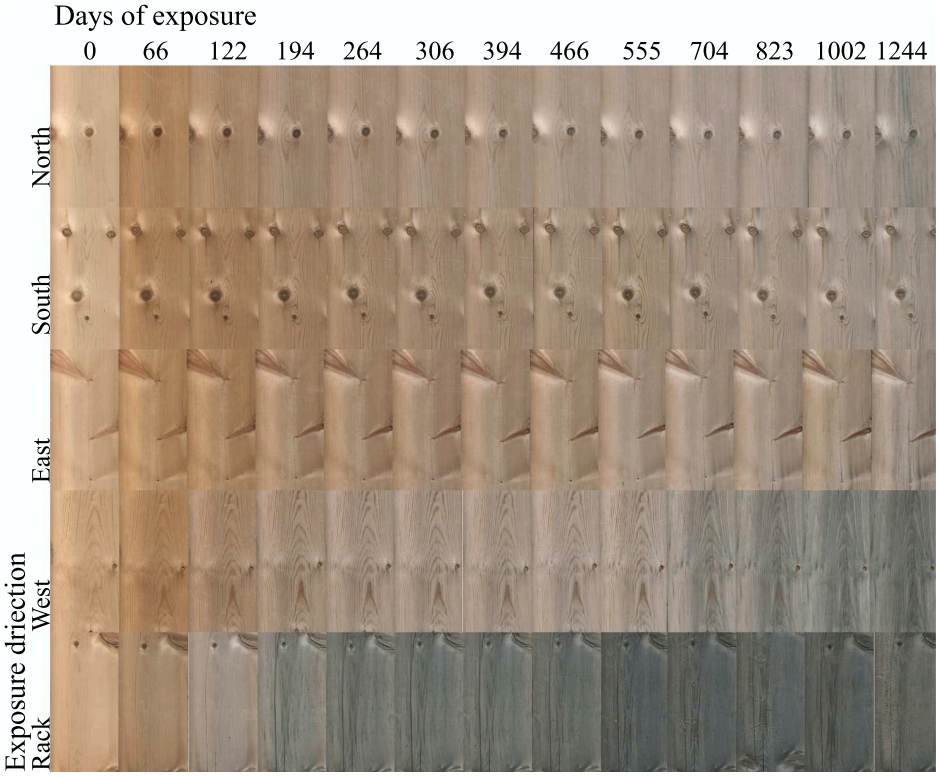


Figure 6.1.: Scots Pine heartwood (Material 3), scanned images from outdoor weathering exposure.

color. All materials show a decrease in L* values compared to the initial state, though to varying extent. The least decrease in L* values was observed for larch (Material 5, south exposure) with 0.78, the most for aspen (Material 4, west exposure) with 37.40. The course of the color changes varies with the respective exposure direction (see 6.1.2). However, the visual appearance and final color values depend little on the wood species.

The color changes of treated materials do not follow a similar distinct pattern. Kebony Furu (Material 6) shows an initial lightening (increase in L* values), and increase in chroma (a* and b* values), followed by slow changes in color values. Kebony SYP (Material 7) shows increasing lightness values and loss in chroma from the start, while royal impregnated wood (Material 8) also showing increasing lightness values shows little changes in a* and b* values, as well as pressure treated wood (Material 9). a* values vary from -1.17 to 2.83. b* values from 8.88 to 18.76. In comparison to the initial state all treated samples show an increase in L* values, varying from 2.94 to 15.01. A collection of scanned images and figures for color values may be found in Appendix A.

### 6.1.2. Exposure direction

As an example representing the group of untreated wood materials, Figure 6.2 shows color values (L*, a*, b*) over exposure time in days for Scots Pine heartwood (Material 3) for all exposure directions: north, south, east, west, and rack. While north, south, and east exposure for this sample are rather similar, west and rack exposed samples stand out. The greying process for rack exposed sample starts quickly after exposure, and is characterized by a decrease in both L*, a*, and b* values. The same process can be observed for all other untreated wood species. For treated wood species color changes cannot be easily described on a general basis. Kebony Furu (Material 6) follow somewhat the same development as the untreated samples, only that instead of a decrease in L* values an increase can be observed. Kebony SYP (Material 7) with its very dark initial color, does not follow any specific pattern, however, color changing values for the east exposed samples are rather little and samples exposed

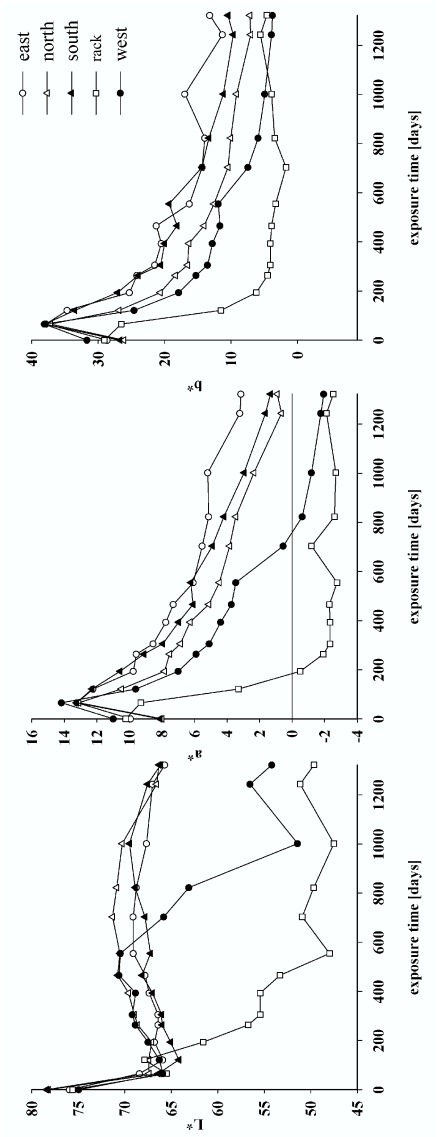


Figure 6.2.: Scots Pine heartwood (Material 3), color values L*, a*, and b* plotted against exposure time.

on the rack and to the west also show the characteristic greying. For royal impregnated and pressure treated wood, the color changes are in general small, though also greying of the rack exposed samples occurs.

For all exposure directions the rate of color changes is decreasing over time. However, the final state does not seem to be reached except for samples exposed on the rack. Due to the rapid changes in color in the beginning of the outdoor exposure, the rack exposed samples reached its final state faster. Irradiation and wind driven rain values for the different exposure directions have been presented in Table 4.3. A comparison of exposure directions with values for rack exposure shows that irradiation values for rack exposure are increased with a factor between 1.4 (south) and 3.8 (north). Wind driven rain values are increased with a factor ranging from 6.2 (west) to 167 (east) compared to precipitation values which are assumed to be relevant for rack exposure. Since all vertically exposed samples seem to converge, the color values for the rack exposed samples might be considered to be the final state of color development of vertically exposed samples.

### 6.1.3. Limit-state

In many applications (e.g. above-ground) the service life of untreated wood cannot simply be quantified by functional parameters. The performance requirement is dominated by the surface aesthetics. Aesthetics again depend strongly on perception and are therefore subjective. Hence, a limit-state for aesthetic appearance cannot be universally valid. However, a limit-state for color differences could involve a limit value for $\Delta$E, which is constituted by the user. A possible application are color differences within a facade from untreated cladding material, e.g. as shown in Figures 6.3 and 1.1. The human eye can distinguish ten million colors. The smallest color difference the human eye can recognize is $\Delta$E=1, though only when samples are located side by side [82]. To illustrate color differences $\Delta$E between different wood surfaces, Figure 6.4 shows larch samples exposed to the west for : (a) 122 days, (b) 306 days, (c) 1322 days, and (d) 1322 days. (a), (b), and (c) are images of the same sample at different stages, whereas (d) is a different larch sample from the same exposure

Figure 6.3.: Different colors of aspen cladding, Tyholt crematory, Trondheim, Norway

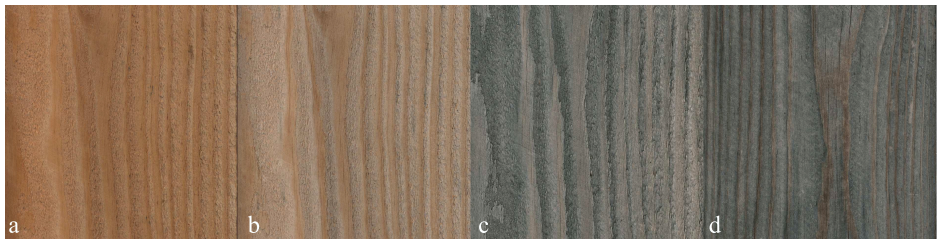


Figure 6.4.: Larch samples (Material 5) exposed to the west, different stages of exposure

direction. Table 6.1 presents color values for those samples. As pointed out earlier, an aesthetic limit-state can be regarded as highly subjective. Some observations made by comparing the images in Figure 6.4 to the values in Table 6.1: 1) All color differences can be recognized with the naked eye, though $\Delta$E=5.9 (sample (c) and (d)) might be difficult to distinguish when not seen side by side. 2) Color differences (a)-(b) and (b)-(c) are perceived differently, though the absolute value is in the same range.While sample (b) appears *bleached* in relation to sample (a), (c) appears *grey*, due to low values of a* and b*. The human eye does not detect differences in hue (red, yellow, green, blue, etc.), chroma, or lightness equally. In fact, the average observer will see hue differences first, chroma differences second, and lightness differences last. Thus, differences in chroma are perceived more dramatic that differences in lightness (L*) [83]. Color difference limit values can vary for different applications, materials and users. For instance, color tolerances in the automotive painting industry, graphics, and textile industry are much lower than what would be reasonable for building applications. These special fields have developed methods and equations to weigh the different perceptions of chroma and lightness caused by the perception of the human eye. Some of these approaches might be applicable in a building materials context.

## 6.2. Laboratory exposure

Figure 6.5 shows images from all weathering cycles conducted in the laboratory for Scots Pine (Material 3). Each row contains samples from one

Table 6.1.: L*, a*, and b* values and ΔE for larch samples (Material 5) exposed to the west

| Sample (see figure 6.4) | L* | a* | b* | ΔE |
|---|---|---|---|---|
| a | 60.3 | 15.7 | 37.1 | 36.3 |
| c | 54.8 | -1.1 | 5.4 | |
| a | 60.3 | 15.7 | 37.1 | 17.9 |
| b | 64.2 | 8.1 | 21.3 | |
| b | 64.2 | 8.1 | 21.3 | 20.7 |
| c | 54.8 | -1.1 | 5.4 | |
| c | 48.9 | -1.3 | 5.6 | 5.9 |
| d | 54.8 | -1.1 | 5.4 | |

weathering cycle (see Table A.10). A complete set of images and graphs for all nine materials and weathering cycles can be found in Appendix A. The starting point for the accelerated laboratory tests were weathering cycles based on literature [33, 25, 84]. However, the evaluated material property in those tests were erosion rates and the correlation between erosion rate and wood density.

### 6.2.1. Material

As for outdoor weathering, untreated wood species (Material nos. 1-5) and treated wood (Material nos. 6-9) react differently to the different laboratory weathering cycles. In Figure 6.6 the color values for all laboratory weathering cycles are shown for Scots Pine (Material 3). Note that the RCC (Rotating Climate Chamber) graph is referring to the x-axis on top of the figure, since a different time scale applies. All accelerated weathering cycles conducted in the ASS follow the same course: L* values decrease (darkening), the rate decreasing with time, followed by an increase (lightening) in L* values until the end of the test period. a* and b* values generally show a decrease in values. Treated samples showed a different course, depending on the material. Especially L* values vary

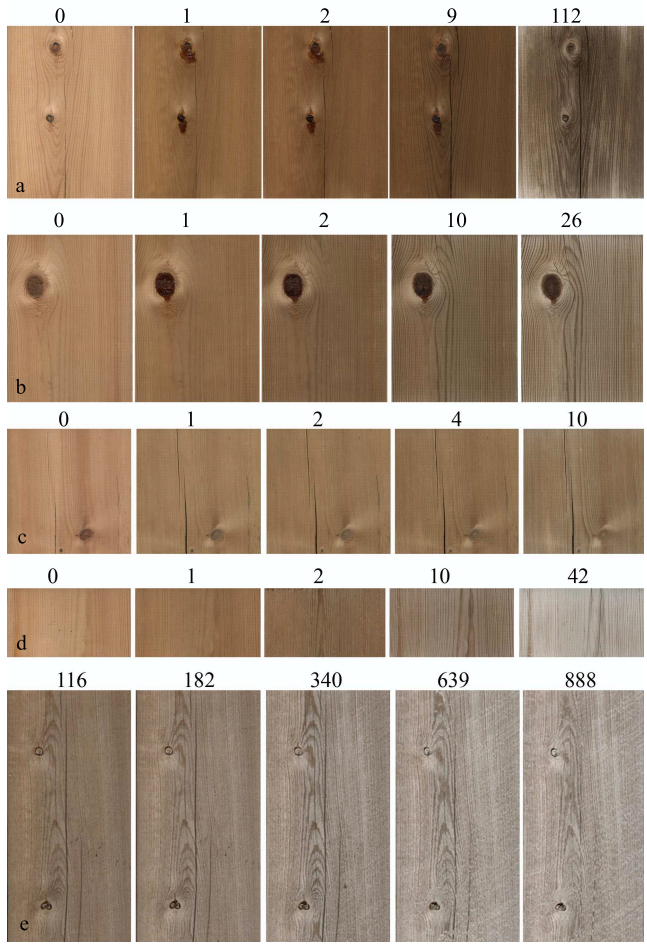


Figure 6.5.: Scanned images from Scots Pine heartwood (Material 3) after laboratory weathering, Run 1-a, Run 2-b, Run 3-c, Run 4-d, RCC-e. Numbers on top indicate exposure time in days.

depending on the weathering cycle. However common to all materials is an increase in lightness values for RCC exposure that does not conform to the other weathering cycles conducted in the ASS.

### 6.2.2. Weathering cycle

As shown in Table 6.2 the sum of the climatic strains per 24 hours is similar for run 1 and run 2. However, for none of the tested materials the color response was similar for run 1 and 2, i.e. by splitting the 24 hour irradiation dose and the amount of water into smaller cycles has a major influence on the color response. From observations made from run 1 and several test runs, the reason for this is likely to be loss in moisture content due to prolonged exposure to high temperatures. Thus, run 2 was designed to section the same dose. In order to assess the influence of temperature in this experiment the temperature was lowered to 22° for run 3. For run 4 the radiation level was lowered by 50% with help of a filter, and the temperature was set back to 63 °C. Generally, the color response of the material showed that a lower temperature has a greater influence on the rate of color change than a lower radiation level, though both modifications reduce the rate of changes in color values.

## 6.3. Outdoor vs. laboratory exposure

Whether or not the accelerated laboratory testing reflects outdoor weathering can be seen by plotting results from laboratory exposure and outdoor exposure in the same graph, see Figure 6.7 [1]. Note, that in order to show those results, the values for run 3 have to be plotted in a different time scale. In general, color values follow the course of the outdoor exposures south in this graph. Taking into account that part of the chroma loss for a* and b* values is due to greying caused by mold growth, which is not present for in laboratory exposure, the color values fit rather well. However, a direct comparison of the color values for outdoor and acceler-

[1] The figure for Material 3 represents an example, observations apply to all materials where not stated differently

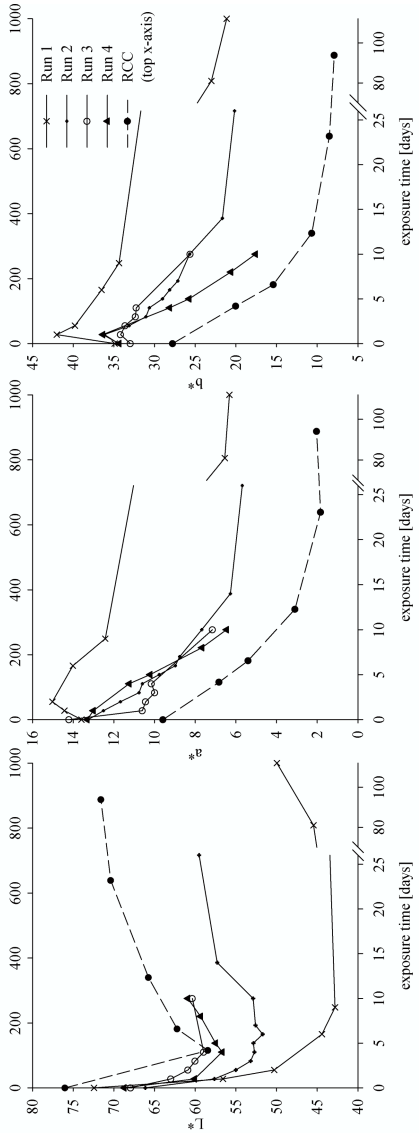


Figure 6.6.: Scots Pine heartwood (Material 3), color values (L, a and b) for laboratory exposure in the ASS

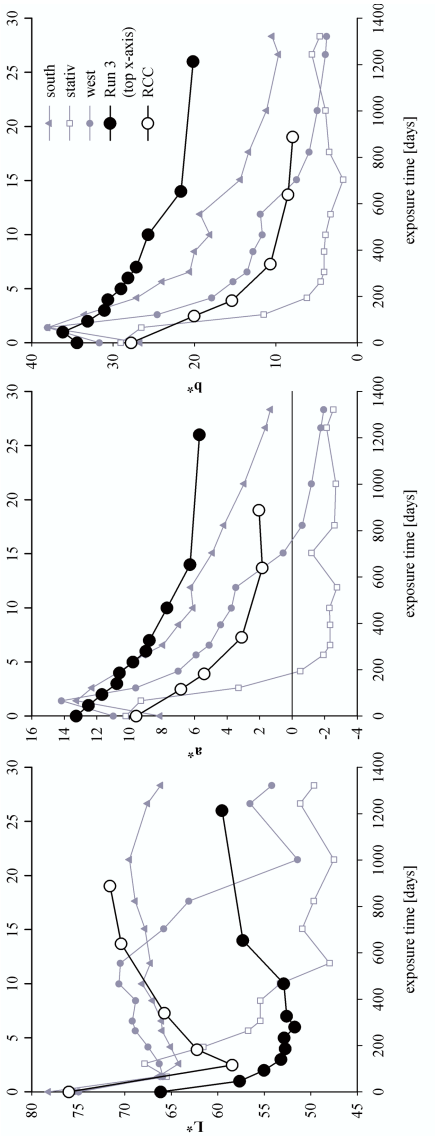


Figure 6.7.: Relation of Scots Pine heartwood (Material 3) color values for ASS laboratory run 3, RCC and outdoor exposure

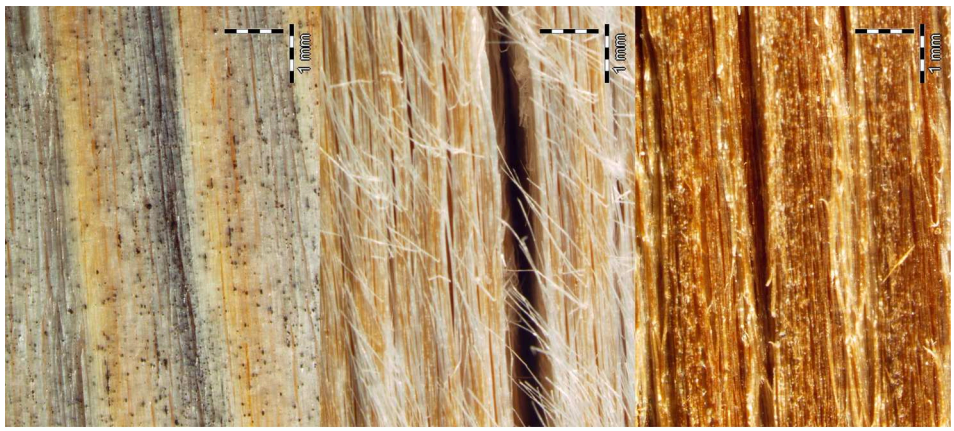


Figure 6.8.: Microscopic images of Pinus Silvestris (Material 1) after (a) 1244 days exposed to the east with vertically oriented annual rings, (b) 888 days of weathering in the RCC, and (c) 500 days of accelerated weathering in ASS (run 1).

ated laboratory weathering has to be seen critical. Due to experimental restrictions samples exposed in the lab could not be conditioned prior to color measurement, which might influence the color values significantly. The microscopic images of Norway spruce presented in Figure 6.8 confirm those findings. Surface mold growth dominates the appearance of outdoor weathered wood (a), while samples weathered in the RCC are characterized by loose fibres attached to the surface (b). (c) shows a sample weathered in the ASS; the significant differences in surface appearance are evident.

## 6.4. Dose-response relation

Assumably, the changes in any material property are related to the dosage of the relevant environmental factors, a so called dose-response relation or function. For many applications, especially for structural critical applications, the identification of those relations might be expedient. Furthermore, for accelerated test design the knowledge of these damage functions

is valuable. The identification of relevant environmental factors and the acquisition of relevant and reliable data are a complex task. In case of the weathering of wood, solar radiation and wind driven rain are assumed to be the two main driving factors for changes in appearance. Radiation and wind driven rain data over time are accumulative, while color differences $\Delta$E can roughly be characterized by an exponential decay function. As stated in Section 3.3.1, the processes related to e.g. temperature dependency of the chemical reactions involved in the photodegradation of wood are not fully understood. Spectral distribution of the solar radiation devices used in laboratory weathering and water additionally may have a major role. The complexity of the reactions and the materials might make a direct derivation of a dose-response function in this case impossible.

## 6.5. Acceleration factors

Acceleration factors may be calculated in order to relate accelerated weathering to the desired service life of a product [85, 86]. In the present study, acceleration factors for two exposure agents are calculated, i.e. UV radiation and temperature. Since temperature levels for the conducted accelerated weathering tests are significantly higher than estimated for outdoor weathering, they need to be considered. Input values for natural weathering are based on the EOTA Technical Report 010 [87], and represent average estimated values for certain regions.

A higher UV intensity [W/m$^2$] and total energy [kWh/m$^2$] in the laboratory weathering apparatus, results in a higher acceleration factor for the accelerated weathering. The UV acceleration factor $\mathrm{AF_{uv}}$ may be calculated as directly proportional to the ratio between the total UV energy in the laboratory weathering apparatus $\Phi_{lab}$ and the natural outdoor weathering $\Phi_{nat}$ for a given time period:

$$AF_{uv} = \Phi_{lab}/\Phi_{nat} \tag{6.1}$$

This is valid as long as one may assume that all the UV radiation contributes to initiate degradation reactions, in addition to an equal spectral

distribution for artificial and natural UV radiation, which naturally is never completely fulfilled.

Chemical degradation processes increase exponentially with increasing temperature (Arrhenius equation) [86]:

$$k = C\, e^{-E_a/(RT)} \tag{6.2}$$

where $k$ [1/s] indicates the reaction rate for the chosen reaction, $C$ [1/s] is a pre-exponential factor, $\mathrm{E_a}$ [J/(mol K)] is the activation energy, R [J/mol] is the gas constant, and T [K] is the temperature. A temperature acceleration factor $\mathrm{AF_{temp}}$ may then be calculated as the ratio between the reaction rate in the laboratory weathering apparatus $\mathrm{k_{lab}}$ and the natural outdoor weathering $\mathrm{k_{nat}}$:

$$AF_{temp} = k_{lab}/k_{nat} = \frac{C_{lab}\, e^{-E_{a,lab}/(RT_{lab})}}{C_{nat}\, e^{-E_{a,nat}/(RT_{nat})}} \approx \frac{e^{-E_{a,lab}/(RT_{lab})}}{e^{-E_{a,nat}/(RT_{nat})}} \tag{6.3}$$

where $\mathrm{T_{lab}}$ and $\mathrm{T_{nat}}$ denote the temperature in laboratory weathering apparatus and the natural outdoor weathering, respectively. Assuming that the pre-exponential factor C is temperature independent gives $C_{lab} \approx C_{nat}$. Furthermore, it is assumed that the activation energy E is temperature independent, e.g. set to $\mathrm{E_{lab}}$=$\mathrm{E_{nat}}$ = 70 kJ/mol.

In a simplified model one may assume that the total acceleration factor $\mathrm{AF_{tot}}$ equals the product of $\mathrm{AF_{uv}}$ and $\mathrm{AF_{temp}}$:

$$AF_{tot} = AF_{uv} \cdot AF_{temp} \tag{6.4}$$

Calculated total acceleration factors $\mathrm{AF_{tot}}$ are given in Table A.10, ranging from about 5 to 250 for the given input parameters. The calculations may most easily be performed based on 24 h cycles. Note that these values are based on temperature acceleration factors corrected (reduced) for the colder ($T_{lab} \leq T_{nat}$) time periods where the prevailing temperature is lower that the reference temperature of 10 °C. In addition, $\mathrm{T_{nat}}$ = 22°Cand $\Phi_{nat} = 0.67 \cdot 5\ GJ/m^2 = 3.35\ GJ/m^2$ have been chosen as the natural

Table 6.2.: Test conditions for laboratory weathering, total strains, and calculated acceleration factors.

| Run | Exposure time [days] | Irradiation [kWh/m$^2$] per 24 hrs | Water [l/(m$^2$)] per 24 hrs | Temperature[b] [℃] | RH[b] [%] | $AF_{tot}$ [-] |
|---|---|---|---|---|---|---|
| 1 | 112 | 24 | 408 | 63 | 50 | 250 |
| 2 | 26 | 24 | 408 | 63 | 50 | 250 |
| 3 | 10 | 24 | 408 | 22 | 50 | 8 |
| 4 | 42 | 12 | 408 | 63 | 50 | 130 |
| RCC | 888 | 1.5 [c]<br>0.0924 [d] | 75 | 63 | - | 5 |

[a] accumulated entire exposure time [b] during solar radiation [c] calculated solar radiation
[d] measured UV radiation

outdoor weathering temperature and the annual solar radiation reference levels respectively (borderline between moderate and severe climate). The assumptions made for the above calculations are based on values given in [87]. These calculations are of course a strong simplification. Other climate factors as mentioned above, e.g. water, will influence $AF_{tot}$. The introduced simplified model may be applied for mutual comparisons for accelerated climate weathering in the laboratory. Nevertheless, the comparison to outdoor weather depends strongly on the chosen input values to the calculations. Whilst the temperature level for laboratory weathering is assured, temperatures for outdoor weathering are subject to great variations, both on a daily (day-night) and a seasonal level (summer-winter). The results from temperature acceleration factors calculations strongly dependent upon the chosen reference level, i.e. the natural outdoor weathering comparison exposure level $T_{nat}$. The reaction rates of chemical reactions increase exponentially with increasing temperature, following the *Arrhenius* equation (see Equation 6.2). Thus, periods of higher temperatures contribute significantly more to the reaction rate and acceleration factor of the respective chemical reaction than periods with lower temperatures.

Hence, in order to determine the real $AF_{temp}$ and thereby $AF_{tot}$ it is not recommended to base calculations upon annual or daily values for $T_{nat}$ ($k_{nat}$). On the contrary, calculations should be performed using short time intervals which hence are integrated. To determine the effective tem-

Table 6.3.: Solar radiation values and calculated acceleration factors for the present study compared to laboratory run 3.

| Exposure | Radiation [kWh/m$^2$][a] | $AF_{temp}$ [-] | $AF_{uv}$ [-] | $AF_{tot}$ [-] |
|---|---|---|---|---|
| horizontal | 2.2 | 3.3 | 110 | 367 |
| north | 0.7 | 3.3 | 322 | 1073 |
| south | 2.1 | 3.3 | 116 | 385 |
| east | 1.6 | 3.3 | 154 | 514 |
| west | 1.6 | 3.3 | 150 | 501 |
| rack | 2.9 | 3.3 | 83 | 278 |

[a] average daily radiation dose (based on Table 4.3)

perature to be used in a simplified calculation of a real acceleration factor, temperature values measured on site by *DNMI* were assessed for the exposure period from February 2005 until August 2008. The determination of the effective temperature $T_{eff}$ is based on the following equation:

$$e^{-E_a/(R\,T_{eff})} = \frac{1}{(t_{end} - t_0)} \sum_{t_i=t_0}^{t_{end}} e^{-E_a/(R\,T_{(t_i)})} \Delta t_i \qquad (6.5)$$

where $\Delta\, t = t_{i+1} - t_i$ is the chosen time step, $E_a$ is the activation energy, e.g. 70 [kJ/mol], and R is the gas constant. The results from this calculation depend on the time step $\Delta$t chosen. For hourly values $T_{eff}$ corresponds to 10.1 ℃, which leads to a calculated acceleration factor of $AF_{temp}$=3.3 for laboratory run 3. Note that the chosen temperatures are average hourly air temperatures, whereas temperatures close to the surface of the different walls might vary significantly. The strong dependence of temperature acceleration factors on $T_{nat}$ is also illustrated by the graphical plots in Figure 6.9. An extensive assessment of different acceleration models may be found in [88]. Radiation acceleration is presumed to be linear. Table 6.3 presents radiation values from the test site adapted from *SoDa* and the corresponding agglomeration factors $AF_{uv}$ and $AF_{tot}$. $AF_{temp}$=3.3 is common to all exposure directions, and radiation for laboratory exposure is chosen to be 24kWh/m$^2$, corresponding to run 3. By plotting color response ($\Delta$E) against exposure time for both laboratory

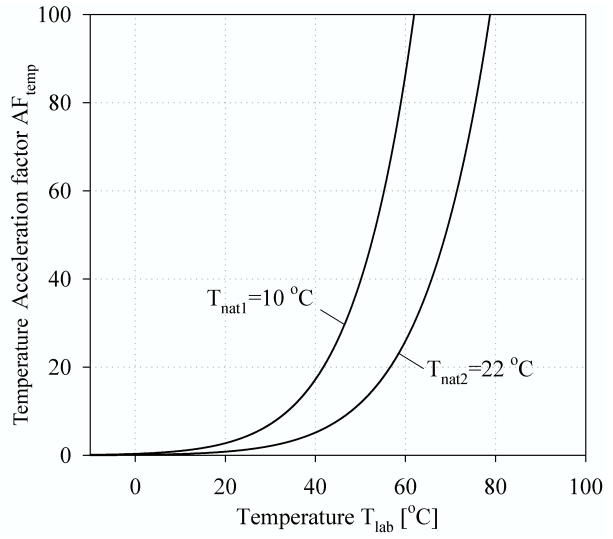


Figure 6.9.: Temperature acceleration factor $AF_{temp}$ dependence on temperature $T_{lab}$ for two different natural weathering temperatures $T_{nat}$.

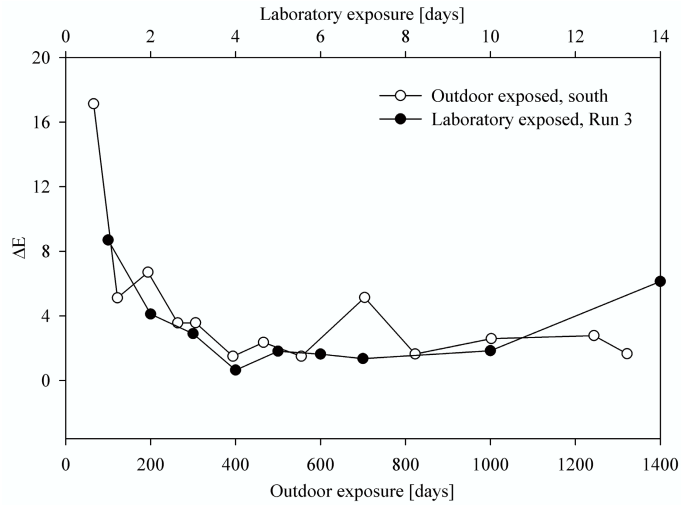


Figure 6.10.: Assessment of acceleration factor for ΔE for laboratory weathering run 3 and outdoor exposed sample (south) for Scots Pine (Material 3).

and outdoor weathering it was found that the acceleration factor for the example case in Figure 6.10 corresponds approximately to $AF_{tot}$=100. Table 6.3 denotes the acceleration factor to $AF_{tot}$=385 for south exposed samples vs. laboratory run 3. This result indicates that a simplified calculation of acceleration factors is precarious, since the results are very sensitive to the chosen temperature $T_{eff}$.

## 6.6. Surface growth

One major difference between outdoor and laboratory exposure are biological components, more precisely fungal spores that result in an additional dark coloring of untreated wood surfaces. At the end of the exposure time, i.e. after three and a half years, samples of fungal organisms on the sample surfaces were taken with a tape lift. Of 227 samples exposed at the outdoor test site, 27 were chosen for analysis: One of each Scots Pine samples (Material 3) from each exposure direction (both vertical and hor-

izontal annual rings), one sample of each of the nine materials on the west exposed side, one Kebony Furu (Material 6), and one Scots Pine impregnated sample (Material 9) from all exposure directions. Fungal species on the tape were identified using a microscope using a evaluation scale from 1 to 4 :*1*) no mold growth, *2*) sparse growth (up to 10% of the surface), *3*) moderate growth (between 10% and 70% of the surface), and *4*) rich growth (over 70% of the surface). Table 6.4 gives an overview of the results from the mold growth analysis. Where nothing else is indicated the detected fungal species is *Aureobasidium pullulans*, a common fungus that colonizes organic materials [37, 46]. All outdoor exposed samples showed fungal growth of varying amount. Growth patterns could not be distinguished for the different samples with this test method. Fungal hyphae grow in the wood cells longitudinal direction and in clots on the surface. Assessment of the results in detail:

1. **Exposure direction** Tendencies of strongest mold growth on west exposed samples and least growth on south exposed samples. No clear difference between east and north exposed samples could be found. Samples exposed on the rack facing 30° south showed a larger amount of growth than the ones from the south wall, similar to the ones on the west wall.

2. **Materials** No clear difference could be found between the different samples from the west wall.

3. **Treatment** No clear differences could be found between untreated and impregnated materials. However, there was a tendency to less mold growth on the Keboby SYP and pressure treated samples exposed on the south, east and north wall.

4. **Laboratory** There was no surface growth on the samples taken from the RCC. However, *Paecilomyces variotii* was found on the sample weathered in the ASS, which is a common contaminant found in laboratories.

5. **Annual rings** For west exposed samples, no difference could be found between vertically and horizontally exposed annual rings. For north and east exposed samples strongest growth was observed for horizontally exposed annual rings. For south exposed samples, strongest growth

Table 6.4.: Results for mold growth analysis from outdoor weathering

| Sample no. | Material | Exposure | Annual rings | Mold growth |
|---|---|---|---|---|
| M3e5 | Scots Pine | east | v | 3 |
| M3e8 | Scots Pine | east | h | 4 |
| M7e5 | Kebony SYP | east | v | 2 |
| M9e5 | Pressure treated | east | v | 2 |
| M3n1 | Scots Pine | north | v | 3 |
| M7n1 | Kebony SYP | north | v | 3 |
| M9n1 | Pressure treated | north | v | 2 |
| M3n2 | Scots Pine | north | h | 4 |
| M1w5 | Norway Spruce | west | v | 4 |
| M2w5 | Norway Spruce | west | v | 4 |
| M3w5 | Scots Pine | west | v | 4 |
| M3w8 | Scots Pine | west | h | 4 |
| M4w5 | Aspen | west | v | 4 |
| M5w5 | Larch | west | v | 4 |
| M6w5 | Keborny Furu | west | v | 4 |
| M7w5 | Kebony SYP | west | v | 4 |
| M8w5 | Royal impregnated | west | v | 3 |
| M9w5 | Pressure treated | west | v | 4 |
| M3s1 | Scots Pine | south | v | 3 |
| M3s3 | Scots Pine | south | h | 2 |
| M7s1 | Kebony SYP | south | v | 3 |
| M9s1 | Pressure treated | south | v | 2 |
| M9st1 | Pressure treated | rack | v | 4[a] |
| Mst1 | Scots Pine | rack | v | 4 |
| M3k | Scots Pine | RCC | v | 1 |
| M3a | Scots Pine | ASS | v | 3[b] |

[a] additionally sparse growth of *Cladosporium*, ass. deposited.

[b] spare/moderate growth of *Paecilomyces variotti*, common contaminant in laboratories.


Figure 6.11.: Norway Spruce (Material 2), annual rings horizontally (a) and vertically (b) oriented , east exposure 1322 days, magnification 10.

was found for vertically exposed annual rings of the Scots Pine samples.

In general, the number of samples analyzed was too little to draw further conclusions about the different parameters, and has to be seen as a first indication on what results can be expected from this analysis. However, with respect to the subject of vertically vs. horizontally mounted annual rings, generally more mold growth was found on the samples mounted with horizontally oriented annual rings by visual inspection of samples of the same material, as illustrated in Figure 6.11. As shown in Table 6.5 lightness values for samples that are mounted with vertically oriented annual rings differ considerably from the ones mounted with horizontally oriented annual rings. Most of the samples mounted with horizontally mounted annual rings show a lower final lightness value, i.e. these samples are darker than the ones mounted with vertically oriented annual rings. This observation suggests a higher mold growth rate for samples mounted with horizontally oriented annual rings. The analysis of the tape lift from fungal samples taken from Pine heartwood somewhat confirms that observation: For all exposure directions except west, there is more mold growth to be observed on the samples exposed with horizontally oriented annual rings.

Table 6.5.: Average lightness values of all samples after exposure for 1322 days for vertically and horizontally oriented annual rings.

| Material | 1 | 2 | 3 | 4 | 5 | 6 | 7 | 8 | 9 |
|---|---|---|---|---|---|---|---|---|---|
| North | | | | | | | | | |
| Vertical | 60.5 | 65.6 | 66.3 | 55.3 | 55.2 | 39.9 | 44.7 | 53.3 | 60.2 |
| Horizontal | 47.3 | 50.9 | 56.3 | 51.3 | 40.9 | 36.5 | 34.3 | 47.6 | 51.1 |
| South | | | | | | | | | |
| Vertical | 57.7 | 66.2 | 68.5 | 57.7 | 63.9 | 40.8 | 30.8 | 56.9 | 53.5 |
| Horizontal | 56.5 | 56.7 | 57.8 | 43.1 | 42.5 | 30.1 | 30.5 | 52.8 | 46.7 |
| East | | | | | | | | | |
| Vertical | 52.0 | 64.6 | 65.5 | 63.4 | 49.4 | 35.8 | 28.5 | 54.6 | 51.4 |
| Horizontal | 43.3 | 43.3 | 46.4 | 41.6 | 40.6 | 25.4 | 29.7 | 45.1 | 52.0 |
| West | | | | | | | | | |
| Vertical | 53.7 | 54.3 | 53.5 | 50.6 | 52.5 | 37.5 | 31.4 | 58.0 | 48.1 |
| Horizontal | 46.2 | 46,8 | 45,6 | 48,3 | 39,9 | 26,3 | 19,2 | 49,6 | 44,9 |

Figure 6.11 a shows a microscope picture of an east exposed sample which was mounted with horizontally oriented annual rings, and Figure 6.11 b shows the respective picture for vertically oriented annual rings. There is a considerable difference in the amount of mold growth for the two samples. One possible reason ist that horizontally oriented annual rings offer an increased surface area with trapped moisture where biological material is more likely to deposit. This result could be observed for all materials, and could be verified by color analysis of all samples after exposure.

# 7. Conclusions

## 7.1. Main findings

Color alterations of untreated wood have been assessed by means of color measurements. Differences in color development depending on exposure directions have been determined and assessed. These differences are mainly induced by different doses of solar radiation and wind-driven rain. However, no quantitative relation between these two climatic strains and the color alterations could be established.

A method for determination of color values using a scanner has been developed. This method has proven to be an efficient supplement for color measurements conducted by a colorimeter. Larger samples, but also a greater amount of samples may be processed in a reasonable amount of time particularly by the automation of image processing. Color variations within samples exposed to the same strains proved to be minor, despite the fact that no clear wood samples were used.

The results from this study could be used in the development of a modeling tool for color development of outdoor exposed untreated wooden materials. However, other geometrical factors , e.g. shading by roof overhang, cladding board design, inclination of the surface, and facade openings as windows and doors, have to be taken into consideration.

Annual ring orientation (vertical or horizontal) has a significant influence on the color changes after three years of exposure. Microscopy confirmed that on samples with horizontally mounted annual rings, there was a higher density of mold growth to be found. This is most likely due to an increased surface caused by horizontal cracks and eroded early wood. Here, dust and dirt can gather easily, forming a medium for mold to grow on. A higher density of mold growth appearing as grey dots on the surface

results mainly in a darker color, a lower value for Lightness.

Mold growth appears on all outdoor exposed samples investigated. There are some differences depending on the exposure direction of the sample: as expected most mold growth was observed on samples exposed facing west and on the rack, least on samples exposed facing south. The reason is most likely, in case of south exposure, high amounts of solar radiation (high temperatures). In case of north exposed samples, the combination low solar radiation levels and reduced access to moisture (wind driven rain) explains the lower amounts of mold growth. However, a more extensive analysis of all samples would be required to draw further conclusions.

Several accelerated weathering tests were performed. None could reproduce the surface appearance of the samples exposed to natural weathering. Though, the rotating climate chamber (RCC) seems to be the one that strains the samples in a similar way. However, cellulose fibres remain on the surface whereas they are eroded by wind and wind driven rain in the field. Surface mold growth is difficult to reproduce in accelerated weathering test which combine several climatic strains. This is a major drawback, which denotes a significant difference for the measured color values for outdoor and accelerated weathering. None of the weathering cycles found in literature could be confirmed to be even close to appropriate or realistic; always considering that the test material was wood. Based on the results of the present study, the weathering cycle that gives results closest to those from outdoor weathering was the one with the lowest radiation level and lowest temperatures.

When using laboratory weathering it is important to evaluate the outcome of high acceleration factors versus realistic results. Though a high acceleration factor might be desirable due to time restrictions for laboratory testing, results might be worthless because of chemical reactions caused by high radiation levels or temperatures.

Service life considerations are often based on ascertained boundary conditions, end of service life or a certain material property that has to fulfill certain conditions. For many building materials and parts, the aesthetic condition is the determining function; obsolescence, the replacement of components before functional failure (e.g. due to changes in fashion) is

the foremost reason for replacement or maintenance. In this case, the definition of the *end of service life* is subjective. Hence, a quantitative determination of limit-state values for untreated wood surfaces in terms of the aesthetic appearance is difficult. Absolute color changes of an untreated wooden cladding are not decisive, especially since the *natural* appearance is intended. However, relative color differences within one particular part or building component are most likely not intended. An individual definition of a limit state value for color variations is a possible approach to make subjective performance requirements accessible to objective assessment.

Dose-response functions for color differences due to weathering could not be established. A greater amount of input data would be necessary. However, a dose-response relationship is valuable for the design of accelerated weathering tests. The knowledge of dose-response functions, hence the exact degradation mechanism and all relevant degradation agents, and their interaction, allows to recreate and accelerate weathering of a material. However, due to the complexity of many materials, there have not been established many dose-response relationships. The calculation of acceleration factors for laboratory weathering is only possible, if degradation processes are understood completely. Rough estimations and calculations of radiation and temperature acceleration factors, have shown that the temperature reference level for outdoor exposure has a major impact on the result of the calculation. Nevertheless, regardless of absolute acceleration factor determinations, these evaluations may be very useful for comparing various materials and accelerated weathering methods.

Through this research project, it has become evident that service life prediction of untreated non-structural wooden building components is a complex task. The methodology suggests a bottom-up approach, i.e. from the determination of dose-response functions (chemical reactions) to material degradation (on a microscopic level) and further to the definition of limit states for building parts and components. For an application in a building context this methodology seems disproportionately cumbersome. Therefore, the focus should be on the development of a more holistic approach (top-down) by breaking buildings down into components (e.g. facade, cladding). The development of tailor-made methods taking into account all aspects of the performance of a building component (e.g. function,

aesthetics, and economics) could be a way of getting hold of the task of service life prediction and maintenance planning in the light of sustainable development.

## 7.2. Future work

Service life prediction of materials and building parts where the limit-state is related to the aesthetic appearance has proven to be a complex task. In order to develop a holistic assessment tool for this type of application additional important factors should be taken into account: Firstly, the design of a facade assembly including *a)* inclined surfaces (other than horizontal and vertical), *b)* facade openings as windows and doors, and *c)* shaded parts as roof overhangs and balconies. Also the work execution and maintenance level should be assessed in a larger context. In the course of this, the data collection should be extended with respect to different climate conditions. Further research may also involve the modeling of color changes and the extension of the study to other materials.

# 8. Introduction to papers

## 8.1. Paper 1

### Influence of material quality and climate exposure on moisture condition of a wooden facade[1]

P. Lauter, B. Time, P.J. Hovde, K. Nore

presented at the *10th International Conference on Durability of Building Materials and Components*, Lyon, France 2005

This paper analyzes data collected in the framework of the research programme *Climate 2000*, conducted by *SINTEF Building and Infrastructure* initiated in 2003. The objective of this investigation was to study if and how different material qualities influence the moisture conditions of the cladding.

## 8.2. Paper 2

### A method to assess the effects of climate and material parameters on the moisture condition of a wooden facade[2]

P. Lauter, B. Time

presented at the *Nordic Building Physics Symposium in Reykjavik*, Island, 2005

This paper introduces a method for the assessment of climatic conditions and material parameters. Data from *Climate 2000* was used to evaluate the parameters influencing on moisture condition of a wooden cladding. Local location, surface treatment, material quality, and micro-location were assessed.

[1] published under maiden name Lauter
[2] published under maiden name Lauter

## 8.3. Paper 3

### Color changes in wood boards during weathering

P. Rüther

presented at the *World Timber Engineering Conference* in Portland, U.S.A., 2006

This paper presents first results from the outdoor and laboratory weathering experiments conducted.

## 8.4. Paper 4

### Color changes of wood and wood based materials due to natural and artificial weathering

P. Rüther, B.P. Jelle

Submitted for publication, currently under review at *Wood Material Science and Engineering*

This paper presents results from the outdoor and laboratory exposure experiments conducted. Differences between different exposure directions, primary solar radiation and wind driven rain are investigated. The relation of outdoor vs. laboratory weathering is discussed and the calculation of acceleration factors is been focused on.

# 9. Scientific publications

## 9.1. Paper 1

**Influence of material quality and climate exposure on moisture condition of a wooden facade**

P. Lauter, B. Time, P.J. Hovde, K. Nore

presented at the 9th International Conference on the Durability of Building Materials and Components, Lyon, France, 2005

*10DBMC International Conference on Durability of Building Materials and Components*
*LYON [France] 17-20 April 2005*

# Influence of material quality and climate exposure on moisture condition of a wooden façade

**P. Lauter**[1], B. Time[2], P.J. Hovde[1], K. Nore[1,2]

[1]Norwegian University of Science and Technology NTNU
Høgskoleringen 7A, 7491 Trondheim, Norway
petra.lauter@ntnu.no
[2]Norwegian Building Research Institute NBI
Høgskoleringen 7B, 7491 Trondheim
TT02-129

**ABSTRACT**

In the framework of the research programme *Climate 2000*, the Norwegian Building Research Institute is running field exposure tests of claddings on an experimental building in Trondheim, Norway. The eastern and western façades are divided into fourteen fields respectively, using different material qualities, painting systems and assemblies concerning building physics. The building is equipped with temperature and moisture measuring devices, continuously logging data since January 2004.
Data gathered from January 1, 2004 until July 31, 2004 are analysed and special attention is directed to the fields of the façade containing untreated wood. These fields contain fast and slow grown Norway spruce (*picea abies*) respectively, and the objective of this investigation is to study how different material qualities influence the moisture conditions of the cladding. In addition to this, the measured data were compared to data logged at the meteorological station located on the same site, in order to see if and how the moisture data mirror the climatic conditions.
At this point of time no clear conclusion can be drawn regarding the different moisture contents of the two material qualities. Though, the moisture content of the fast grown material seems to vary more than for the slow grown one. Crack formation due to greater variations in moisture content can be interpreted as a first sign of differences in the moisture condition of the two material qualities. This can lead to increased moisture absorption by and by.
Additionally, it was investigated if and to what extent the measured moisture content reflects meteorological parameters. It appears that by adding a time delay of 12 hours the goodness of fit, namely the coefficient of determination, can be improved significantly from an average of 0.5 to an average of 0.97. That means that 97 % of the measured values of moisture content can be explained by the chosen meteorological parameters.
The results provide useful information considering further investigation regarding the durability of wood materials exposed to climatic strains.

**KEYWORDS**

Durability, Service Life, Wood, Material Properties, Climate Exposure

*10DBMC International Conference on Durability of Building Materials and Components*
*LYON [France] 17-20 April 2005*

## 1 INTRODUCTION

As the concern and interest in sustainable materials and buildings increase, it is significant to acquire knowledge for innovative and enhanced use of wood as a renewable resource and sustainable material. A crucial issue for the application of wood as a sustainable material is the durability and service life. The standard ISO 15686 – *Buildings and constructed assets, Service life planning* [ISO 15686, 2000] contains general principles for the prediction of service life and maintenance planning. The standard contains the so-called factor method to determine the influence of different stresses on the service life of a building, material or component. The service life estimation is based on a Reference Service Life (RSL) and seven factors regarding the quality of components, the design level, the work execution level, the indoor environment, the outdoor environment, the in-use conditions and the maintenance level. Apart from determining the reference service life it is of interest to explore the factors itself. The present study investigates the factors quality of components and outdoor climate.
At present studies carried out by Siemes [2003] or Moser [2002] focus on the further development of theoretical models presented in ISO 15686 [2000 & 2001]. Another important issue is the characterisation, mapping and modelling of the environment. Stresses and strains caused by weather as for example wind, rain and radiation are the main reasons for degradation of all kinds of building materials in outdoor use [Haagenrud [1997] and Högberg [2002]]. In terms of wood used as a building material Scheffer [1971] developed already in 1971 a map showing the risk of fungal decay for wood based on meteorological data. Newer research is directed towards the development of a prediction model for wood decay not only taking into account the environmental factors but also the design and shape of a building or object [Foliente et al. [2002]].
As a part of the ongoing NBI (Norwegian Building Research Institute) programme *Climate 2000 – Building constructions in a more severe climate* [Lisø et al. [2002]], an experimental investigation of wooden cladding design has been set up at a test building. The overall aim of the investigation is a better understanding of the connection between macro and micro climate conditions, the implications for the building stock in general and for wooden façades in particular.
The present study focuses primarily on investigations regarding the material quality of a untreated wooden façade and secondly on the characterisation of the climatic strains it is exposed to.

## 2 MATERIALS AND METHODS

### 2.1 Test Site

The test site comprising the experimental building and a meteorological station (property of *The Norwegian Meteorological Institute* (DNMI)) is owned by the *Norwegian University of Science and Technology* (NTNU) and the *Norwegian Building Research Institute* (NBI). The test site is located in Trondheim, Norway (longitude 10°27’14’’, latitude 69°24’40’’, 129 m above sea level). Located in an open field, no surrounding buildings are likely to have an influence on the measurements.

The experimental building consists of a rectangular structure, the minor walls oriented towards south and north respectively so that the major walls are exposed to the east and west respectively. Each of the major walls is divided into fourteen fields, each of them 585 mm wide and 3200 mm high, each consisting of 27 horizontal boards.
Data are logged continuously since January 1, 2004, logging one value an hour. The present study considers data logged from January 1, 2004 until July 31, 2004.

*10DBMC International Conference on Durability of Building Materials and Components*
*LYON [France] 17-20 April 2005*

### 2.2 Design

The present study is focused on two fields containing material left untreated i.e. without any painting, on the western side of the experimental house. Each board is 585 mm long, 142 mm high and 19 mm thick, moulded on both the upper and the lower edge to achieve a plane surface on the back of the cladding. Both inner and outer side are left rough sawn. Between the back of the cladding and the wind barrier a 23 mm gap guarantees the ventilation of the cladding boards. Furthermore, the gap serves the desiccation of the claddings' reverse side and the equalisation the pressure on the façade.

### 2.3 Materials

Norway Spruce (*picea abies*) in two different material qualities is used for all fields, slow grown material with an average density of 687 kg/m$^3$ and fast grown material with an average density of 574 kg/m$^3$. The following Table 1 lists the accurate values for the instrumented boards of the investigated fields.

| | | *Density [kg/m$^3$]* | *Moisture content [weight %]* |
|---|---|---|---|
| 1 | fguMt | 565.3 | 18.6 |
| 2 | fguMb | 592.7 | 18.8 |
| 3 | sguMt | 631.5 | 18.0 |
| 4 | sguMb | 630.3 | 15.9 |

see Figure 1 or Table 3 for abbreviations

**Table 1 Density and initial moisture content of the instrumented boards**

### 2.4 Measurement Devices

Each field is instrumented with two temperature measuring devices and two moisture measuring devices respectively, located 550 mm from the top edge of the field, and 875 mm above the lower edge of the field, as illustrated in Figure 1.

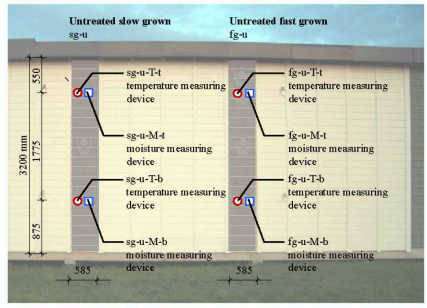


**Figure 1 Instrumentation and location of measuring devices**

*10DBMC International Conference on Durability of Building Materials and Components*
*LYON [France] 17-20 April 2005*

The measuring device for the temperature consists of a type T thermocouple and a compensation cable, measuring the temperature at the back of the cladding. The maximum measuring range is -270 °C to 400 °C corresponding to a signal between 0 mV and 21 mV. The tolerance in the used area between -59 °C and 93 °C constitutes ± 1.1 °C.
The moisture content of the boards is measured using the regular impedance; the electrical resistance between two steel nails located 25 mm apart from each other. The two steel nails used for the measuring of the moisture content penetrated the whole cross section from the back ending 3 mm behind the surface of the board.

## 3 RESULTS AND DISCUSSION

### 3.1 Material quality

Data were analysed to detect differences in moisture conditions caused by material quality and the location of the measuring device in the field. The different data sets were compared and the mean monthly values and the respective standard deviation were calculated. Table 2 lists the monthly mean values and the respective standard deviations for the moisture content of the two untreated fields.

| | | | *Jan [%]* | *Feb [%]* | *Mar [%]* | *Apr [%]* | *May [%]* | *Jun [%]* | *Jul [%]* | *Mean [%]* |
|---|---|---|---|---|---|---|---|---|---|---|
| 1 | fguMt | Mean | 19.5 | 21.0 | 17.3 | 15.5 | 15.1 | 14.5 | 14.5 | **16.8** |
| | | StDev | 1.05 | 1.48 | 2.21 | 2.18 | 2.85 | 2.31 | 1.24 | **1.90** |
| 2 | fguMb | Mean | 20.1 | 21.2 | 17.5 | 15.5 | 14.8 | 14.1 | 14.3 | **16.8** |
| | | StDev | 1.20 | 1.30 | 2.20 | 1.90 | 2.30 | 1.80 | 1.10 | **1.70** |
| 3 | sguMt | Mean | 19.9 | 20.8 | 17.4 | 15.5 | 14.7 | 14.2 | 14.4 | **16.7** |
| | | StDev | 1.06 | 1.13 | 1.95 | 1.60 | 1.92 | 1.62 | 0.96 | **1.46** |
| 4 | sguMb | Mean | 21.4 | 22.4 | 18.1 | 16.0 | 15.5 | 14.8 | 15.0 | **17.6** |
| | | StDev | 1.40 | 1.40 | 2.20 | 1.70 | 2.20 | 1.60 | 1.00 | **1.60** |

1: fast grown, untreated, top; 2: fast grown, untreated, bottom; 3: slow grown, untreated, top; 4: slow grown, untreated, bottom

**Table 2 Mean monthly values and respective standard deviations of the moisture content of the untreated fields**

The fast grown material (fgu) had an average moisture content of 16.8 % at both the measuring points on the top and bottom. Here, the respective slow grown material (sgu) had an average moisture content of 16.7 % and 17.6 % respectively. In this case, the standard deviation is a measure of the variation of the moisture content. However, the fast grown material is the one with greater variation in moisture content, namely 1.90 % at the top and 1.70 % at the bottom measuring point, compared to 1.46 % and 1.60 % for the slow grown material respectively.

Though, the fast grown material seems to have a certain tendency to vary more in moisture content than the slow grown one. The standard deviation of the moisture content is always greater for the fast grown

material than for the slow grown material. Likewise, the increase of the variation of the standard deviation is greater for the fast grown than for the slow grown material. However, since there are only seven values available these results are not conclusive, even though this trend shows expected results.

### 3.2 Climate Exposure

Another interesting aspect is to investigate if and to what extent the moisture conditions of the cladding mirror the weather conditions. Therefore, the measured data were compared to the weather data logged at the meteorological station located on the same site as the experimental building.
Regression analyses were used to review how the different weather parameters affect the moisture content of the cladding material. The meteorological station logs altogether 28 different meteorological parameters; temperature, relative humidity, wind speed and direction, precipitation, air pressure, and global and long wave radiation. Some of the parameters are measured several times, for example as maximum, minimum and average value.
The first regression analysis with a set of example data revealed the most important parameters used for further investigations, listed in Table 3. Radiation, global radiation as well as longwave radiation, is omitted in the regression analyses since they correlate highly with the air temperature.

| *Symbol* | *Meteorological parameter* | *Unit* |
|---|---|---|
| TTM | Temperature, average last hour | $^{o}$C |
| UUM | Relative humidity, average last hour | % |
| FM | Wind speed, average last hour | m/s |
| DM | Wind direction, belongs to FM | $^{o}$ (*) |
| RT | Number of minutes precipitation last hour | 0-60 min |

(*) 0$^{o}$ = north, 90$^{o}$ = east, 180$^{o}$ = south, 270$^{o}$ = west

**Table 3 Meteorological parameters, abbreviations and units**

The first regression analyses of the moisture content show comparatively poor coefficients of determination, ranging from 0.04 to 0.12. To improve the fit of the regression the moisture content values were compared to weather parameters delayed by 1 to 240 hours.
For each measuring device of the cladding 240 regression analyses – that equals a time delay of 10 days - were carried out. The objective was to detect if the particular weather parameter influenced the moisture content immediately and to determine the dimension of a possible time delay. First, regression analyses have been carried out for all data together, second for the data of each month separately and third for special weather conditions (such as periods with a lot of rain or cold or warm periods).
The coefficient of determination is used to estimate how well the measured data correspond to the weather parameters. First, regression analyses were carried out for each of the parameters listed in Table 3.

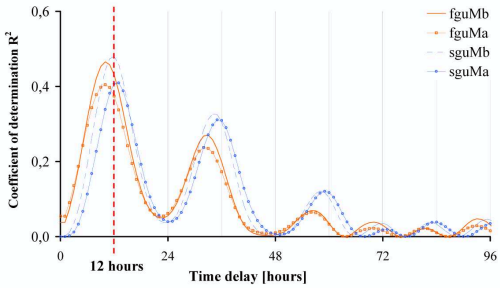


**Figure 2 Coefficient of determination for the regression analyses of moisture content and relative humidity for July 2004**

Figure 2 shows the connection between the coefficient of determination ($R^2$) and the time delay for all four measuring devices. The regression coefficient $R^2$ is frequently interpreted as the fraction of the variability explained by the independent variable, in this case the meteorological data. The measured moisture content for July 2004 is in this case compared to the relative humidity (*UUM*). It appears that the coefficient of determination reaches a maximum value at a time delay of approximately 12 hours. This way, $R^2$ can be increased from 0.06 to 0.47 for example for the measuring device *fguMb*.
All parameters show a significant increase in the values for $R^2$ from no time delay to a 12 hour time delay, though the maximum is not necessarily exactly at this point of time. In the case of no time delay the measured values are compared to the weather parameters logged at the same time, whereas a 12 hour time delay means that the measured values are compared to the weather parameter logged 12 hours earlier.
To investigate if and to what extent the goodness of fit increases by adding a time delay of 12 hours, multiple regression analyses where conducted with all relevant parameters, *TTM*, *UUM*, *FM*, *DM*, and *RT*.

| *time delay* | *fguMb* | *fguMt* | *sguMb* | *sguMt* |
|---|---|---|---|---|
| 0 | 0.513 | 0.496 | 0.499 | 0.495 |
| 12 | 0.975 | 0.937 | 0.984 | 1.000 |

see Table 2 for abbreviations

**Table 4 Improvement of the coefficient of determination by adding a 12 hour time delay**

It appears that the regression coefficient $R^2$ can be increased considerably; in average an improvement from 0.50 to up to 0.97 can be achieved, see Table 4.

The next steps will be first to investigate if the revealed assumption mentioned in 3.1 pursues for data measured after July 2004. Second it will be studied if the results found by regression analyses in 3.2 also apply for data measured in the autumn and winter 2004/2005 to focus on the further development of the characterisation of the micro climate.

## 4 CONCLUSION

The first investigated influence of the material quality and location of the measuring device on the moisture content of the untreated cladding boards did not reveal any significant difference between the four measuring devices. Usually, the fast grown material is supposed to absorb more moisture than the slow grown one, but this can not be affirmed at that point of time. However, the fast grown material appears to have a tendency to vary stronger in moisture content than the slow grown one. This can lead to greater dimensional changes in the cladding boards by and by, followed by the development of cracks. More moisture can be absorbed by these cracks, leading to increased moisture content of the fast grown material. Though, this is only a possible scenario of how the materials quality can gain importance by and by, at this early stage of the experiments such ageing effects can not be revealed clearly.

Second, the effects of different weather parameters on the moisture content of the cladding boards were investigated. The following four meteorological parameters seem to have an influence on the moisture content of the cladding boards: the average temperature *TTM*, the average relative humidity *UUM*, the number of minutes precipitation *RT*, the wind speed *FM*, and the wind direction *DM*. Regression analyses were carried out to reveal if the parameters influence the moisture content with a time delay. It appears that a time delay of 12 hours results in the best regression fit. The coefficient of determination can be increased from about 0.5 to 0.97 or even 1.0 in one case. Hence, the moisture content of the cladding can mostly be explained by the prevailing weather conditions.

The observation of the moisture content of different wooden materials over the years can provide valuable insight in ageing processes of wooden materials used above ground. Likewise, the characterisation of the micro climate results in better comprehension of the influence of weather parameters on the performance of the material. The advance of understanding the processes that influence the performance of building materials is an important step towards the operability of service life prediction models.

## ACKNOWLEDGEMENT

These experiments have been conducted within the ongoing NBI Research & Development Programme *Climate 2000 - Building constructions in a more severe climate* (2000 - 2006). The authors gratefully acknowledge the Norwegian Building Research Institute, the construction industry partners in the *Climate 2000* and the Research Council of Norway.

## REFERENCES

Foliente, G.C., Leichester, R.H. & Cole, I. 1999, 'Development of a reliability-based durability design method for timber construction', Proc. 8th International Conference on Durability of Building Materials and Components, National Research Council Canada, Ottawa, Canada.

Haagenrud, S.E. 1997, *Environmental Characterisation including Equipment for Monitoring*, CIB W80/RILEM 140-PSL, Sub Group 2 Report, Norwegian Institute for Air Research (Norsk institutt for luftforskning, NILU), Kjeller, Norway.

Högberg, A. 2002, *Microclimate Load: Transformed Weather Observations for Use in Design of Durable Buildings*, Department of Building Physics, Chalmers University of Technology, Gothenburg, Sweden.

ISO 15686-1, 2000, *Building and Construction assets – Service Life Planning; Part 1: General Principles*, The International Organization for Standardization, Geneva, Switzerland.

ISO 15686-2, 2001, *Building and Construction assets – Service Life Planning; Part 2: Service life Prediction Procedures* , The International Organization for Standardization, Geneva, Switzerland.

Lisø, K.R., et al. 2002, *Climate 2000 – Building Constructions in a more severe climate; Programme 2000-2006*, Programme Description, Norwegian Building Research Institute, Oslo, Norway

Moser, K. 2002, *Engineering Design Methods for Service Life Prediction*, CIB W80/RILEM 175, SLM: Service Life for Buildings and Components, Task Group Performance based Methods of Service Life Prediction, Swiss Federal Laboratories for Material Testing and Research, Dübendorf, Switzerland.

Siemes, T. 2003, *Prediction of service life of building materials and components, Service life methodologies*, CIB W80/RILEM 175, SLM: Service Life for Buildings and Components, Task Group Probabilistic methods, TNO Building and Construction Research, Delft, The Netherlands.

Scheffer, T.C. 1971, 'A Climate Index for Estimating Potential dor Decay in Wood Structures Above Ground', in *Forest Products Journal*, Forest Products Society, Madison, USA.
pp. 25-31

## 9.2. Paper 2

**A method to assess the effects of climate and material parameters on the moisture condition of a wooden facade**

P. Lauter, B. Time

presented at the Nordic Building Physics Symposium in Reykjavik, Island, 2005

# A method to assess the effects of climate and material parameters on the moisture conditions of a wooden façade

***Petra Lauter***
***Norwegian University of Science and Technology***
***petra.lauter@ntnu.no***

***Berit Time***
***Norwegian Building Research Institute***
***berit.time@byggforsk.no***

***KEYWORDS****: climate exposure, moisture content, wooden façade, material parameters, service life prediction*

***SUMMARY****: The present study introduces a method for the assessment of climatic conditions and material parameters as an example applied to a wooden façade in view of service life prediction. The moisture content is used as evaluation criteria since enduring high moisture content is known to be one main cause for fungal and insect attack. Data is used from the ongoing project Climate 2000 – Building constructions in a more severe climate, conducted by the Norwegian Building Research Institute (NBI), where among other things an experimental investigation of wooden cladding design has been set up at a test building. Four parameters are introduced to evaluate the significance of different material parameters: local location, surface treatment, material quality, and micro location. In each case boards differing in only one of the parameters are compared by calculating a nondimensional factor. Thus, the importance of the different factors can be evaluated simply by comparing them among each other. The results indicate that local location, i.e. orientation towards west or east, has the greatest influence. Next, the investigations on the parameter surface treatment, i.e. oil-based paint, water-based paint, and untreated surface, already reveal differences in moisture content for the different surface treatments. Finally, the parameters material quality and micro location seem to be of rather marginal significance at that time. The results confirm the assumptions about the influence of the different parameters on the moisture content. However, since data is so far only available for a period of one year, the further observation of the detected developments will be an interesting task. As well, advances in understanding the processes that affect the performance of building materials are important both to meet the requirements of sustainable constructions and the prediction of their service lives.*

## 1. Introduction

In order to meet future requirements regarding a sustainable development, it is significant to devise methods, tools, and solutions for the planning and design of buildings and constructions in order to increase their durability and the reliability of their performance [Lisø et.al. 2003]. Therefore, the careful selection of building materials and components is vital. Service life prediction or estimation is needed to meet these requirements. In the process of service life prediction data of among other things the prevailing exposure environment and the influence of different material parameters are required. *Service life* is defined as the 'period of time after installation during which a building or its parts meets or exceeds the performance requirements'. The estimated service life is defined as 'the service life that a building or parts of a building would be expected to have in a set of specific in-use conditions, calculated by adjusting the reference in-use conditions in terms of materials, design, environment, use, and maintenance' [ISO 15686]. Studies carried out by Siemes [2003] or Moser [2002] focus on the further development of theoretical models presented in ISO 15686 [2000 & 2001]. Another important issue in this context is the characterisation, mapping and modelling of the environment. Stress caused by weather as for example wind, rain, and radiation are the main reasons for degradation of all kinds of building materials in outdoor use [Haagenrud [1997] and Högberg [2002]]. In terms of wood used as a building material Scheffer [1971] developed a map showing the risk of fungal decay for wood based on meteorological data. A simplified method to determine the estimated service life is introduced in ISO 15686-1[2000], where seven factors affect the estimated service life, viz quality of components, design level, work execution level, indoor environment, outdoor environment, in-use conditions, and maintenance level. The investigation of the factors itself and their importance for the performance level are the primary intentions of the present study. At the same time, this implies a better understanding of the prevailing climate conditions, the implications for the building stock in general and wooden building envelopes in particular. This case investigates the influence of surface treatment, material quality, micro-, and local climate on the moisture

condition of a wooden façade. The moisture content of wood is presumed to be a predominant factor when considering its susceptibility to fungal attack. Wood kept at moisture content of 20% or less are not normally subject to fungal attack [Råknes, 1985]. Depending on its location and material parameters, the moisture content of wood is likely to differ. Therefore, it will be utilised in the present study as a criteria in order to assess the influence and importance of the different parameters.

## 2. Test design

### 2.1 Test site

The test site comprising the experimental building and a meteorological station (property of *The Norwegian Meteorological Institute* (DNMI)) is owned by the *Norwegian University of Science and Technology* (NTNU) and the *Norwegian Building Research Institute* (NBI). The test site is located in Trondheim, Norway (longitude 10°27'14'', latitude 69°24'40'', 129 m above sea level). Located in an open field, no surrounding buildings are likely to have an influence on the measurements.

The experimental building consists of a rectangular structure, the minor walls oriented towards south and north respectively so that the major walls are exposed to the east and west respectively. Each of the major walls is divided into fourteen fields, each of them 585 mm wide and 3200 mm high, each consisting of 27 horizontal boards. Data are logged continuously since January 1, 2004, logging one value an hour.

The present study considers data logged from January 1, 2004 until December 31, 2004.

### 2.2 Design

This study investigates the moisture content of board samples influenced by different experimental setups. The experimental setup consists basically of an experimental building where various material combinations of board samples are mounted. In principle, there are two different material qualities being exposed in two different orientations, such as east and west. The material used in this study is Norway Spruce (*Picea abies (L.) Karst.*) in two material qualities. The slow grown has an average dry density of 459 kg/m$^3$ and the fast grown 385 kg /m$^3$, respectively. In addition, two fields of each of the different qualities are treated with surface coating and one is left untreated. The surface treatments are on the one hand an oil-borne alkyd based paint (*Drygolin Extreme Oljemaling by Jotun A/S*) and on the other hand a water-borne alkyd-acrylate based paint (*Demidekk Optimal by Jotun A/S*).

Each board is 585 mm long, 142 mm high and 19 mm thick, moulded on both the upper and the lower edge to achieve a plane surface on the back of the cladding. Both inner and outer side are left rough sawn. Between the back of the cladding and the wind barrier a continuous 23 mm gap in connection with a 4 mm gap at inlet and outlet provides the ventilation of the cladding boards. For more detailed information see Nore et al. [2005]. The mounted board samples in all the different combinations used in this study are illustrated in Fig. 1. As an example the west side is shown. The given field numbers apply to the present study.

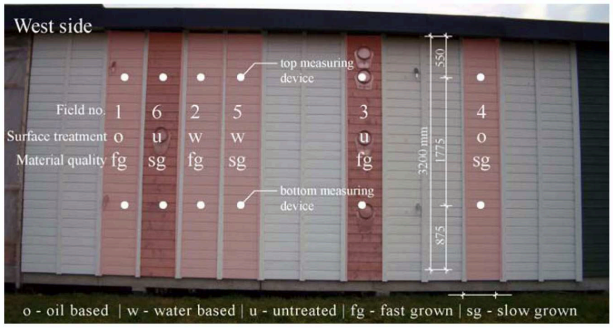


*FIG. 1: Picture of the west façade; investigated fields highlighted*

### 2.3 Measurement devices

Each board is instrumented with two temperature and two moisture measuring devices. One is located 550 mm from the roof and the other 875 mm from the ground, as illustrated in Fig.1. Only the data from moisture measuring devices are used in the present study. Moisture content (weight %) of the boards is measured using the regular impedance; the electrical resistance between two steel pins located 25 mm apart from each other. The two steel nails used for the measuring of the moisture content penetrated the whole cross section from the back ending 3 mm behind the surface of the board.

## 3. Results and discussion

The analysis of the data focuses on the moisture content in the wooden cladding boards mounted to the test house in various experimental configurations. It is expected that the moisture content varies with different configurations. For a better understanding, four factors are introduced: Local location (LL), surface treatment (ST), material quality (MQ), and micro location (ML). To determine these values, the monthly average of the moisture content, its standard deviation, minimum, and maximum are determined and compared to each other. The result is a nondimensional factor that can be evaluated thoroughly. To increase the reliability of the results each factor can be calculated twice; first for the top measuring device, second for the bottom measuring device.

The following Table.1 shows the parameters and the configuration alternatives used to calculate the quotient. For the factor *local location* (LL) the values for the field on the west side are divided by the values of the respective field on the east side having the same material configuration. Three different subdivisions can be distinguished for the factor *surface treatment* (ST): the combination oil divided by water (ST I), oil divided by untreated (ST II) and finally water divided by untreated (ST III). For the *material quality* (MQ) the values for the slow grown material are divided by the values for the fast grown ones. The *micro location* describes the location of the measuring device within the field, dividing the values for the top measuring device by the ones for the bottom ones.

*TABLE. 1: Configuration of the comparing parameters*

| Factor | Configuration A | Configuration B | Quotient |
|---|---|---|---|
| **Local location** | West | East | West/East |
| **Surface treatment I** | Oil | Water | Oil/Water |
| **Surface treatment II** | Oil | Untreated | Oil/Untreated |
| **Surface treatment III** | Water | Untreated | Water/Untreated |
| **Material quality** | Slow grown | Fast grown | Slow/Fast |
| **Micro location** | Top | Bottom | Top/Bottom |

Altogether thirty-one different factors can be calculated, five for the *local location* (LL), ten for the *surface treatment* (four ST I, three ST II, and three ST III), five for the *material quality* (MQ), and eleven for the *micro location* (ML). The below given Fig.2 illustrates the combinations for the factors *LL*, *ST*, and *MQ*.

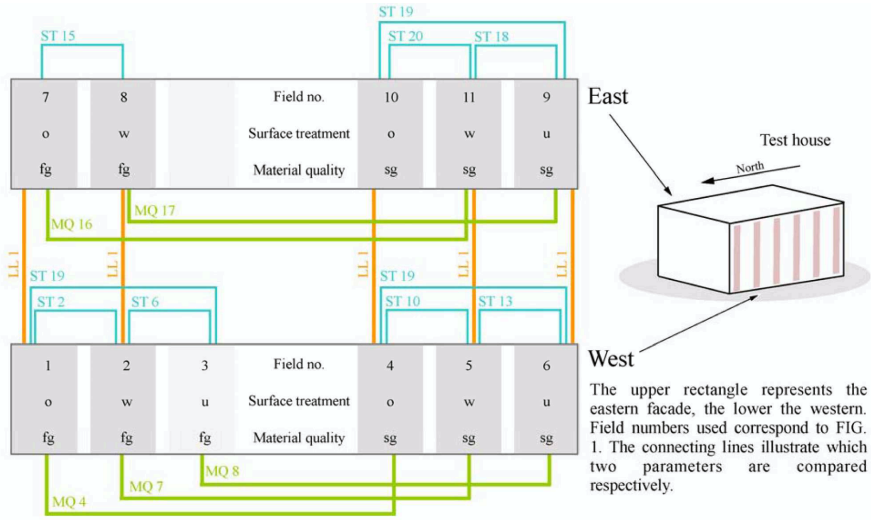


*FIG. 2: Overview over different configurations*

### 3.1 Local location

The following Table 2 lists the results for the factors *local location*. It includes the numbers of the field (as in Fig. 1 and Fig. 2, the calculated factor for the average moisture content and the respective standard deviation. A factor greater than one indicates greater moisture content for the field on the west façade, a factor smaller than one greater moisture content for the respective field on the east façade.

*TABLE. 2: Results for the factor local location (LL)*

| | LL 1 | LL 5 | LL 9 | LL 12 | LL 14 |
|---|---|---|---|---|---|
| **Quotient [Config. A/Config. B]** | 1/7* | 2/8 | 4/10 | 5/11 | 6/9 |
| **Average top [-]** | 1.16 | 1.05 | 1.07 | 1.13 | 1.07 |
| **Average bottom [-]** | 1.16 | 1.04 | 1.03 | 1.06 | 1.05 |
| **Standard deviation top [-]** | 1.63 | 1.16 | 1.29 | 1.17 | 1.94 |
| **Standard deviation bottom [-]** | 1.60 | 1.20 | 1.59 | 1.34 | 1.62 |

*The numbers used here correspond to Fig.1 and Fig.2

The values for all quotients are greater than one, varying between 1.05 and 1.16 for the average moisture content of the top measuring point, and between 1.03 and 1.16 for the bottom measuring point. Likewise, the variations in moisture content, here expressed by the standard deviation of the average moisture content, vary between 1.17 and 1.94 for the top and between 1.2 and 1.62 for the bottom measuring point respectively. Those values indicate up to 16% higher moisture content and up to 94% greater variations in moisture content for the fields at the west façade.

The results correspond with the presumptions, since the prevailing wind direction on site is southwest and driving rain is considered to be the primary reason for increased moisture content.

### 3.2 Surface treatment

The quotients for the factor *surface treatment* (ST) can be subdivided into three categories. First, ST I, comparing oil based paint with water based paint. Second, ST II, comparing oil based paint with untreated surface, and finally, ST III comparing water based paint with untreated surface. A quotient greater than 1.0 indicates higher moisture content for the respective numerator for each quotient. TABLE. 3able 3 summarises the results for the surface treatment factor.

*TABLE. 3: Results for the factor surface treatment (ST)*

| | **ST I** | | | | **ST II** | | | **ST III** | | |
|---|---|---|---|---|---|---|---|---|---|---|
| | **ST 2** | **ST 10** | **ST 15** | **ST 20** | **ST 3** | **ST 11** | **ST 19** | **ST 6** | **ST 13** | **ST 18** |
| **Quotient [Config. A/Config. B]** | 1/2* | 4/5 | 7/8 | 10/11 | 1/3 | 4/6 | 10/9 | 2/3 | 5/6 | 11/9 |
| **Average top [-]** | 1.01 | 0.99 | 0.92 | 1.04 | 1.03 | 1.05 | 1.04 | 1.02 | 1.06 | 0.99 |
| **Average bottom [-]** | 1.01 | 0.96 | 0.91 | 0.99 | 1.05 | 0.96 | 0.98 | 1.04 | 1.00 | 0.99 |
| **Standard dev. top [-]** | 1.18 | 0.86 | 0.84 | 0.78 | 0.63 | 0.51 | 0.61 | 0.54 | 0.60 | 0.78 |
| **Standard dev. bottom [-]** | 0.96 | 0.94 | 0.68 | 0.79 | 0.65 | 0.56 | 0.57 | 0.68 | 0.59 | 0.71 |

*The numbers used here correspond to Fig.1 and Fig.2

Though, some trends can be identified. Results are less clear than for the factor local location. For ST I quotients the values oscillate around 1.0, with a minimum of 0.91 and a maximum of 1.04. ST 15 is the one with the most significant difference in average moisture content. Here, the moisture content of the field containing water based paint is 8% higher for the top and 9% for the bottom measuring device. Quotient ST 10 shows the same result, whereas ST 2 shows the opposite. However, since ST 20 is not definite no clear conclusion can de drawn. The standard deviation of the ST I factors vary from 0.78 to 1.18 for the top, and from 0.68 to 0.96 for the bottom measuring point. Assuming that the outstanding value 1.18 for the quotient ST 2 is a random mistake, the values are all less than 1.0. Thus, the variations in moisture content seem to be greater for the water based surface treatment than for the oil based one.

For ST II quotients, the situation is similar to ST I; the values oscillate around 1.0 and no obvious conclusion can be reached. However, variations in moisture content show a definite result. They are always less for the one with oil based paint than for the untreated surface, namely down to 51%. Although no significant differences can be detected in the average moisture content, the results show the buffering capability of the oil-based coating.

The ST III quotients vary for the average moisture content as the ST I and ST II quotients do. Nevertheless, variations in moisture content are significantly greater for the untreated materials, expressed by the standard deviation, i.e. between 46% and 22%.

Comparing the standard deviations for all three types of ST quotients, the variations in moisture content are lowest for oil based paint, followed by water based paint and finally the untreated material. Oil borne coating systems are known to have smaller pores than water borne coating systems resulting in slower and less moisture sorption [Christiansen, 1999; Råknes 1985]. However, it is important to note that experiments are still in an initial stage, so that the behaviour of the surface treatments concerning moisture content can change as the ageing process proceeds.

### 3.3 Material quality

The results for the factor material quality (MQ) are shown in TABLE. 4able 4. The values for the slow grown material are divided by the values for the fast grown ones. A quotient greater than 1.0 indicates higher moisture content for the slow grown material, and vice versa.

*TABLE. 4: Results for the factors material quality (MQ)*

| | MQ 4 | MQ 7 | MQ 8 | MQ 16 | MQ 17 |
|---|---|---|---|---|---|
| **Quotient [Field no. A/Field no. B]** | 4/1* | 5/2 | 6/3 | 10/7 | 11/8 |
| **Average top [-]** | 0.99 | 1.02 | 0.98 | 0.98 | 0.95 |
| **Average bottom [-]** | 0.99 | 1.01 | 1.05 | 1.07 | 0.99 |
| **Standard deviation top [-]** | 0.69 | 0.95 | 0.85 | 0.85 | 0.95 |
| **Standard deviation bottom [-]** | 0.70 | 0.94 | 1.08 | 0.98 | 0.84 |

*The numbers used here correspond to Fig.1 and Fig.2

Considering the average moisture content the results are not conclusive. Values oscillate around 1.0, minimum being 0.95 for the top measuring point, maximum 1.02. Respectively, minimum for the bottom measuring point is 0.99 and maximum 1.07. Variations in moisture content, apart from the value 1.08 for the factor MQ 8, are always higher for the fast grown material.

### 3.4 Micro location

The factor micro location describes the influence of the location of the measuring device within a field with otherwise equal material properties. The following Table 5TABLE. 5 comprises the results, dividing the top measuring point by the bottom measuring point respectively. Values greater than 1.0 reveal higher moisture content for the top measuring device; values less than 1.0 indicate higher moisture content for the bottom measuring device.

*TABLE. 5: Results for the factors micro location (ML)*

| | West | | | | | | East | | | | |
|---|---|---|---|---|---|---|---|---|---|---|---|
| | ML 1* | ML 2 | ML 3 | ML 4 | ML 5 | ML 6 | ML 7 | ML 8 | ML 9 | ML 10 | ML 11 |
| **Average [-]** | 0.99 | 1.02 | 1.02 | 1.03 | 1.00 | 0.94 | 0.99 | 0.98 | 0.93 | 0.99 | 0.94 |
| **Standard deviation [-]** | 1.00 | 0.76 | 1.05 | 1.10 | 0.83 | 0.82 | 1.07 | 0.87 | 0.89 | 0.96 | 0.94 |

*The numbers used here correspond to Fig.1 and Fig.2

No clear tendency applies to all results. Though, on the eastern façade, average moisture content is always higher for the bottom measuring device, even though not dramatically; the values vary from 0.93 to 0.99. Considering the average of the average values, which is 0.98, the moisture content is slightly higher for the bottom measuring point. Same applies to the standard deviation, meaning a greater variation in moisture content for the bottom measuring device. In case of the standard deviation more values can be found that are a lot lower than 1.0 than vice versa, indicating a tendency for greater variations in moisture content for the bottom measuring device.

Recapitulating, the results gained through the assessment using the introduced factor correspond closely to the assumptions. The local location affects the moisture content to greatest extent. Both average moisture content and its variations are relatively higher for all fields of the western façade, 16% for the average, and up to 94% for the

variations of the moisture content. Furthermore, the data shows differences in moisture condition caused by different surface treatments. Although the differences are not as distinct as for the local location, performance characteristics of surface treatments can be distinguished. The coating of oil-based paint is known to consist of smaller pores than water-based paint, causing less moisture uptake. Due to better elasticity properties water-based paint compensates the dimensional changes better than oil-based paint. In contrast, oil-based paint hardens over time, resulting in reduced elasticity. Finally, this can cause crack formation resulting in greater moisture sorption rates than the water-based coating system [Christiansen, 1999; Råknes 1985]. The extent of such effects might be seen by further monitoring. Since the experiments are still in an initial stage, the surface treatments might undergo changes in moisture uptake as ageing processes proceed.

Additionally, the results illustrate the buffering effect for both painting systems in comparison with the boards left untreated. At this stage, the material quality does not seem to have a major importance for the moisture content, though slight greater variations can be detected for the fast grown material, i.e. the lower density. The same applies to the micro location. Though, slightly higher values for both the average moisture content and the variations can be determined for the bottom measuring device.

Summarising the results it can be stated that all parameters affect the moisture content to some extent. For the factor local location and surface treatment, the influence is rather well-defined. The influence of the factor surface treatment might increase in importance with the ageing of the coating film. The factors material quality and local location show only limited impact on the moisture conditions.

## 4. Conclusions

This study is carried out using data from the ongoing project *Climate 2000 – Building constructions in a more severe climate*, conducted by the *Norwegian Building Research Institute* (NBI). Part of the project is an experimental investigation of wooden cladding design which has been set up at a test building in Trondheim, Norway. This study presents a method to assess the influence of surface treatment, material quality, micro-, and local climate on the moisture content of a wooden façade. The results confirm the presumptions about the influence of the different parameters on the moisture content. Four factors are introduced to evaluate the significance of different parameters: local location, surface treatment, material quality, and micro location. Of these, local location, i.e. whether the cladding is oriented towards west or east, has the greatest influence. Next, the investigations on the factor surface treatment, i.e. oil-based paint, water-based paint, and untreated surface, indicate differences in moisture content for the different surface treatments. Finally, the factors material quality and micro location seem to be of rather marginal significance up to now. Since data are so far only available for a period of one year, the further observation of the detected developments will provide valuable insight into the functionality of wooden façade materials. Advances in understanding those processes that affect the performance of building materials are important both for the design of sustainable constructions and their service life prediction. The introduced method is one possible approach to the numerical implementation of the factor method proposed in ISO 15686 [2000&2001].

## 5. Acknowledgement

This paper has been written using data within the ongoing NBI Research & Development program *Climate 2000 – Building Constructions in a More Severe Climate* (2000 – 2006), strategic institute project *Impact of climate change on the built environment*. The authors gratefully acknowledge all construction industry partners, the Research Council of Norway, and the Northern Periphery Programme project *External Timber Cladding in Maritime Conditions*.

## 6. References

BSI 7543 (2003). Guide to durability of buildings and building elements, products and components, British Standards Institution, London, U.K.

Christiansen, H. (1999). Råteskader i trepanel - Resultater fra Dekkbeisfondet, Project report 248, Norwegian Building Research Institute, Oslo, Norway.

Haagenrud, S.E. (1997). Environmental Characterisation including Equipment for Monitoring, CIB W80/RILEM

140-PSL, Sub Group 2 Report, Norwegian Institute for Air Research (NILU), Kjeller, Norway.

Högberg, A. (2002). Microclimate Load: Transformed Weather Observations for Use in Design of Durable Buildings, Department of Building Physics, Chalmers University of Technology, Gothenburg, Sweden.

ISO 15686-1 (2000). Building and Construction assets – Service Life Planning; Part 1: General Principles, The International Organization for Standardization, Geneva, Switzerland.

ISO 15686-2 (2001). Building and Construction assets – Service Life Planning; Part 2: Service life Prediction Procedures, The International Organization for Standardization, Geneva, Switzerland.

Lisø, K.R., Aandahl et.al. (2003). Preparing for climate change impacts in Norway's built environment, Building Research & Information, Vol. 31 (3-4), pp.200-209, London, U.K.

Lisø, K.R., et al. (2002). Climate 2000 – Building Constructions in a more severe climate; Programme 2000-2006, Programme Description, Norwegian Building Research Institute, Oslo, Norway

Moser, K. (2002). Engineering Design Methods for Service Life Prediction, CIB W80/RILEM 175, SLM: Service Life for Buildings and Components, Task Group Performance based Methods of Service Life Prediction, Swiss Federal Laboratories for Material Testing and Research, Dübendorf, Switzerland.

Norberg P. (1996). Monitoring of moisture conditions on painted wood panels exposed outdoors in a temperate climate, Proceedings of the 7th Conference oh Building Materials and Components, Stockholm, Sweden.

Nore, K., Thue, J.V., Time, B., Rognvik, E. (2005). Ventilated wooden claddings–A field investigation. 7th Nordic Symposium on Building Physics, June 13-15, 2005, Reykjavik, Iceland, (submitted).

Råknes E. (1985). Råte i ytterkledning, Norsk Treteknisk Institutt, Oslo, Norway.

Siemes, T. (2003). Prediction of service life of building materials and components, Service life methodologies, CIB W80/RILEM 175, SLM: Service Life for Buildings and Components, Task Group Probabilistic methods, TNO Building and Construction Research, Delft, The Netherlands.

Scheffer, T.C. 1971, 'A Climate Index for Estimating Potential of Decay in Wood Structures above Ground', Forest Products Journal, Volume 21 (19), pp. 25-31, Forest Products Society, Madison, USA.

## 9.3. Paper 3

**Color changes in wood boards during weathering**

P.Rüther

presented at the World Timber Engineering Conference in Portland, U.S.A., 2006

# Color changes in wooden boards during weathering

**Petra Rüther**
**PhD student**
**Department for Civil and Transport Engineering**
**NTNU, Trondheim, Norway**
**petra.ruether@ntnu.no**

## Summary

In the present study color changes of wooden samples due to exposure to natural and artificial weathering are investigated. The materials showed considerable differences in color development. Color changes due to exposure types vary for the two material types, untreated and treated samples. Whilst exposure on rack accelerates color changes for untreated materials, treated ones do not differ much from the vertically exposed ones. For exposure in a climate simulation apparatus, the same as for rack exposure applies; none of them correlates clearly with either one of the natural ageing tests. The quantification of wood surface degradation by means of image analysis provides insight into the problems raised by natural and artificial aging of building materials exposed to the outdoor environment. The benefits of a controlled exposure environment such as the climate carousel are overruled by the difficulties of designing an exposure environment matching the prevailing outdoor exposure conditions.

## 1. Introduction

Building materials and structures are affected by environmental impacts throughout their lifetime. Those impacts affect performance and service life of materials and objects and therefore their effect on the environment. Environmental simulation deals with effects of climate exposure on materials' performance, their long-term behavior and service life, and interaction between material and environment. Questions of accelerated and artificial aging play a major role in the context of aging and weathering processes.

Weathering mechanisms of untreated wood were investigated by Feist and Mraz (1978) [1]. They exposed untreated wooden samples both to natural and artificial weathering, quantifying the degradation by measuring erosion rates. Sell and Leukens (1971) exposed 20 different wood species to outdoor weathering and described the observed weathering phenomena in [2]. A more general work on testing and evaluation methods was carried out by Lewry and Crewdson (1994) [3], in which they underline amongst others the importance of objective evaluation methods for the degradation of building materials. Furthermore, computer image processing is mentioned as an appropriate tool to this evaluation. Due to increasing computer power over the last decades, it is now possible to process images as used in the present study on a commercial PC.

This study investigates color changes of wooden samples due to exposure to both natural and artificial aging. The appearing color changes are quantified by calculating differences in appearance by means of the *CIELAB* model developed by the *International Commission on Illumination (CIE)*, an organization dedicated to the creation of standards for all aspects of light [4].

## 2. Materials and Methods

Nine different wooden materials are exposed to the outdoor climate both at an experimental site in Trondheim and a climate simulation apparatus, the so called *climate carousel* at the laboratory. Five of the nine materials are untreated boards of wood species commonly used in facades. Four are treated in different ways, two are treated with Furfuryl alcohol and two are pressure impregnated.

### 2.1 Test specimens

Test specimens used for the test are 50 cm in length and approximately 150 mm in width. Accurate measures were taken after conditioning at standard climate of 20°C at 60% relative humidity for 6 days. The edges of the samples are not rounded, except material #1, which is a ready shaped cladding board from the manufacturer. All other surfaced are rough sawn. The following Table 1shows the types of materials used together with their density, thickness and width of the boards.

*Table 1 Material types used in the study*

| No. | Wood species | Latin name | Density [kg/m$^3$] | Thickness [mm] | Width [mm] |
|---|---|---|---|---|---|
| 1 | Norway spruce | Picea abies (L.) Karst. (Ruptimal® surface) | 411,71 | 18,72 | 142,8 |
| 2 | Norway spruce | Picea abies (L.) Karst. | 456,56 | 17,76 | 140,51 |
| 3 | Pine heartwood | Pinus silvestris L. | 478,53 | 21,28 | 142,98 |
| 4 | Larch | Larix decidua Mill. | 439,50 | 19,58 | 151,66 |
| 5 | Aspen | Populus tremula L. | 493,84 | 21,42 | 145,89 |
| 6 | Kebony 30 | Southern yellow pine (Pinus taeda), *Wood Polymer Techn.* treatment method with Furfuryl alcohol | 542,09 | 19,34 | 144,58 |
| 7 | Visorwood | Pine (Pinus sylvestris L.), *Wood Polymer Techn.* treatment method with Furfuryl alcohol | 731,09 | 19,96 | 153,75 |
| 8 | Pressure treated | class AB (according to Norwegian classification system for use above ground) | 496,53 | 18,55 | 144,1 |
| 9 | Royal treatment | Møre Røyal® - royal impregnation | 432,86 | 18,02 | 143,59 |

### 2.2 Exposure

The specimens are exposed to outdoor climate at a test site as well as in a climate simulation apparatus at the laboratory, thoroughly described in 2.2.2.

#### 2.2.1 Experimental site

The test house is located in Trondheim, Norway at a longitude of 10°27'14'' and latitude of 69°24'40'' at 120 m above sea level. The test site is owned by the *Norwegian University of Science and Technology (NTNU)* and *SINTEF Building and Infrastructure*. It comprises several test assemblies and a meteorological station owned by *The Norwegian Meteorological Institute (DNMI)*. The test site is located on an open field; no surrounding buildings are likely to have an influence on the exposure conditions.

Table 2 lists monthly average values for average temperature and precipitation for the last normal period (1961-1990) measured at Trondheims' airport Værnes and meteorological data collected at the test sites' station during the exposure period.

*Table 2 Temperature and precipitation at experimental site*

| | | jan | feb | mar | apr | may | jun | jul | aug | sep | oct | nov | dec | Average/Total |
|---|---|---|---|---|---|---|---|---|---|---|---|---|---|---|
| Temperature [°C] | Normal period | -3,4 | -2,5 | 0,1 | 3,6 | 9,1 | 12,5 | 13,7 | 13,3 | 9,5 | 5,7 | 0,5 | -1,7 | 5,03 |
| | Exposure 2005 | 1,6 | -1,2 | 0,0 | 5,6 | 7,2 | 11,1 | 15,7 | 12,9 | 10,8 | 7,6 | 4,0 | -0,8 | 6,2 |
| | Exposure 2006 | 0,2 | -0,7 | -4,2 | - | - | - | - | - | - | - | - | - | - |
| Precipitation [mm] | Normal period | 63 | 52 | 64 | 49 | 53 | 68 | 94 | 87 | 113 | 104 | 71 | 84 | 892 |
| | Exposure 2005 | 118 | 59 | 22 | 33 | 47 | 74 | 20 | 119 | 106 | 41 | 82 | 109 | 829 |
| | Exposure 2006 | 108 | 106 | 45 | - | - | - | - | - | - | - | - | - | - |

*Figure 1 Test house, eastern facade (feb 2005)*

Test specimens are exposed on a test house, its walls facing north, south, east and west respectively. Nine samples of each species are exposed on the east and west side of the building, two of each material on the north and south facing side. Additionally, two samples of each material are exposed on a rack at the test site exposing the samples to the south at an angle of 30 degrees. Figure 1shows a picture of the east facing wall taken in February 2005. Test samples were mounted at the experimental site on February 2005, the last evaluation was performed March, 3rd 2006 after altogether 394 days of exposure.

### 2.2.2 Climate carousel

The apparatus used for this test is designed based on the recommendations given in [5]; *Building materials and components in the vertical position: Exposure to accelerated climatic strains*. This document describes a common method for the Scandinavian countries. The apparatus consists of four test chambers, closed and insulated at the back, each for a maximum size of test specimens of 1,5 m x 2,5 m. The central unit containing the test chambers rotates 90° every hour, rotating the test chambers through three different exposure environments before returning to laboratory climate. The three exposure climates in the apparatus are UV and IR radiation, water spray, and frost. Table 3 summarizes the required test conditions according to [5], also described in [6].

*Table 3 Test conditions according to [5].*

| | | |
|---|---|---|
| 1 | UV and infrared radiation | Perpendicular to the test specimen with a relative spectral distribution in the UV band close to that of global solar irradiance. Black panel temperature 65±3ºC, controlled by means of infrared halogen lamps, Current values: UVA: 1,1 W/m$^2$; UVB: 1,1 W/m$^2$ |
| 2 | Water spray | Water with a spray of de-mineralized water 15±2 l/(m$^2$h) |
| 3 | Cooling and freezing | Air temperature -20±5ºC, measured by white panel temperature |
| 4 | Laboratory climate | Thawing at ambient laboratory climate 23±5ºC, 50±10% RH |

### 2.3 Color analysis

Different color models can be used to quantify color changes. They attempt to describe the color which can be seen by the human eye using different methods to describe and classify color. All color models use numeric values to represent the visible spectrum of color. A color model determines the relationship between values, and the color space defines the absolute meaning of those values as colors. Some models, as the *CIELAB* color space, have a fixed color space and are therewith device independent. The *CIELAB* color space is a model produced by the *International Commission on Illumination (CIE)*, an organization dedicated to the creation of standards for all aspects of light [4].

The *CIELAB* model describes color on terms of its lightness component (L) and two chromatic components, a (greenness-redness) and b (blueness and yellowness). Together, those three components form a three-dimensional space. L, the lightness components, ranges from 0 (black) to 100 (white), representing the achromatic axis of grays. Changes in lightness can be determined by $\Delta L^{*}=L^{*}_{1}- L^{*}_{0}$. Absolute color differences can be calculated using the Euclidean distance between two colors defined as $\Delta E^{*}=[ (\Delta L^{*})^{2} +(\Delta a^{*})^{2}+(\Delta b^{*})^{2}]^{1/2}$.

Test samples are demounted periodically for evaluation. After conditioning in a standard climate (20ºC, 60% RH), samples are scanned by a commercial scanner, deactivating all color correction functions to obtain equal light conditions for all scans. Only the middle 30 cm are used for evaluation to rule out regions of greater degradation close to the end grain. The average color values and their standard deviation are determined.

## 3. Results

The colors measured are transformed into plots to evaluate differences in color development due to different exposure conditions. The following Table 4 summarizes the exposure conditions at the experimental site for the exposure period. The average temperature for the exposure period was 5,61ºC with an average relative humidity of 73%. The predominant wind direction is almost exactly from the south. Note that the amount of global radiation during winter is significantly less than during summer.

*Table 4 Exposure conditions at experimental site.*

| Scan No. | Scan date | Days of Exposure | Exposure interval | TTM [ºC] | UUM [%] | FM [m/s] | DM | RR [mm] | QO [kW/m$^2$] |
|---|---|---|---|---|---|---|---|---|---|
| 1 | 2005-02-08 | 0 | | | | | | | |
| 2 | 2005-05-03 | 66 | 66 | 1,75 | 68 | 2,39 | 169 | 85 | 187 |
| 3 | 2005-06-28 | 122 | 56 | 8,98 | 70 | 2,78 | 194 | 117 | 222 |
| 4 | 2005-09-08 | 194 | 72 | 14,08 | 74 | 2,12 | 183 | 157 | 253 |
| 5 | 2005-11-10 | 264 | 70 | 8,60 | 73 | 2,93 | 179 | 135 | 67 |
| 6 | 2005-12-22 | 306 | 42 | 1,96 | 79 | 2,80 | 181 | 158 | 3 |
| 7 | 2006-03-20 | 394 | 88 | -1,69 | 72 | 2,86 | 178 | 268 | 53 |
| | | | | Ø 5,61 | Ø 73 | 2,7 | Ø 181 | ∑ 920 | ∑ 785 |

TTM – average temperature; UUM – average relative humidity, FM – average wind speed, DM – wind direction (0º north, 90 º east etc.); RR - precipitation, QO – accumulated global radiation

Samples have been exposed 394 days altogether starting in February 2005; last evaluation took place end of March 2006. The artificial aged samples have been exposed since august 2005 with some maintenance intervals at the apparatus, for altogether 185 days.

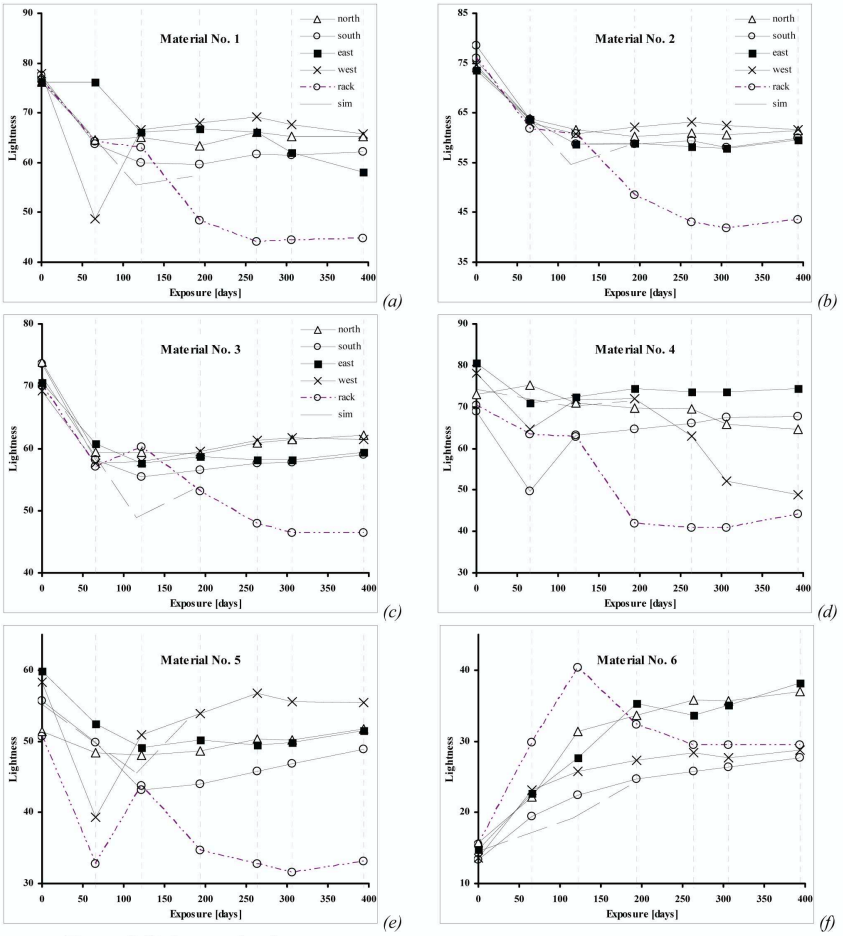


*Figure 2 Lightness development*

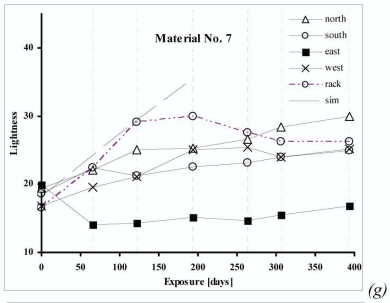


(g)

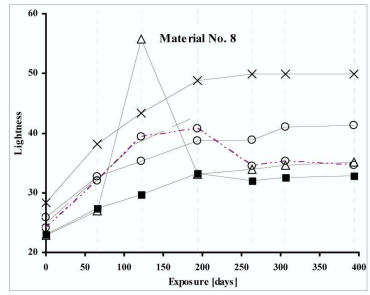


(h)

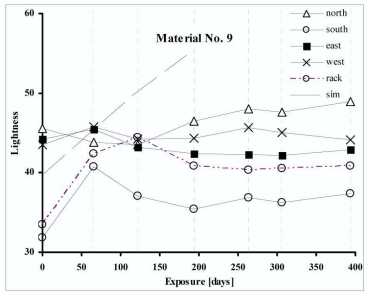


(i)

*Figure 3 Lightness development (continued)*

## 4. Discussion

First results after 394 days of exposure (February 2005 until March 2006) show that samples of untreated wood (Material No.1 to No.5) grow significantly darker during the first exposure period of 66 days. Darkening ranges from 5% up to 20% percent for untreated species. The differences between the different types of vertical exposure play only a minor role in this first phase. As seen Figure 2 lightness values for the untreated samples vary little up to an exposure time of 122 days; that includes the samples exposed on the rack. Those samples get significantly darker than the vertically exposed samples starting end of July. The lightness gradients of samples exposed on rack is similar for all untreated wood species. Common to all species is a fast decrease followed by a more slight increase of lightness. Changes in lightness seem to flatten out with time. As for the artificial aged samples, values are also given in the above chart. Likewise, samples exposed in the artificial weathering apparatus also get darker first and lighter with time. For materials No.1, No.2 and No.3 darkening is even greater as for samples exposed on rack. However, all untreated samples get lighter with longer exposure in the weathering apparatus. At evaluation after 184 days, some samples (#2, #4, #5) show approximately the same lightness values as samples from outdoor exposure, whereas others (#1, #3) are still darker than all vertically exposed ones.

In contrast, most samples of treated wood (Materials No.6 to No.8) get evenly lighter in the course of time, as seen from Figure 2. Material No. 9 is an exception, with lightness values varying a little in the beginning and flattening out with time without any identifiable trend. For materials # 6, #7 and #8, lightness increases between 10% and 20% compared to initial stage. Furthermore, differences between exposure types are different from the pattern observed for untreated samples: values for samples exposed on rack do not stand out clearly as for untreated samples. For example, increase in lightness for material #8 is greatest for exposure facing west, whereas for #6 exposure facing north and east seem to undergo greatest changes in lightness. For exposure in the climate simulation apparatus, variations in lightness development can be observed; #7 and #9 get darker and darker exceeding all other exposure types, whereas #6 is still lighter than all samples exposed outdoor and #8 seems to correlate quite well with exposure on rack.

Determination of both Chroma ($\Delta C^*$) and Euclidean distance ($\Delta E^*$) support the above described results; changes in color are decreasing for all samples with time.

Another interesting topic in this context is the repeatability of outdoor exposure tests. As a result of variations of the exposure environment itself, namely the weather conditions, the progress of surface degradation can vary to a great extent. Artificial weathering devices as the one used for the present study offer the opportunity of a controlled exposure environment. But, as shown in this study, the degradation rate, quantified by means of color changes, depends greatly on the exposed material itself. The attempt to obtain similar degradation rated for natural and artificial aging is one of the major tasks of climatic simulation techniques.

Changes in surface color are expected to overlap with an increasing colonization of mold fungi on the surface. Samples of surface growth will be taken to determine the extend of such microbiological activity. Changes in color due to fungal growth can hardly be simulated in the climate carousel, since all microorganisms are killed by the prevailing temperatures. Same applies to increased surface erosion due to driving rain, sand or other particles on materials exposed outdoors, together with darkening of the surface by dirt and dust sticking to the surface, especially for exposure on rack.

The process of color changes does not seem to be terminated yet. It will be interesting to see whether decreases in color changes occur due to for example reduced radiation energy during the winter months or whether color development is final after a little more than one year of exposure.

## 5. Conclusion

In the present study color changes of wooden samples caused by exposure to both natural and artificial aging were investigated. After 394 days of outdoor and 184 days of artificial aging samples showed significant changes in color. The used materials, five untreated wood species and four materials treated in different ways, showed significant differences in color development. Generally, untreated samples grow significantly darker in the first exposure period of 66 days. Darkening ranges from 5% up to 20% percent for untreated species. Afterwards they get lighter again. In contrast, treated samples get evenly brighter in the course of time. Differences in exposure types vary for the two material types. Whilst exposure on rack seems to accelerate changes in color to an extend which will probably never be reached by vertically exposed samples for the untreated ones, rack exposure for the treated ones does not differ much from the vertically exposed ones. No clear conclusion can be drawn regarding differences in orientation. For exposure in the climate simulation apparatus, the same principles as for

rack exposure apply; though untreated and treated samples each show a certain pattern, none of them correlates clearly with either one of the natural aging tests. Further, it will be interesting to observe further development of color changes, fungal growth on the surface, cracks and other degradation measurements. The quantification of wood surface degradation by means of image analysis provides insight into the problems raised by natural and artificial aging of wooden, and more general, building materials exposed to the outdoor environment. The benefits of a controlled exposure environment as the climate carousel seem to be overruled by problems with designing an exposure environment matching prevailing outdoor exposure conditions.

## 6. References

[1] Feist W.C., Mraz E.A., 1978. Comparison of Outdoor and Accelerated Weathering of Unprotected Softwoods. *Forest Products Journal*.Vol. 28, No.3, pp.38-43.

[2] Sell J., Leukens U., 1971. Verwitterungserscheinungen an ungeschützten Hölzern (Weathering characteristics of untreated wood-in German). *Holz als Roh-und Werkstoff.* Vol. 29, No. 1, pp. 23-31.

[3] Lewry A.J., Crewdson L.F.E. Crewdson, 1994. Approaches to testing the durability of materials used in the construction and maintenance of buildings. *Construction and Building Materials.*Vol. 8, No. 4, pp.211-222.

[4] CIE International Commission on Illumination, 2004. *Technical Report*: Colorimetry, CIE 15, 3rd Edition, Vienna, Austria

[5] NORDTEST Method NT BUILD 495, 2000. Building Materials and Components in the vertical Position: Exposure to accelerated climatic strains. Nordtest, Espoo, Finland

[6] Brandt E., Nilsen T.-N., Experiences with Equipment for Large Scale Accelerated Ageing Tests. *Proceedings of the 9th Conference on Durability of Building Materials & Components*, Brisbane, Australia

## 9.4. Paper 4

**Color changes of wood and wood based materials due to natural and artificial weathering**

P. Rüther, B.P. Jelle

Submitted for publication, currently under review at *Wood Material Science and Engineering*

# Surface color changes of wood and wood based products due to natural and artificial weathering

P. Rüther[1,a,*], B.P. Jelle[1,b,]

[a] *Department for Civil and Transportation Engineering, Norwegian University of Science and Technology, Høgskoleringen 7a, 7491 Trondheim, Norway*
[b] *SINTEF Building and Infrastructure, Høgskoleringen 7b, 7491 Trondheim, Norway*

**Abstract**

Color changes of unpainted wood surfaces caused by weathering are an aesthetic problem and the understanding of the underlying processes is a complex task. This study investigates color changes of wooden boards both outdoors on a test house and in the laboratory. The CIE L*a*b* color system is used to compare exposure directions outdoors, laboratory weathering, and materials used in this study. Results indicate that there is a common pattern for color changes. Solar radiation and wind driven rain are assumed to be the main driving forces behind color changes, together with graying caused by mold growth. However, no quantitative correlation between color changes and the two main climatic strains could be found. Laboratory weathering is a useful tool when it comes to recreate similar exposure conditions. The present study indicates that results from laboratory weathering can hardly be compared to results from outdoor weathering. Though, how close they are to actual exposure conditions is a widely discussed question. However, color measurement is a useful tool to objectively document changes in appearance.

*Keywords:* Wood, Weathering, Color changes, Acceleration factor, Mold growth

## 1. Introduction

Wood is a versatile material that is widely used both in indoor and outdoor applications. Wood undergoes several transformations during weather exposure. The weathering of wood involves color changes, loss of surface fibers, roughening and cracking of the surface, and changes in chemical composition (1, 2, 3). However, durability and serviceability are not usually impaired by weathering. Environmental agents, e.g. solar radiation and precipitation have a major role in wood weathering. Color changes are rapidly superposed by mold fungus colonization (4, 5, 6). Solar radiation, mainly the high-energy short-wave part is known to cause degradation in wood. However, UV light is can only penetrate the upper most surface, about 80 $\mu$m (7, 8). However, the initial chemical reaction leads to photodegradation, the parts of the cellular structure rich in lignin (e.g. the middle lamella) is eroded first, water washed out soluble degradation products and the surface remains rich in cellulose (9, 10). Higher temperatures favor chemical reactions in general, also wood weathering (11, 12). However, the role of temperature in the chemical reactions, wavelength dependency and the influence of the presence of water are subject to ongoing research (13). Weathering studies might be conducted under natural, i.e. outdoor conditions, or artificial, e.g. laboratory conditions (14). For outdoor weathering, the evaluation method for wood degradation chosen is often erosion rate. Erosion rates for natural weathering were found to correlate strongly with wood density (15, 16). Samples are often exposed tilted facing south, in order to maximize solar radiation doses (17). Laboratory weathering is chosen to accelerate or compress degradation processes. However, the spectral distribution of the light source, the composition of the weathering cycles, and the chosen temperature levels have a great influence on the chemical reactions (18, 19, 20, 21, 22). Changes in appearance caused by wood weathering have so far been evaluated subjectively (23), i.e. by visual inspection. However, color measurement provides the possibility to objectively assess changes in appearance, since lighting variations and differences in the observers' perception are excluded. This is done by describing color develop-

*P. Rüther
*Email addresses:* petra.ruether@ntnu.no (P. Rüther), bjorn.petter.jelle@sintef.no (B.P. Jelle)

ment in an objective way by means of the CIE L*a*b* model (24) verifying that the chosen method of color analysis is suitable for this purpose. Quantifying color development in terms of two major climatic strains, i.e. solar radiation and wind driven rain is another aspect in this study. Furthermore, differences and similarities between outdoor and laboratory weathering are being investigated. Acceleration factors for different laboratory weathering cycles are calculated and discussed. The results from this study might be suitable as input data for the simulation of surface color changes of wood. A proven dependency of climatic strains and color development could help to improve simulation of wood surface color changes, either by laboratory simulation or numerical simulation.

## 2. Experimental

Nine different wood species and wood based products are included in this study, five untreated wood species and four materials that are treated by means of different impregnation techniques. Table 1 presents the materials used in this study, together with average mass densities and initial average color values. Regular materials were used to include the whole range of variations in appearance, including knots and defects. Test specimens used in this study are approximately 150 mm in width. Different lengths are used for different exposures, depending on the available space, 500 mm length for outdoors and in the Rotating Climate Chamber (RCC), and 200 mm for exposure in the ATLAS solar simulator.

### *2.1. Outdoor exposure site*

The specimens are exposed on a test house at Voll in Trondheim, Norway (longitude 10°27'16", latitude 63°24'39" elevation above sea level 120 m). The test specimens are exposed vertically on the walls of the test building facing north, south, east and west. Test specimens are mounted with both vertically and horizontally oriented annual rings. Additionally, samples of each material were exposed on a rack at the test site facing south with an angle of 30° from the ground. The samples were exposed at the test site for 1322 days. Table 2 gives an overview of the climatic conditions at the test site during the exposure period and the current normal period (NP). Temperature, precipitation, and solar radiation on a horizontal plane are measured on site. The primary wind direction is 202.5 degrees from north, equivalent with SSW. Solar radiation and wind driven rain are assumed to be the main driving forces behind color changes and surface degradation of wood samples. Solar radiation varies substantially with the latitude of the location. Close to the equator, there are almost no seasonal variations to be found, hence, solar radiation values are fairly constant throughout the year. Further north, close to the arctic circle, variations in solar radiation is remarkable due to seasonal variations. Moreover, radiation values vary with the locations' elevation above sea level, the time of the day, and the nature of the cloud cover (26). Solar radiation data for inclined surfaces may be obtained from various data bases. A comparison of solar radiation data measured on site and data obtained from a solar radiation database (SoDA) showed good correlation. To emphasis variation in climatic strains for different exposure directions, Table 3 presents solar radiation and wind driven rain data for vertical surfaces (inclination 90°) exposed north, south, east, and west, and rack (inclination 30°). Wind driven rain data is measured at another test building on the same site. A more detailed description of those measurements and its test set up can be found in Nore et al. (27).

### *2.2. Artificial weathering*

Artificial weathering tests were performed in two apparatuses: An ATLAS solar simulation chamber and a rotating climate chamber (RCC). The ATLAS solar simulator can be programmed according to the users' requirements, while the RCC runs in a fixed cycle that is defined in NT Build 495 (28). The ATLAS SC 600 MHG solar simulation chamber is equipped with a 2500 W metal halide global lamp which dissipates a spectral distribution similar to that of sunlight, wavelengths ranging from 280 nm to 3000 nm. Samples are exposed on a horizontal grillage. The rotating climate chamber (RCC) is designed based on specifications in NT Build 495, see also Brandt and Nilsen (29). The apparatus consists of a rotating central unit containing the test specimens located on four sides, each capable of carrying a vertically mounted test specimen of maximum 1.5 m x 2.5 m (width x height). The central unit rotates 90° every hour, which thus passes the test specimens into four different exposure environments: UV and IR radiation, water spray, frost, and laboratory climate. Four different test cycles were run in the ATLAS solar simulator, one in the RCC. Table 4 presents test specifications for the different runs for the artificial laboratory ageing tests.

## 3. Color analysis

Color models may be used to quantify color and color changes. Most of them are based on a standard devel-

Table 1: Materials, oven-dried densities, and average initial color values for all materials used

| No. | Material | Latin name | Density [kg/m$^3$] | Initial color values L-value | a-value | b-value |
|---|---|---|---|---|---|---|
| 1 | Norway Spruce[a] | *Picea abies (L.) H. Karst.* | 411.7 | 80.6 | 6.0 | 24.5 |
| 2 | Norway Spruce | *Picea abies (L.) H. Karst.* | 456.6 | 79.2 | 6.1 | 24.2 |
| 3 | Scots Pine heartwood | *Pinus silvestris L.* | 478.5 | 73.1 | 11.3 | 31.0 |
| 4 | Aspen | *Popolus tremula L.* | 493.8 | 79.3 | 5.0 | 23.8 |
| 5 | Larch | *Larix decidua Mill.* | 492.8 | 56.2 | 12.6 | 31.9 |
| 6 | Kebony Furu (Scots pine)[b] | *Pinus silvestris L.* | 542.1 | 23.3 | 5.9 | 18.5 |
| 7 | Kebony SYP (Southern yellow pine)[c] | *Pinus taeda* | 731.1 | 27.7 | 4.0 | 16.0 |
| 8 | Scots Pine, royal impregnation[d] | *Pinus silvestris L.* | 432.9 | 48.2 | 1.3 | 35.2 |
| 9 | Scots Pine, pressure treated[e] | *Pinus silvestris L.* | 496.5 | 34.0 | 5.2 | 24.5 |

[a] Ruptimal® surface, mechanically roughened surface [b] untreated heartwood and sapwood treated with furfuryl alcohol [c] sapwood, treated with furfuryl alcohol [d] as no. 7, add. impregnation with colored linseed oil [e] class NP5 (chemical treated according to (25)).

Table 2: Temperature, precipitation, and solar radiation on a horizontal plane measured by *DNMI* at the Voll test site (Trondheim) during exposure period.

| | | Jan | Feb | Mar | Apr | May | June | July | Aug | Sep | Oct | Nov | Dec | Average | Total |
|---|---|---|---|---|---|---|---|---|---|---|---|---|---|---|---|
| Temperature [°C] | NP | -3.3 | -2.7 | 0.1 | 3.6 | 8.7 | 12.0 | 13.2 | 12.7 | 9.0 | 5.6 | 0.3 | -2.0 | 4.7 | |
| | 2005 | 1.6 | -1.2 | 0.1 | 5.6 | 7.2 | 11.1 | 15.8 | 12.9 | 10.5 | 7.7 | 4.0 | -0.8 | 6.2 | |
| | 2006 | 0.2 | -0.7 | -4.1 | 4.5 | 9.3 | 12.4 | 15.8 | 17.3 | 12.7 | 6.7 | 4.2 | 4.5 | 6.9 | |
| | 2007 | -0.5 | -4.0 | 3.5 | 4.7 | 8.2 | 14.1 | 15.7 | 13.3 | 8.6 | 6.0 | 1.0 | 0.2 | 5.9 | |
| | 2008 | 0.6 | 1.3 | 0.5 | 5.6 | 9.3 | 13 | 16.1 | 13.7 | 10.4 | 6.5 | 2.2 | -0.6 | 6.6 | |
| Precipitation [mm] | NP | 76 | 59 | 59 | 49 | 46 | 63 | 81 | 76 | 110 | 103 | 78 | 90 | 74 | 890 |
| | 2005 | 116 | 60 | 23 | 32 | 45 | 73 | 21 | 117 | 105 | 41 | 66 | 125 | 69 | 633 |
| | 2006 | 94 | 126 | 49 | 29 | 46 | 37 | 54 | 40 | 69 | 98 | 74 | 99 | 68 | 815 |
| | 2007 | 138 | 59 | 51 | 82 | 49 | 18 | 128 | 105 | 115 | 97 | 200 | 30 | 89 | 1072 |
| | 2008 | 62 | 107 | 61 | 22 | 34 | 54 | 38 | 58 | 52 | 69 | 124 | 31 | 59 | 712 |
| Solar radiation [kWh/m$^2$] | 2005 | 3 | 18 | 56 | 109 | 122 | 122 | 141 | 87 | 53 | 29 | 6 | 2 | 62 | 748 |
| | 2006 | 3 | 15 | 63 | 109 | 139 | 129 | 148 | 120 | 55 | 24 | 6 | 1 | 68 | 812 |
| | 2007 | 3 | 21 | 55 | 75 | 112 | 161 | 133 | 93 | 51 | 24 | 5 | 2 | 61 | 711 |
| | 2008 | 3 | 14 | 61 | 101 | 134 | 143 | 155 | 113 | 69 | 23 | 6 | 2 | 69 | 824 |

Table 3: Solar radiation and wind driven rain on inclined (vertical) surfaces at Voll test site (Trondheim), accumulated over exposure period, for Voll test site, Trondheim, February 2005 to August 2008.

| | Horizontal | North | South | East | West | Rack |
|---|---|---|---|---|---|---|
| Solar radiation [kWh/m$^2$] | 3557 | 986 | 2745 | 2060 | 2111 | 3805 |
| Percentage of solar radiation on a horizontal plane [%] | 100 | 27.7 | 77.2 | 57.9 | 59.4 | 107.0 |
| Wind driven rain [l/m$^2$] | (2998) | 74 | 315 | 18 | 482 | - |
| Percentage of precipitation [%] | 100 | 2.5 | 10.5 | 0.6 | 16.1 | - |

oped by the International Commission on Illumination (CIE) (24). They attempt to describe color according to human color perception. These color models use numeric values to represent the visible spectrum of color. The color model determines the relationship between values, and the color space defines the absolute meaning of those values as colors. The CIE L*a*b* model describes color in terms of its lightness component (L*) and two chromatic components, a* and b*. A positive value of a* denotes a more red color on a green-red scale, whereas a positive value of b* denotes a more yellow color on a blue-yellow scale. Together, those three components form a three-dimensional color space. L*, the lightness component ranges from 0 (black) to 100 (white), representing the achromatic axis of grays. a* and b* range from -128 to 127. According to (30) color differences can be calculated by determining the Euclidean distance between two colors as (31, 32)

$$\Delta E^* = \sqrt{(\Delta L^*)^2 + (\Delta a^*)^2 + (\Delta b^*)^2} \quad (1)$$

By summing up $\Delta E^*$ for all analyzed points in time, the course of the color changes can be taken into account:

$$\sum_{i-1,i}^{n} = \Delta E^*_{0,1} + \Delta E^*_{1,2} + ... + \Delta E^*_{n-1,n} \quad (2)$$

Chroma C* is defined as the Euclidean distance between a color and its achromatic point of the same lightness:

$$C^* = \sqrt{a^{*2} + b^{*2}} \quad (3)$$

Chroma differences can be calculated as

$$\Delta C^*_{1,2} = C^*_2 - C^*_1 = \sqrt{a^{*2}_2 + b^{*2}_2} - \sqrt{a^{*2}_1 + b^{*2}_1} \quad (4)$$

To determine the color development of the outdoor exposed samples, test specimens are demounted periodically. After conditioning in a standard climate (20°C, 60 % RH) until equilibrium moisture content, samples are scanned. Samples tested in the laboratory are taken out for evaluation at the same time of the weathering cycle. Color values are obtained using Matlab® corrected by means of a color profile obtained by a scanner target according to ISO 12641 (1997)(33). Additional color measurements using a colorimeter Datacolor Mercury 3000 showed that the scanning method produced equally reliable results.

### *3.1. Acceleration factors*

Acceleration factors may be calculated in order to estimate required ageing time in the laboratory climate ageing apparatus, thus relating the accelerated climate ageing to the desired service lifetime of the product. The higher UV intensity [W/m$^2$] and total energy [kWh/m$^2$] in the ageing apparatus, the higher acceleration factor for the climate ageing. The UV acceleration factor $AF_{uv}$ may be calculated as directly proportional to the ratio between the total UV energy in the laboratory ageing apparatus $\Phi_{lab}$ and the natural outdoor ageing $\Phi_{nat}$ for a given time period:

$$AF_{UV} = \Phi_{lab}/\Phi_{nat} \quad (5)$$

This is valid as long as one may assume that all the UV radiation contributes to initiate degradation reactions, in addition to an equal spectral distribution for artificial and natural UV radiation, which naturally is never completely fulfilled. The chemical degradation processes increase exponentially with increasing temperature (Arrhenius equation). A temperature acceleration factor $AF_{temp}$ may then be calculated as the ratio between the reaction rate in the laboratory ageing apparatus $k_{lab}$ and the natural outdoor ageing $k_{nat}$:

$$AF_{temp} = k_{lab}/k_{nat} = \frac{C_{lab}e^{E_{lab}/(RT_{lab})}}{C_{nat}e^{E_{nat}/(RT_{nat})}} \frac{e^{E_{lab}/(RT_{lab})}}{e^{E_{nat}/(RT_{nat})}} \quad (6)$$

where $T_{lab}$ and $T_{nat}$ denote the temperature in laboratory ageing apparatus and the natural outdoor ageing, respectively. R is the gas constant. It is here assumed that the pre-exponential factor C is temperature independent which gives $C_{lab} \approx C_{nat}$. Furthermore, it is also assumed that the activation energy E is temperature independent, e.g. set to $E_{lab}$=$E_{nat}$ = 70 kJ/mol. In a simplified model one may assume that the total acceleration factor $AF_{tot}$ equals the product of $AF_{uv}$ and $AF_{temp}$:

$$AF_{tot} = AF_{uv} \cdot AF_{temp} \quad (7)$$

These calculations are of course a strong simplification. The other climate factors as mentioned above, e.g. water, will influence $AF_{tot}$. The acceleration factor is strongly dependent upon the chosen reference level, i.e. the natural outdoor ageing comparison exposure level, e.g. $T_{nat}$. In order to determine the real $AF_{tot}$ one may strictly not base the calculations upon annual or daily values for $\Phi_{nat}$ and $T_{nat}$ ($k_{nat}$), on the contrary rather perform calculations with short time intervals which hence are integrated. Nevertheless, the simplified model may be applied for various mutual comparisons by accelerated climate ageing in the laboratory. One also has to compare the laboratory results with outdoor tests in natural climate.

Calculated total acceleration factors (UV plus temperature) are given in Table 4, ranging from about 5 to 250. The calculations may most easily be performed

based on 24 h cycles. Note that these values are based on temperature acceleration factors corrected (reduced) for the colder ($T_{lab} \leq T_{nat}$) time periods without solar radiation exposure. In addition, $T_{nat}$ = 22°C and $\Phi_{nat} = 0.67 \cdot 5\ GJ/m^2 = 3.35\ GJ/m^2$ have been chosen as the natural outdoor ageing temperature and the annual solar radiation reference levels (borderline between moderate and severe climate), see (34) for further information.

After determining color values L*, a* and b* they are plotted against exposure time. Nine materials are investigated in this study, of which two materials are chosen to illustrate the results within this context: Pine heartwood and Kebony Furu. Pine heartwood presents the group of materials that are untreated, Kebony Furu the group of materials that have been treated.

## 4. Results and discussion

### *4.1. Outdoor weathering*

In Figure 2 (a-c) color values (L*, a*, b*) are plotted against exposure time for Scots Pine heartwood, the respective scanned images are presented in Figure 1. At the end of the investigated exposure time, only minor difference in lightness values for east, south, and north exposed samples can be observed. Lightness values for west and rack exposure end up at the same level which is much lower than the other samples. The rate of change in a* and b* values are decreasing over time. For both a* and b* values, the sample exposed on the rack stands out by a significantly higher rate of color changes in the beginning. a* values for the sample exposed on the rack and to the west drop beneath 0, which means the remaining chromatic values changes from ”red” to ”green”. However, a* or b* values close to zero means that samples are close to being achromatic, i.e. grey. In summary, differences in color development found by visual inspection are supported by the analysis of the graphs. Samples exposed to the north, south, and east are both similar in visual appearance and color values. The samples exposed to the west and on the rack are somewhat similar in appearance after the exposure period, though both visual inspection and color values illustrate clearly the differences in color development. Figure 3 illustrates the course of color changes in Kebony Furu. Lightness values (Figure 3 a) increase rapidly in the beginning of the exposure, the samples turn lighter. At the end of the exposure time, lightness values for all samples vary only by approximately 4 %. a* values show an initial increase for all exposure directions after the first evaluation after 66 days. This increase in chroma, similar with the Scots Pine samples, is terminated after already the second evaluation after 122 days, followed by a decrease, which is of different extent depending on exposure direction. The sample exposed on the rack is experiencing the greatest decrease in a* values. At third evaluation after 194 days, a* values for this sample have dropped beneath zero, from ”red” to ”green”. In the course of time, west and north exposed samples also drop as far as to the ”green” side, while the process seems to have slowed down for the south and east exposed samples. b* values show somewhat the same development. Values for the sample placed on the rack are dropping faster than the others. For the other samples, east and south exposed ones follow the same course, while north and west exposed ones show higher rates in changes in b* values. In summary, also for Kebony Furu, the course of the graphs is supported by visual inspection. Color development is somehow similar for all exposure directions, L* values range little, while a* and b* values, representing chroma can vary widely. But, due to the darker initial color of the Kebony Furu samples, visual inspection is more difficult than for Scots pine. Though, by means of color measurement even minor variations might be detected.

### *4.2. Laboratory weathering*

Color values measured for laboratory exposure are presented in Figure 4for Scots Pine heartwood and in Figure 5 for Kebony Furu. Due to a much longer test period, color values for the Rotating Climate Chamber (RCC) are presented in Figure 2 and 3together with the ones from outdoor exposure. In summary, results obtained from laboratory testing suggest that sectioning the same strain per 24 hours differently, as for run 1 and run 2, plays a major role in color development. Furthermore, results suggest that temperature plays a major role, as L* values develop significantly different for run 2 and run 3, where the testing temperature is lowered from 63 °C to 22 °C. Changes in color values for Kebony Furu, presented in Figure 5 do not show the same distinct pattern as for Scots Pine heartwood. L* values for run 1 are almost unchanged in the beginning of the test, decreasing slightly. Run 2 shows a similar course, though values are increasing and decreasing, so they do not seem to be conclusive. L* values for run 3 stand out from the other runs: L* is increasing fast, the sample turns lighter. The rate of the change is slowing down already after the first evaluation after 24 hours, though, after 10 days of exposure, values differ significantly from those obtained by the other runs. a* values show a decrease with about the same rate for runs 1, 2, and 3. For run 4, a values drop to the ’green side’ already at first evaluation after 1 day. However, the initial

Table 4: Complete overview over test conditions for laboratory weathering for the ATLAS solar simulator (ASS) (Run 1-4) and the rotating climate chamber (RCC).

| Run | Exp. time [days] | Light [hours] per 24 hrs | Irrad. [W/m$^2$] | Irrad. [kWh/m$^2$] per 24 hrs | Total irrad.[a] [kWh/m$^2$] | Water [hours] per 24 hrs | Water [l/(m$^2$h)] | Water [l/m$^2$] per 24 hrs | Total water[a] [l/m$^2$] | Temp.[b] [°C] | RH[b] [%] | $AF_{tot}$ [e] [-] |
|---|---|---|---|---|---|---|---|---|---|---|---|---|
| 1 | 112 | 20 | 1200 | 24 | 2688 | 4 | 102 | 408 | 45 696 | 63 | 50 | 250 |
| 2 | 26 | 5 times 4 | 1200 | 24 | 624 | 1 times 4 | 102 | 408 | 10 608 | 63 | 50 | 250 |
| 3 | 10 | 5 times 4 | 1200 | 24 | 240 | 1 times 4 | 102 | 408 | 4 080 | 22 | 50 | 9 |
| 4 | 42 | 5 times 4 | 600 | 12 | 504 | 1 times 4 | 102 | 408 | 17 136 | 63 | 50 | 130 |
| RCC | 888 | 6 times 1 | 257 [c]<br>15.4 [d] | 1.5 [c]<br>0.0924 [d] | 1369 [c]<br>82 [d] | 6 times 50 min | 15 | 75 | 66 600 | 63 | - | 5 |

[a] accumulated entire exposure time [b] during solar radiation [c] calculated solar radiation [d] measured UV radiation

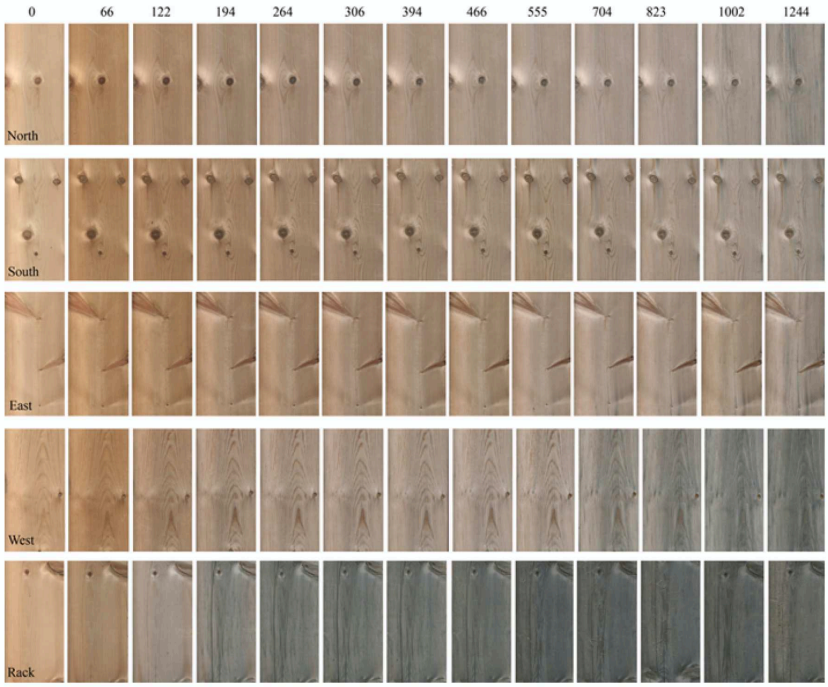


Figure 1: Scots Pine heartwood (sample no. 3), scanned images from the outdoor weathering experiment. Numbers on top indicate exposure time in days. From top to bottom: North, south, east, west, and south facing rack exposure.

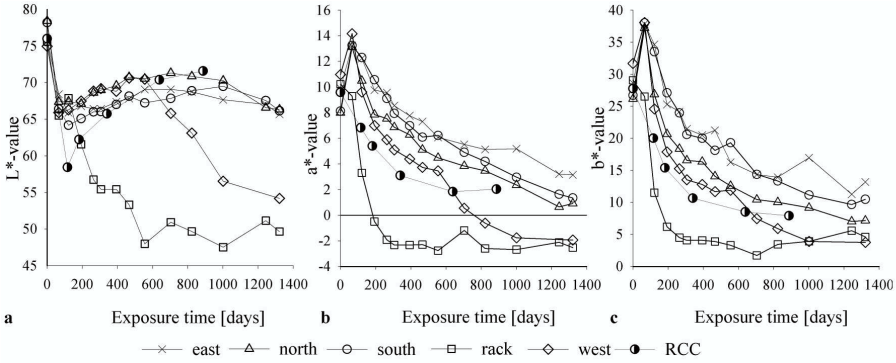


Figure 2: Scots Pine heartwood (sample no. 3), color values (L, a and b) for outdoor exposure and for RCC laboratory exposure.

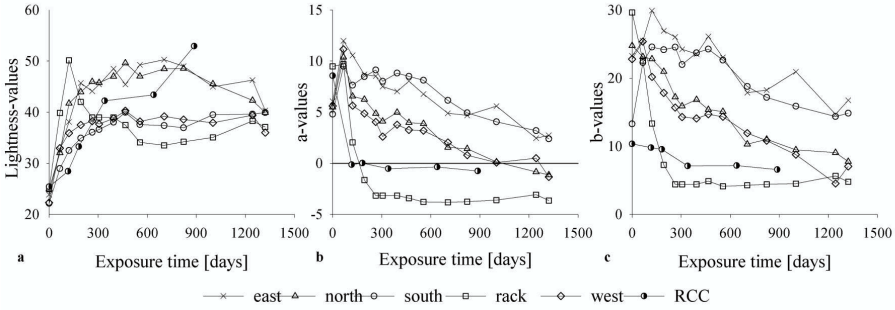


Figure 3: Kebony Furu (sample no. 6), color values (L, a, b) for outdoor exposure and for RCC laboratory exposure.

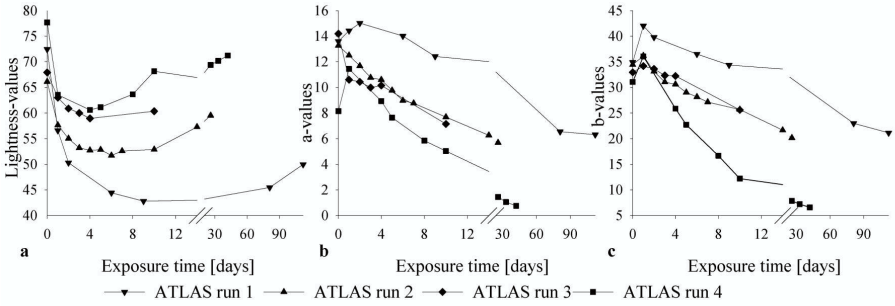


Figure 4: Scots Pine heartwood (sample no. 3), color values (L, a and b) for *ATLAS* laboratory exposure.

a* value for run 4 differs considerably from the ones for run 1 to 3, so the result is inconclusive. The same applies to b* values, the rate of decrease for run 4 matches the changes for the other runs, but the initial value differs considerably. Both a* and b* values decrease from the beginning, their rate decreasing after already the first evaluation after one day. The only exception are b* values for run 3 where a considerable increase can be observed up until the second evaluation, before values start to decrease at about the same rate as for the other runs. Color values for Kebony Furu samples exposed in the RCC are shown in Figure 5. Lightness values increase from the start, first with a lower, later with a higher rate than the outdoor exposed samples. Also, the changes in lightness values do not seem to stop and the sample gets lighter and lighter. a* and b* values for the RCC exposed sample show a decrease from the beginning on and a rate that is decreasing over time. Altogether, results differ from the ones found for Scots Pine heartwood. Run 1 and 2 cause an approximate similar course of color change, that means in this case, the same load causes approximately the same result. Furthermore, taking into account the deviation of the initial color values for the sample in run 4, color changes caused by run 4 are in accordance with color changes from run 1 and 2. These results suggest that the irradiation level does not play a major role for the observed color changes in these experiments, since for this run radiation is reduced with 50 % compared to the other runs. Also, run 3, where the temperature is reduced to 22 °C, shows a very different pattern of color development.

### *4.3. Outdoor vs. laboratory weathering*

For Scots Pine heartwood, the overall course of the color changes is somewhat similar for all the runs conducted in the laboratory, but also appears to be quite different from observations made at outdoor exposure. Outdoor exposed samples get darker at first and then turn lighter and lighter, which is supported by both visual inspection and color measurements. Samples exposed to the laboratory weathering cycles used in this study, turn darker to varying extend. Exposed over a longer period to those cycles though, samples also to show a form of bleaching, where they turn lighter again. For a* and b* values, only the test in the RCC can somewhat recreate the development quantitatively. In summary, samples exposed to the different runs in ATLAS show less loss in chroma compared to outdoor exposed samples. Also, there is no initial increase in a* and b* values that is common to all the samples exposed outdoors. For Kebony Furu, the course of changes in L* values is significantly different for outdoor and laboratory exposure tests. Outdoor exposed samples turn lighter, the rate of the changes slowing down with time, before they start to turn darker again. Samples exposed to ATLAS weathering cycles are relatively stable in L* values for run 1, 2, and 4, while run 3 causes a significant increase in L* values. In summary, none of the weathering cycles conducted in the ATLAS solar simulator recreated the effects of outdoor weathering, neither for Scots Pine heartwood nor for Kebony Furu. Acceleration factors for laboratory ageing are calculated in section 3.1. The results of the color analysis suggest that run 3, with a calculated acceleration factor of 8 and ageing in the RCC with a calculated acceleration factor of 5 are most suitable in terms of recreating somehow the color changes observed outdoors.

### *4.4. Overall color changes delta E*

In order to describe and compare the observed color changes and the different materials further, three measures are implemented: $\Delta E^*$ (see Equation 1) is defined as the color difference between the initial and the final stage. $\sum \Delta E^*$ (see Equation 2) is the sum of all color differences between each analyzing date and $\Delta C^*$ (see Equation 4) is the chroma difference between the initial and final stage.

Table 5 and Table 6 give an overview over the initial and final color values for both outdoor and laboratory exposure. Measured values L*, a*, and b* are presented together with the calculated values for C. For Scots Pine heartwood, values for $\Delta C$ are positive for all outdoor exposure directions, all samples decrease in chroma, turn grey. Though this is common to all exposure directions, west and rack exposure result in the highest values for $\Delta C$. The same applies to $\Delta E$. West and rack exposure result in the highest values, hence the largest changes in appearance. East shows the lowest rate of color changes, though values for north and south range in the same dimension. Values for $\Delta E$ indicate that the course of the color changes is quite similar for all exposure directions. The final $C$ values for west and rack exposure are the lowest ones, in accordance with visual observations, these samples experiences the greatest loss in color. In contrast, south and east exposed samples are the ones that are the most chromatic after the exposure period. Compared to the results for Scots Pine heartwood, results for Kebony Furu show certain differences. Though total color changes $\Delta E$ are highest for rack exposure, values for north and west exposure are somewhat alike, so are values south and east exposure. The values for $\Delta E$ suggests that the samples experienced the same overall color changes as the

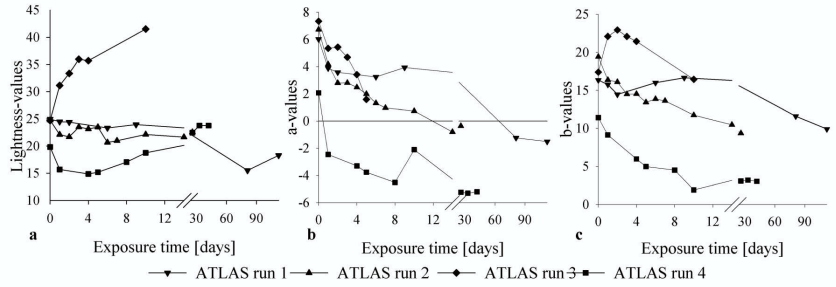


Figure 5: Kebony Furu (sample no. 6), color values (L, a and b) for *ATLAS* laboratory exposure.

Table 5: Color values and color changes for outdoor for Scots Pine heartwood (sample no. 3).

| | | Exposure direction | | | | |
|---|---|---|---|---|---|---|
| | | North | South | East | West | Rack |
| Initial color values | L | 78.41 | 78.20 | 75.93 | 74.94 | 75.60 |
| | a | 7.99 | 8.12 | 9.92 | 10.98 | 10.22 |
| | b | 26.16 | 26.70 | 28.62 | 31.67 | 29.07 |
| | C | 27.35 | 27.90 | 30.29 | 33.52 | 30.81 |
| Final color values | L | 66.31 | 66.14 | 65.69 | 54.18 | 49.64 |
| | a | 0.91 | 1.33 | 3.14 | -1.95 | -2.53 |
| | b | 7.17 | 10.48 | 13.18 | 3.75 | 4.60 |
| | C | 7.22 | 10.56 | 13.55 | 4.22 | 5.25 |
| Color differences | $\Delta E$ | 23.60 | 21.32 | 19.73 | 37.12 | 37.88 |
| | $\sum\Delta E$ | 53.48 | 55.26 | 52.44 | 61.52 | 59.94 |
| | $\Delta C$ | 20.13 | 17.34 | 16.74 | 29.30 | 25.56 |

Table 6: Color values and color changes for outdoor exposure for Kebony Furu (sample no. 6).

| | | Exposure direction | | | | |
|---|---|---|---|---|---|---|
| | | North | South | East | West | Rack |
| Initial color values | L | 24.97 | 22.17 | 23.88 | 22.29 | 24.96 |
| | a | 5.49 | 4.81 | 6.07 | 5.61 | 9.48 |
| | b | 24.74 | 13.29 | 23.27 | 22.79 | 29.63 |
| | C | 25.35 | 14.13 | 24.04 | 23.47 | 31.11 |
| Final color values | L | 39.93 | 39.93 | 40.33 | 36.00 | 37.11 |
| | a | -1.13 | 2.39 | 2.74 | -1.32 | -3.63 |
| | b | 7.76 | 14.84 | 16.74 | 7.05 | 4.80 |
| | C | 7.84 | 15.04 | 16.97 | 7.17 | 6.01 |
| Color differences | $\Delta E$ | 23.59 | 17.98 | 18.01 | 22.00 | 30.60 |
| | $\sum\Delta E$ | 51.61 | 43.01 | 68.24 | 43.07 | 59.79 |
| | $\Delta C$ | 17.51 | -0.91 | 7.08 | 16.30 | 25.10 |

Pine samples. *C* values range in the same magnitude as for Pine with south and east exposed samples being the most chromatic after exposure, indicating that there is an increase in chroma.

### *4.5. Interrelation of climatic strains and color changes*

No direct interrelation between solar radiation dose and changes in lightness values could be established. Similarly, there is no strong connection to be found between the other color values a* and b*, and other climatic factor investigated as driving rain, temperature or relative humidity. These findings suggest that the interrelation between climatic strains and color changes is rather complex. Hence, the identification of the predominant climatic strain is a difficult task. There are several factors that interact, solar radiation and elevated temperature, water and temperature (e.g. freezing and thawing), wind and rain (wind-driven rain).

In contrast, the number of climatic strains in the laboratory is reduced to what is assumed to be the predominant ones: controlled amounts of solar radiation, water spray, and temperature. Run 1 and 2 apply the same amount of radiation and water spray only in a different succession, run 3 applies a lower temperature, and run 4 reduces the radiation dose. Hence, color development should be similar for run 1 and 2. Run 1 causes considerable greater changes in lightness values than run 2. For Kebony Furu, see Figure 5, color changes for run 1 and run 2 result in a similar course of changes in lightness values. Hence, similar radiation doses can cause different color development depending on the succession of the applied strains.

### *4.6. All nine materials*

The above findings for the development of color changes apply also to the other materials investigated in this study. The pattern for color changes, both for outdoor and laboratory exposure is somewhat distinct for untreated wood species (Norway Spruce, Norway Spruce (Ruptimal surface), Scots Pine heartwood, Aspen, and Larch) and treated materials (Kebony Furu, Kebony SYP, Scots Pine royal treated, and Scots Pine pressure treated). As an example to illustrate the above findings, Figure 6 shows color values for all materials

Table 7: Average lightness values of all samples after exposure for 1322 days for vertically and horizontally oriented annual rings.

| Mat. | 1 | 2 | 3 | 4 | 5 | 6 | 7 | 8 | 9 |
|---|---|---|---|---|---|---|---|---|---|
| North | | | | | | | | | |
| Vert. | 60.5 | 65.6 | 66.3 | 55.3 | 55.2 | 39.9 | 44.7 | 53.3 | 60.2 |
| Hori. | 47.3 | 50.9 | 56.3 | 51.3 | 40.9 | 36.5 | 34.3 | 47.6 | 51.1 |
| South | | | | | | | | | |
| Vert. | 57.7 | 66.2 | 68.5 | 57.7 | 63.9 | 40.8 | 30.8 | 56.9 | 53.5 |
| Hori. | 56.5 | 56.7 | 57.8 | 43.1 | 42.5 | 30.1 | 30.5 | 52.8 | 46.7 |
| East. | | | | | | | | | |
| Vert. | 52.0 | 64.6 | 65.5 | 63.4 | 49.4 | 35.8 | 28.5 | 54.6 | 51.4 |
| Hori. | 43.3 | 43.3 | 46.4 | 41.6 | 40.6 | 25.4 | 29.7 | 45.1 | 52.0 |
| West. | | | | | | | | | |
| Vert. | 53.7 | 54.3 | 53.5 | 50.6 | 52.5 | 37.5 | 31.4 | 58.0 | 48.1 |
| Hori. | 46.2 | 46,8 | 45,6 | 48,3 | 39,9 | 26,3 | 19,2 | 49,6 | 44,9 |

used in this study for rack exposure. Note that the initial darkening of the samples is common to all untreated wood species (nos. 1 to 5), while treated ones initially become lighter (nos. 6 to 9). Also the change in a* value from "red" to "green" is common for all materials. In general, all materials are getting more alike in color compared to the initial state. The above mentioned distinction between untreated and treated materials applies to laboratory weathering as well, though in this case pressure treated wood follows the same pattern in color development as untreated materials, see Figure 7.

### *4.7. Mold growth*

One major difference between outdoor and laboratory exposure are biological components, more precisely fungal growth that results in an additional dark coloring of untreated wood surfaces. At the end of the exposure time, samples of fungal organisms on the sample surfaces were taken with a tape lift. Fungal species on the tape were identified using a microscope using an evaluation scale from 0 (no growth) to 4 (rich growth). The species that can be exclusively found on the samples is *Aureobasidium pullulans*, a species that is commonly found on wood substrates. The results indicate most mold growth (for all materials) for west and rack exposed samples and least mold growth for south exposed samples. There is no distinct difference for north and east exposed samples, though there is generally less mold growth for those exposure directions. There is no significant difference to be found between the materials. For west exposure, where there is rich mold growth on all panels, there is somehow a little less on the royal impregnated sample. For the other exposure directions, there is a tendency towards less growth on the impregnated samples and for Kebony SYP for east exposure. Some of the samples exposed on the test building have been mounted with annual rings oriented horizontally. As shown in Table 7 lightness values for samples that are mounted with vertically oriented annual rings differ considerably from the ones mounted with horizontally oriented annual rings. Most of the samples mounted with horizontally mounted annual rings show a lower final lightness value, i.e. the samples mounted with horizontally oriented annual rings are darker that the ones mounted with vertically oriented ones. This observation suggests a higher mold growth rate for samples mounted with horizontally oriented annual rings. The analysis of the lift from fungal samples taken from Pine heartwood somewhat confirms that observation: For all exposure directions except west, there is more mold growth to be observed on the samples exposed with horizontally oriented annual rings. Figure 8 a shows a microscope picture of an east exposed sample which was mounted with horizontally oriented annual rings and Figure 8 b shows the respective picture for vertically oriented annual rings. There is a considerable difference in the amount of mold growth for the two samples. One possible reason for this could be that horizontally oriented annual rings offer an in-creased surface area with trapped moisture where biological material is more likely to deposit.

## 5. Conclusions

Nine different wooden board materials have been investigated in this study by natural outdoor ageing and accelerated laboratory ageing, where color measurements have been applied as a quantitatively tool along with visual inspection. The wooden materials could roughly be assorted in two groups in terms of their pattern of color changes: Untreated wood species and impregnated materials. The underlining cause for the different color development might be the darker initial color of the treated materials, subsequently a higher surface temperature and radiation absorption. This effect combined with the altered surface chemistry is presumably the cause for the color development observed in this study. The wooden samples receiving the highest levels of solar radiation and wind-driven rain, i.e. south on rack and west exposed samples, showed as expected the most rapid and dramatic color developments. After over three years of exposure the different wooden materials could hardly be distinguished, where none of the materials stood out significantly in terms of maintaining its original color. Furthermore, no quantitative relation between climatic strains and color changes could be established.

A comparison between outdoor and laboratory weathering revealed that color changes caused by out-

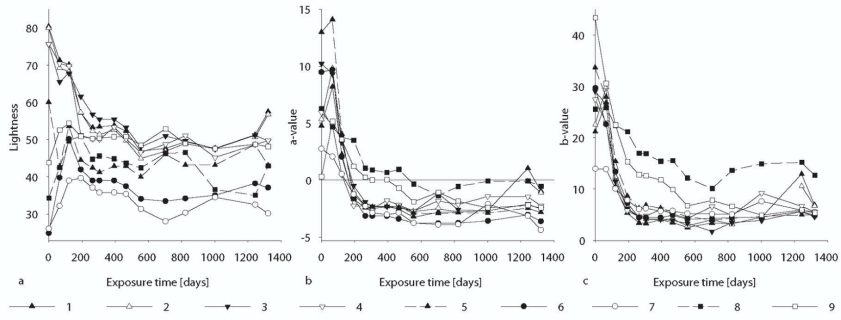


Figure 6: Color values (L, a, and b) for all materials (samples nos.1-9) investigated in this study, numbers refer to Table 1 for exposure on south facing rack.

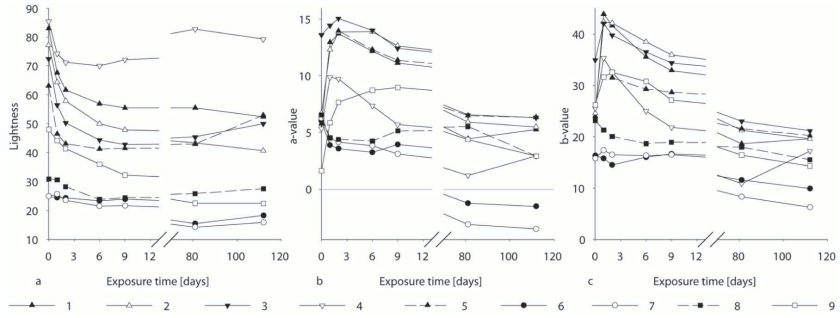


Figure 7: Color values (L, a, and b) for all materials (samples nos.1-9) investigated in this study, numbers refer to Table 1 for *ATLAS* laboratory exposure run 1.

Figure 8: Norway Spruce (Material 2), annual rings horizontally (a) and vertically (b) oriented , east exposure 1322 days, magnification 10.

door exposure lead to the conclusion that none of the laboratory weathering cycles applied managed to recreate the same pattern of color development as outdoor exposure. This suggests that the complexity of the natural exposure conditions cannot be overestimated. Another reason is the lack of fungal spores during laboratory exposure that contribute considerably to the grey appearance of weathered wood. However, laboratory weathering is a useful tool since the climatic strains applied are controllable and may be accelerated substantially. For laboratory weathering it was found that both solar radiation intensity and temperature, but also the succession in which the different strains are applied, play a major role in how fast and extensive the color changes develop. In order to understand color development of wood in exterior applications it is important to be aware of the variations of the exposure environment. This study is a first step towards providing a quantitative overview over both the color changes of commonly used wooden materials for outdoor applications and the prevailing climatic strains that lead to those.

## References


[1] Borgin K. The mechanisms of the breakdown of the structure of wood due to environmental factors. Journal of the Institute of Wood Science 1971;4:26–30.

[2] Hon DNS, Minemura N. Wood and Cellulosic Chemistry; chap. Color and Discoloration. Marcel Dekker, New York; 2 ed.; 2001, p. 385–442.

[3] Pandey KK. Study of the effect of photo-irradiation on the surface chemistry of wood. Polymer Degradation and Stability 2005;90:9–20.

[4] Sell J, Leukens U. Über die aussenklimatische und biologische Beanspruchung von unbehandelten und angestrichenen Holzoberflächen, 1.Teil: Chemische, mechanische und farbliche Alterungserscheinungen. Oberfläche-Surface 1969;10(8):536–9.

[5] Wälchli O. Über die aussenklimatische und biologische Beanspruchung von unbehandelten und angestrichenen Holzoberflächen, 2.Teil: Biologische Aspekte. Oberfläche-Surface 1969;10(9):619–23.

[6] Kühne H, Leukenes U, Sell J, Wälchli O. Scanning electron microscope observations on mold-fungi causing grey stain. Holz als Roh-und Werkstoff 1970;28(6):223–9.

[7] Hon DNS, Chang ST. Surface degradation of wood by ultraviolet light. Journal of Polymer Science 1984;22:2227–41.

[8] Wypych G. Handbook of Material Weathering. ChemTech Publishing; Third ed.; 2003.

[9] Evans P, Schmalzl K, Michell A. Rapid loss of lignin at wood surfaces during natural weathering. Cellulosics: Pulp, Fibre and Environmental Aspects 1993;.

[10] Feist W, Hon DS. Chemistry of weathering and protection. 1984,.

[11] Futó LP. Einfluss der Temperatur auf den photochemischen Holzabbau, 1. Mitteilung: Experimentelle Darstellung. Holz als Roh- und Werkstoff 1976;34:31–6.

[12] Futó LP. Einfluss der Temperatur auf den photochemischen Holzabbau, 2. Mitteilung: Rasterelektronenmikroskopische Darstellung. Holz als Roh- und Werkstoff 1976;34:49–54.

[13] Williams R. Wood Chemistry and Wood Composites; chap. Weathering of Wood. CRC Press; 2005,.

[14] Sharratt V, Hill C, Kint D. A study of early colour change due to simulated accelerated sunlight exposure in scots pine. Polymer Degradation and Stability 2009;.

[15] Feist W, Mraz E. Comparison of outdoor and accelerated weathering of unprotected softwoods. Forest Products Journal 1978;28(3):38–43.

[16] Sell J, Feist WC. Role of density in the erosion of wood during weathering. Forest Products Journal 1986;36(3):57–60.

[17] Evans P. Effect of angle of exposure on the weathering of wood surfaces. Polymer Degradation and Stability 1989;24:81–7.

[18] Arnold M, Sell J, Feist WC. Wood weathering in fluorecent ultraviolet and xenon arc chambers. Forest Products Journal 1991;41(2):40–4.

[19] Brown R. Predictive techniques and models for durability tests. Polymer testing 1995;14(5):403–14.

[20] Meeker W, Escobar L, Lu C. Accelerated degradation tests: Modeling and analysis. Technometrics 1998;40(2):89–99.

[21] Pandey KK, Vuorinen T. Comparative study of photodegradation of wood by uv laser and a xenon light source. Polymer Degradation and Stability 2008;93:2138–46.

[22] Jelle BP, Rüther P, Hovde PJ, Nilsen TN. Proceedings of the 11th international conference on durability of building materials and components. In: Attenuated Total Reflectance (ATR) Fourier Transform Infrared (FTIR) Radiation Investigations of Natural and Accelerated Climate Aged Wood Substrates. 2008,.

[23] Sell J, Leukens U. Weathering phenomena of unprotected wood species. Holz als Roh- und Werkstoff 1971;29(1):23–31.

[24] CIE 115, Colorimetry. Commission Internationale de l'Eclairage; 2004.

[25] EN 351-1. Durability of wood and wood-based products, Preservative treated solid wood, Part 1: Classification of preservative penetration and retention. CEN; 2007.

[26] Iqbal M. An Introduction to Solar Radiation. Academic Press Canada; first ed.; 1983.

[27] Nore K, Blocken B, Jelle BP, Thue JV, Carmeliet J. A dataset of wind-driven rain measurements on a low-rise building in Norway. Building and Environment 2007;42:2150–65.

[28] Nordtest . Nordtest method, NT BUILD 495 Building Materials and Components in the vertical position: Exposure to accelerated climatic strains. Nordtest Method; Nordtest; 2000.

[29] Brandt E, Nilsen TN. Experience with equipment for large scale accelerated ageing tests. In: Proceedings of the 9th International Conference on the Durability of Building Materials and Components. Brisbane, Australia; 2002,.

[30] BS 6923, Method for calculation of small colour differences. British Standards; 1988.

[31] ISO 7724-1, Paints and varnishes. Colorimetry, Part 1: Principles. International Standard; 1984.

[32] ISO 7724-2, Paints and varnishes. Colorimetry, Part 2: Color measurements. International Standard; 1984.

[33] ISO 12641. graphic technology. Prepress digital data exchange. Color targets for input scanner calibration. International standard; 1997.

[34] EOTA, Exposure procedure for artificial weathering, TR010, Technical report. 2001.

# References


[1] Our common future. Report of the World Commission on Environment and Development, United Nations, 1987.

[2] UNEP, Sustainable Building  Construction initiative, Information note. United Nations Environment Programme, 2006.

[3] ECTP, Strategic research agenda for the european construction sector. ECTP, European Construction Technology Platform, 2005.

[4] Council directive on the approximation of laws, regulations, and administrative provisions of the member states relating to construction products. The council of the european communities, 89/106/EEC, 1988.

[5] Durability and the construction products directive. European Commission, Guidance Paper F, 2004.

[6] ISO 15686:2000, Buildings and Constructed Assets, Service Life Planning. International Organization for Standardization, 2000.

[7] C.J. Kibert, J. Sendzimit, and G.G. Bradley. *Construction Ecology: Nature as the basis for green buildings*. Taylor  Francis, London, 2002.

[8] EOTA Guidance Document 002, Assumption of Working Life of Construction Products in Guidelines for European Technical Approval, European Technical Approvals and Harmonized Standards. 1999.

[9] M.A. Lacasse. Advances in service life prediction - An overview of durabilty and methods of service life prediction for non-structural building components. In *Proceedings of the Annual Australasian Corrosion Association Conference, Wellington Convention Centre*, 2008.

[10] T. Kesik and I. Saleff. Differential durability, Building life cycle and sustainability. In *Proceedings of the 10$^{th}$ Canadian Conference on Building Science and Technology, Ottawa, Canada*, pages 38-47, 2005.

[11] A Listerud, S Bjørberg, and P.J. Hovde. Service life estimation of facades- use of the factor method in practice. In *Intenational Conference on Durability of Building Materials and Components*, Porto, Portugal, 2011.

[12] B. Marteinsson. *Service life estimation in the design of buildings.* PhD Thesis, KTH Research School, Stockholm, Sweden, 2005.

[13] A. Sarja. Generic limit state design of structures. In *Proceedings of the 10$^{th}$International Conference on Durability of Building Materials and Components*, 2005.

[14] A. Aikivuori. Periods and demand for private sector housing refurbishment. *Construction Management and Economics*, 14(1):3-12, 1996.

[15] A. Högberg. *Microclimate load: Transformed weather observations for use in design of durable buildings.* PhD Thesis, Chamlmers University of Technology, Gothenburg, Sweden, 2002.

[16] S.E. Haagenrud. Environmental characterization including equipment for monitoring. CIB W80/RILEM 140-PSL, 1997.

[17] J.E. Pickett and M.M. Gardner. Reproduceability of florida weathering data. *Polymer Degradation and Stability*, 90:418-430, 2005.

[18] T.C. Scheffer. A climate index for estimating potential for decay in wood structures above ground. *Forest Products Journal*, 21(10):25-31, 1971.

[19] K.R. Lisø, H.O. Hygen, T. Kvande, and J.V. Thue. Decay potential in wood structures using climate data. *Building Research Information*, 34(6):546-551, 2006.

[20] C.E. MacKenzie, C.-H. Wang, R.H. Leicester, G.C. Foliente, and M.N. Nguyen. Timber service life design guide. Technical Report, Forest and Wood Products Australia, 2007.

[21] D.N.-S. Hon and N. Minemura. *Wood and Cellulosic Chemistry*, chapter Color and Discoloration, pages 385-442. Marcel Dekker, New York, 2nd Edition, 2001.

[22] J. Sell and U. Leukens. Über die aussenklimatische und biologische Beanspruchung von unbehandelten und angestrichenen Holzoberflächen, 1.Teil: Chemische, mechanische und farbliche Alterungserscheinungen. *Oberfläche-Surface*, 10(8):536-539, 1969.

[23] O. Wälchli. Über die aussenklimatische und biologische Beanspruchung von unbehandelten und angestrichenen Holzoberflächen, 2.Teil: Biologische Aspekte. *Oberfläche-Surface*, 10(9):619-623, 1969.

[24] H. Kühne, U. Leukens, J. Sell, and O. Wälchli. Scanning electronmicroscope observations on mold-fungi causing grey stain. *Holz als Roh- und Werkstoff*, 28(6):223-229, 1970.

[25] W.C. Feist and E.A. Mraz. Comparison of outdoor and accelerated weathering of unprotected softwoods. *Forest Products Journal*, 28(3):38-43, 1978.

[26] J. Sell and W.C. Feist. Role of density in the erosion of wood during weathering. *Forest Products Journal*, 36(3):57-60, 1986.

[27] P.D. Evans, K. Urban, and M.J.A. Chowdhury. Surface checking of wood is increased by photodegration caused by ultraviolet and visible light. *Wood Science and Technology*, 42:251-265, 2008.

[28] D.N.-S. Hon and S.-T. Chang. Surface degradation of wood by ultraviolet light. *Journal of Polymer Science*, 22:2227-2241, 1984.

[29] K. K. Pandey. Study of the effect of photo-irradiation on the surface chemistry of wood. *Polymer Degradation and Stability*, 90:9-20, 2005.

[30] K.K. Pandey and T. Vuorinen. Comparative study of photodegradation of wood by uv laser and a xenon light source. *Polymer Degradation and Stability*, 93:2138-2146, 2008.

[31] L.P. Futó. Einfluss der Temperatur auf den photochemischen Holzabbau, 1. Mitteilung: Experimentelle Darstellung. *Holz als Roh- und Werkstoff*, 34:31-36, 1976.

[32] L.P. Futó. Einfluss der Temperatur auf den photochemischen Holzabbau, 2. Mitteilung: Rasterelektronenmikroskopische Darstellung. *Holz als Roh- und Werkstoff*, 34:49-54, 1976.

[33] M. Arnold, J. Sell, and W.C. Feist. Wood weathering in fluorecent ultraviolet and xenon arc chambers. *Forest Products Journal*, 41(2):40-44, 1991.

[34] L. Oltean, A. Teischinger, and C. Hansmann. Wood surface discoloration due to simulated indoor sunlight exposure. *Holz als Roh- und Werkstoff*, 66:51-56, 2008.

[35] T. Schnabel, B. Zimmer, and A. J. Petutschnigg. On the modelling of color changes of wood surfaces. *European Journal of Wood and Wood Products*, 67:141-149, 2009.

[36] W.E. Hillis. *Heartwood and Tree Exudates*. Springer Verlag, Berlin, Heidelberg, 1987.

[37] R.A. Eaton and M.D.C. Hale. *Wood, Decay, Pests and Protection*. Chapman Hall, London, 1993.

[38] K. Borgin and K. Corbett. *Ringer i tre*. C. Huitfeldt Forlag A.S., 1995.

[39] D.M. Dinwoodie. *Timber: Its nature and behaviour*. EFN Spon, London, 2nd Edition, 2000.

[40] W.C. Feist and D.N.-S. Hon. *The chemistry of solid wood*, Chapter Chemistry of weathering and protection, pages 401-451. Advances in Chemistry series. Americal Chemical Society, D.C., 1984.

[41] R.M. Rowell, Editor. *Handbook of Wood Chemistry and Wood Composites*. CRC Press, 2005.

[42] P.D. Evans, K.J. Schmalzl, and A.F. Michell. Rapid loss of lignin at wood surfaces during natural weathering. *Cellulosics: Pulp, Fibre and Environmental Aspects*, 1993.

[43] K. Borgin. The stability, durabilty, and weather resistance of wooden houses under cold climate conditions. *Architect Builder*, June-July, 1969.

[44] J. Sell. Investigations on the infestiation of unterated and surface treated wood by blue stain fungi. *Holz als Roh-und Werkstoff*, 26(6):215-222, June 1968. in german.

[45] H. Viitanen and A.-C. Ritschkoff. Mould growth in pine and spruce sapwood in relation to air humidity and temperature. Report 21, Department of Forest Products, Swedish University of Agricultural Science, 1991.

[46] L.R. Gobakken. *Surface mould growth on painted and unpainted wood; Influecning factors, modelling and aesthetic service life*. PhD Thesis, Norwegian University of Life Science, Aas, Norway, 2009.

[47] J. Sell and U. Leukens. Weathering phenomena of unprotected wood species. *Holz als Roh- und Werkstoff*, 29(1):23-31, 1971.

[48] R.S. Williams. *Handbook of Wood Chemistry and Wood Composites*, Chapter Weathering of wood, pages 139-185. CRC Press, 2005.

[49] K. Borgin. The mechanism of the breakdown of the structure of wood due to environmental factors. *Journal of the Institue of Wood Science*, 4:26-30, 1971.

[50] B. George, E. Suttie, A. Merlin, and X. Deglise. Photogedradation and photostability of wood - The state of the art. *Polymer Degradation and Stability*, 88:268–274, 2005.

[51] M. Arnold and J. Sell. Künstliche Bewitterung von Holz und Holzanstrichen: Vergleich zweier Gertetypen. *Holz als Roh- und Werkstoff*, 48:138, 1990.

[52] H. Derbyshire and E.R. Miller. The photodegradation of wood during solar irradiation Part I: Effects on the structural integrity of thin wood strips. *Holz als Roh- und Werkstoff*, 39(8):341-350, 1981.

[53] H. Derbyshire, E.R. Miller, and H. Turkulin. Investigations into the photodegradation of wood using microtensile testing; Part 1: The application of microtensile testing to measurement of photodegradation rates. *Holz als Roh- und Werkstoff*, 53(1):339-345, 1995.

[54] H. Derbyshire, E.R. Miller, and H. Turkulin. Investigations into the photodegradation of wood using microtensile testing; Part 2: An investigation of the changes in tensile strength of different softwood species during natural weathering. *Holz als Roh- und Werkstoff*, 54(1):1-6, 1996.

[55] H. Derbyshire, E.R. Miller, and H. Turkulin. Investigations into the photodegradation of wood using microtensile testing; Part 1: The application of microtensile testing to measurement of photodegradation rate. *Holz als Roh- und Werkstoff*, 53(5):339-345, 1995.

[56] A.J. Lewry and L.F.E. Crewdson. Approaches to testing the durability of materials used in the construction and maintenance of buildings. *Construction and Building Materials*, 8(4):211-222, 1994.

[57] R.P. Brown. Survey of status of test methods for accelerated durability testing. *Polymer Testing*, 10(1):3-30, 1991.

[58] L.F.E. Jacques. Accelerated and outdoor/natural exposure testing of coatings. *Progress in Polymer Science*, 25(9):1337-1362, 2000.

[59] J.W. Martin, S.C. Saunders, F.L. Floyd, and J.P. Wineburg. *Methodologies for predicting the service life of coating systems*. Federation of Societies for Coatings Technology, 492 Norristown Road, Blue Bell, USA, June 1996.

[60] A.D. McNaught and A. Wilkinson, Editors. *Compendium of Chemical Terminology*. IUPAC International Union of Pure and Applied Chemistry, 1997.

[61] J.W. Martin. Repeatability and reproduceability of field exposure results. In Jonathan W. Martin and David R. Bauer, Editors, *Service life Prediction : Methodology and Metrologies*, Volume 805 of *ACS Symposium Series*, pages 2-22. American Chemical Society, Oxford University Press, 2002.

[62] L. Tolvaj and K. Mitsui. Light source dependence of the photodegradation of wood. *Journal of Wood Science*, 51:468-473, 2005.

[63] S. Geving, T.H. Erichsen, K. Nore, and B. Time. Hygrothermal conditions in wooden claddings-Test house measurements. Project report 407, Norwegian Building Research Institute, Oslo, Norway, 2006.

[64] M. Kottek, J. Grieser, C. Beck, B. Rudolf, and F. Rubel. World map of the Köppen-Geiger climate classification updated. *Meteorologische Zeitschrift*, 15(3):259-263, June 2006.

[65] J.A. Duffie and W.A. Beckman. *Solar Engineering of Thermal Processes*. John Wiley Sons, Inc., USA, 2nd Edition, 1991.

[66] M. Iqbal. *An Introduction to Solar Radiation*. Academic Press Canada, 1st edition, 1983.

[67] C. Rigollier, M. Lefévre, and L. Wald. The method Heliosat-2 for deriving shortwave solar radiation from satellite images. *Solar Energy*, 77(2):159-169, 2004.

[68] M. Lefévre, M. Albuisson, and L. Wald. Joint report on interpolation scheme "Meteosat" and database "climatology in (Meteosat)". 2002.

[69] K. Nore, B. Blocken, B.P. Jelle, J.V. Thue, and J. Carmeliet. A dataset of Wind-Driven Rain Measurements on a Low-Rise Building in Norway. *Building and Environment*, 42:2150-2165, 2007.

[70] NS EN 335-1, Hazard Classes of Wood and Wood-based Products against biological Attack - Part 1: Classification of Hazard Classes. CEN, 1992.

[71] NS EN 350-2, Durability of Wood and Wood-based Products - Natural Durability of Solid Wood - Part 2: Guide to natural Durability of selected Wood species of importance in Europe. CEN, 1992.

[72] P.O. Flæte, F.G. Evans, and G. Alfredsen. Natural durability of different wood species - Results after five years testing in ground contact. *ProLigno*, 4(3):15-24, 2008.

[73] Nordtest. Nordtest Method, NT BUILD 495 Building Materials and Components in the vertical position: Exposure to accelerated climatic strains. Nordtest Method, Nordtest, 2000.

[74] E. Brandt and T.-N. Nilsen. Experience with equipment for large scale accelerated ageing tests. In CSIRO, Editor, *Proceedings of the 9th International Conference on the Durability of Building Materials and Components*, Brisbane, Australia, 2002.

[75] CIE 115, Colorimetry. *Commission Internationale de l'Eclairage*, 2004.

[76] ISO/CIE 10527. CIE Standard Colorimetric Observers. International Organization for Standardization, 1991. 1st edition.

[77] ISO 7724-1. Paints and Varnishes-Colorimetry-Part 1: Principles. International Organization for Standardization, 1984.

[78] ISO 7724-2. Paints and Varnishes-Colorimetry-Part 2: Color measurement. International Organization for Standardization, 1984.

[79] BS 6923. Method for Calculation of small Colour Differences. British Standards, 1988.

[80] ISO 12641, Graphic Technology-Prepress digital Data Exchange-Color Targets for input Scanner Calibration. International Organization for Standardization, 1997.

[81] W. Faust. Scanner calibration. Personal communication, November 2008.

[82] W.G.K. Backhaus, R. Kliegl, and J.S. Werner, Editors. *Color Vision: Perspectives from different Disciplines*. Walter de Gruyter, 1998.

[83] A. Valberg. *Light Vision Color*. Wiley-Blackwell, 2005.

[84] J. Sell and K. Weiss. Apparat fr die künstliche Bewitterung von Holz und Holzanstrichen. *Farbe + Lack*, 95(6):417-418, 1989.

[85] R.P. Brown. Predictive techniques and models for durability tests. *Polymer Testing*, 14(5):403-414, 1995.

[86] W.Q. Meeker, L.A. Escobar, and V. Chan. Using accelerated tests to predict service life in highly variable environments. In Jonathan W. Martin and David R. Bauer, Editors, *Service life Prediction : Methodology and Metrologies*, Volume 805 of *ACS Symposium Series*, pages 396-412. American Chemical Society, Oxford University Press, 2002.

[87] EOTA Technical Report 010. Exposure Procedure for artificial Weathering. European Organisation for Technical Approvals, 2004. Edition May 2004.

[88] W.Q. Meeker, L.A. Escobar, and J.C. Lu. Accelerated degradation tests: Modeling and analysis. *Technometrics*, 40(2):89-100, May 1998.

# A. Tables and Figures

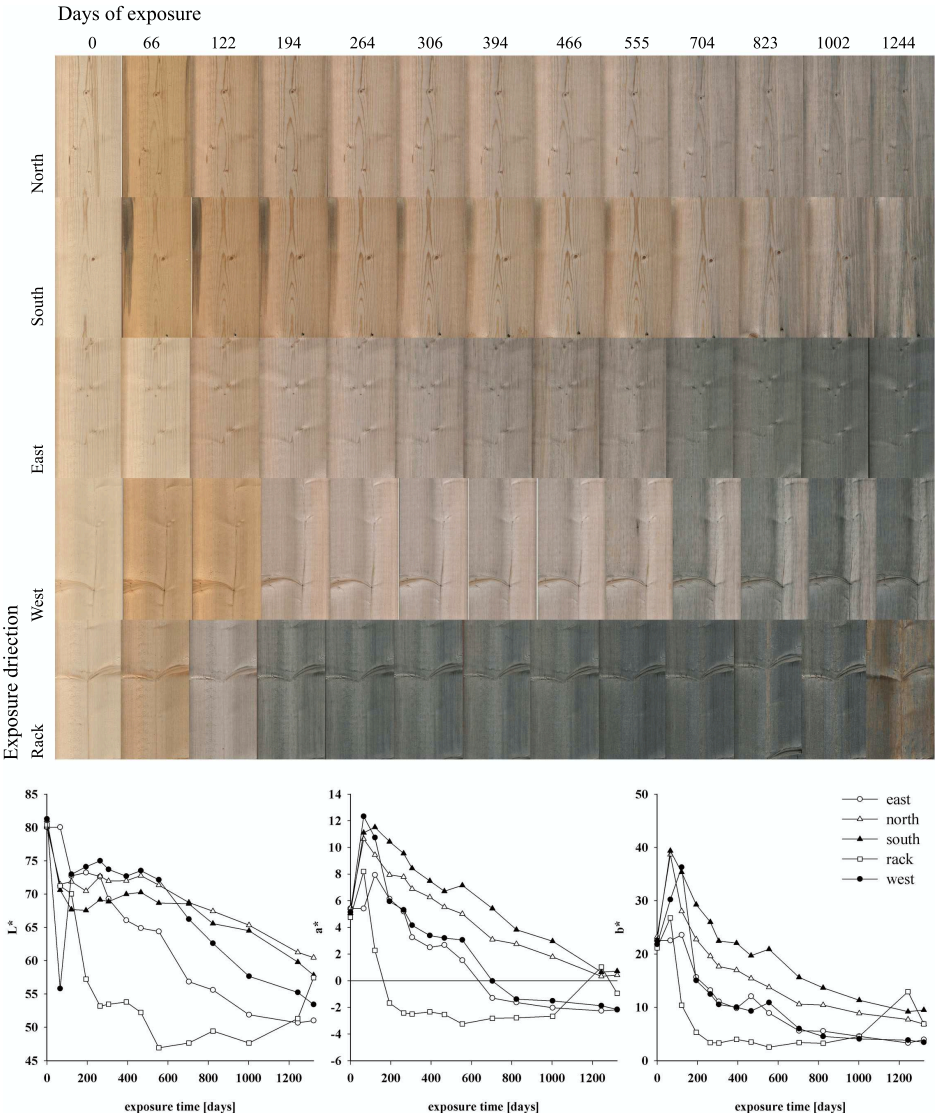


Figure A.1.: Scanned images for Material 1 (Norway spruce, Ruptimal surface) above and color values L*, a*, b* for outdoor exposure below

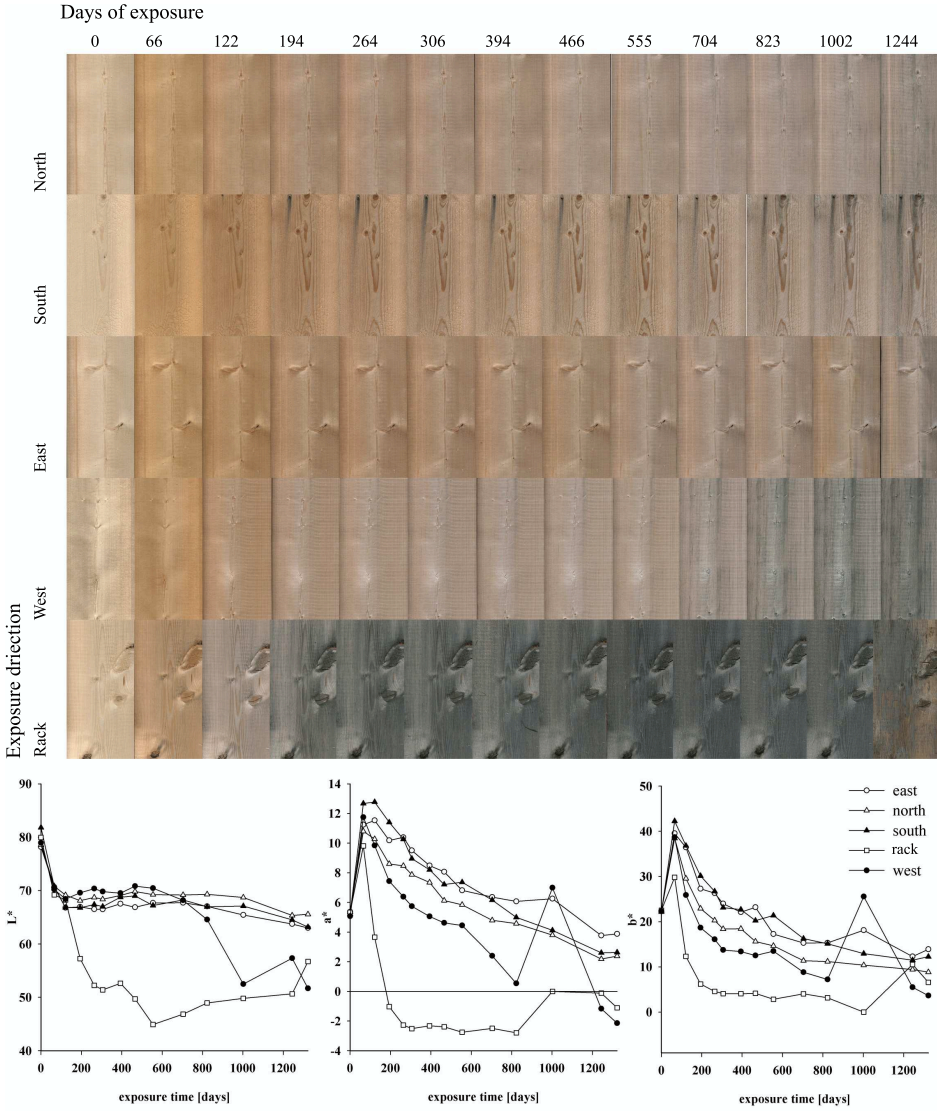


Figure A.2.: Scanned images for Material 2 (Norway spruce) above and color values L*, a*, b* for outdoor exposure below

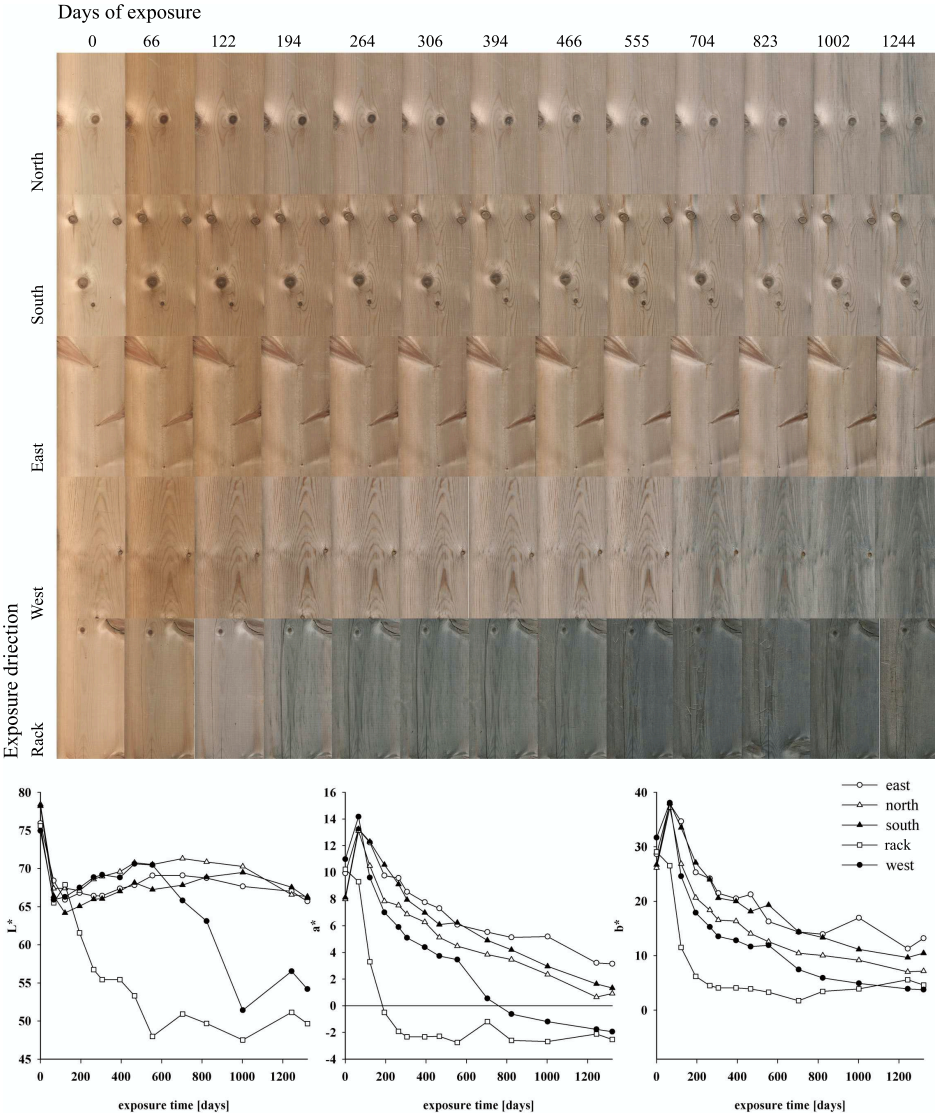


Figure A.3.: Scanned images for Material 3 (Scots Pine) above and color values L*, a*, b* for outdoor exposure below

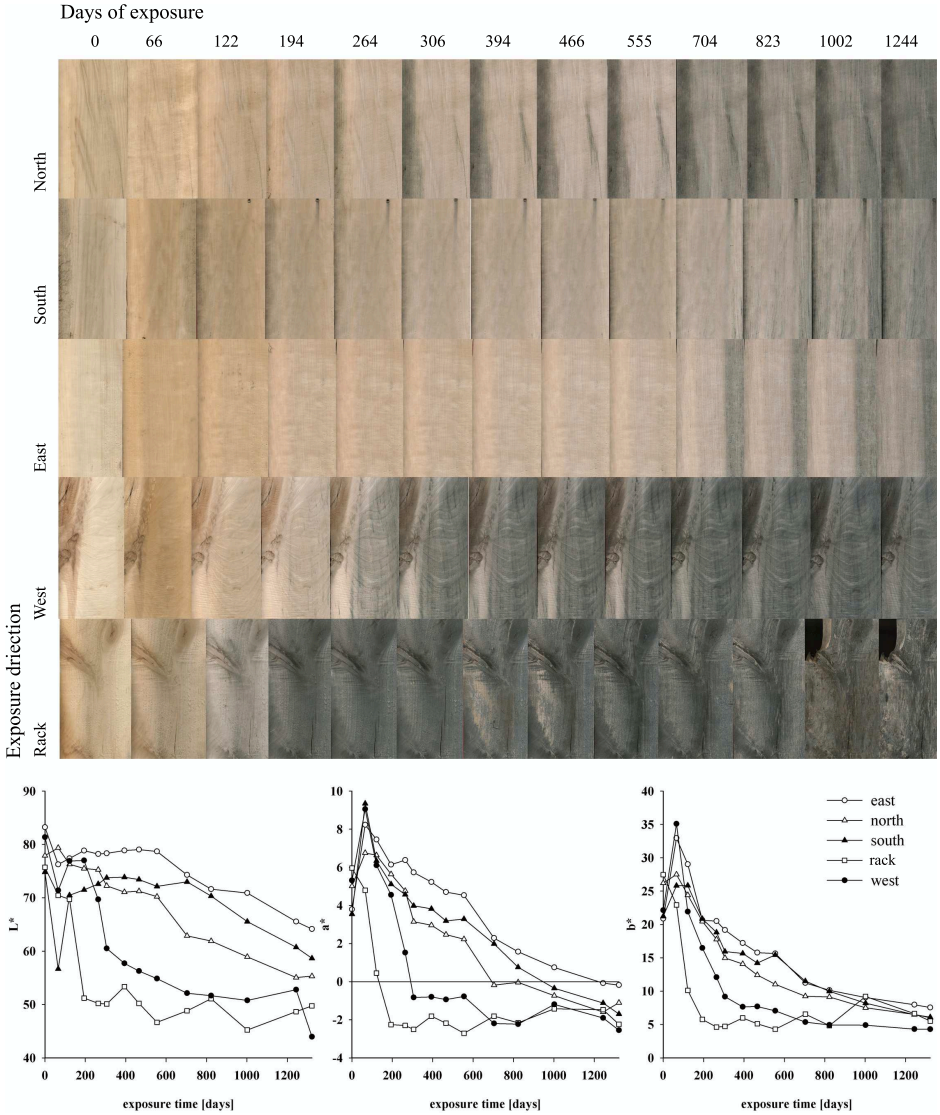


Figure A.4.: Scanned images for Material 4 (Aspen) above and color values L*, a*, b* for outdoor exposure below

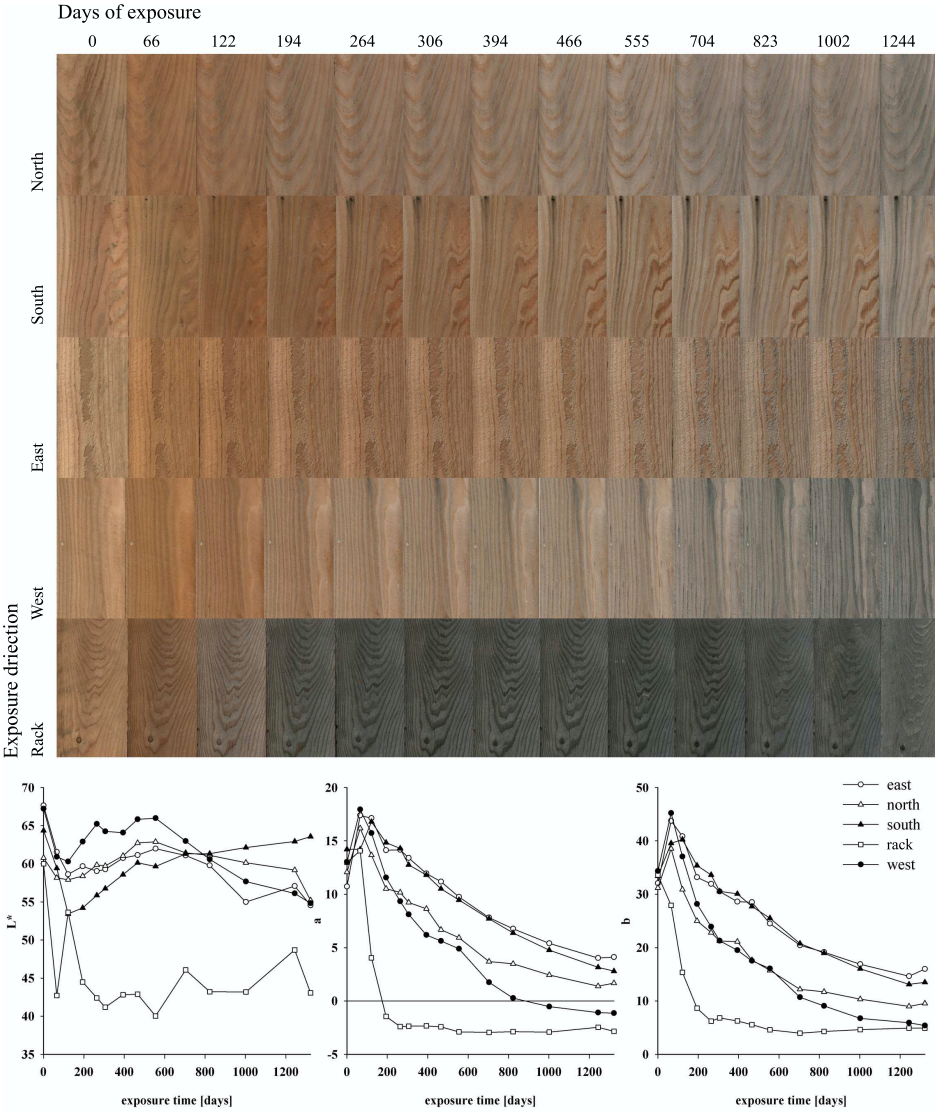


Figure A.5.: Scanned images for Material 5 (Larch) above and color values L*, a*, b* for outdoor exposure below

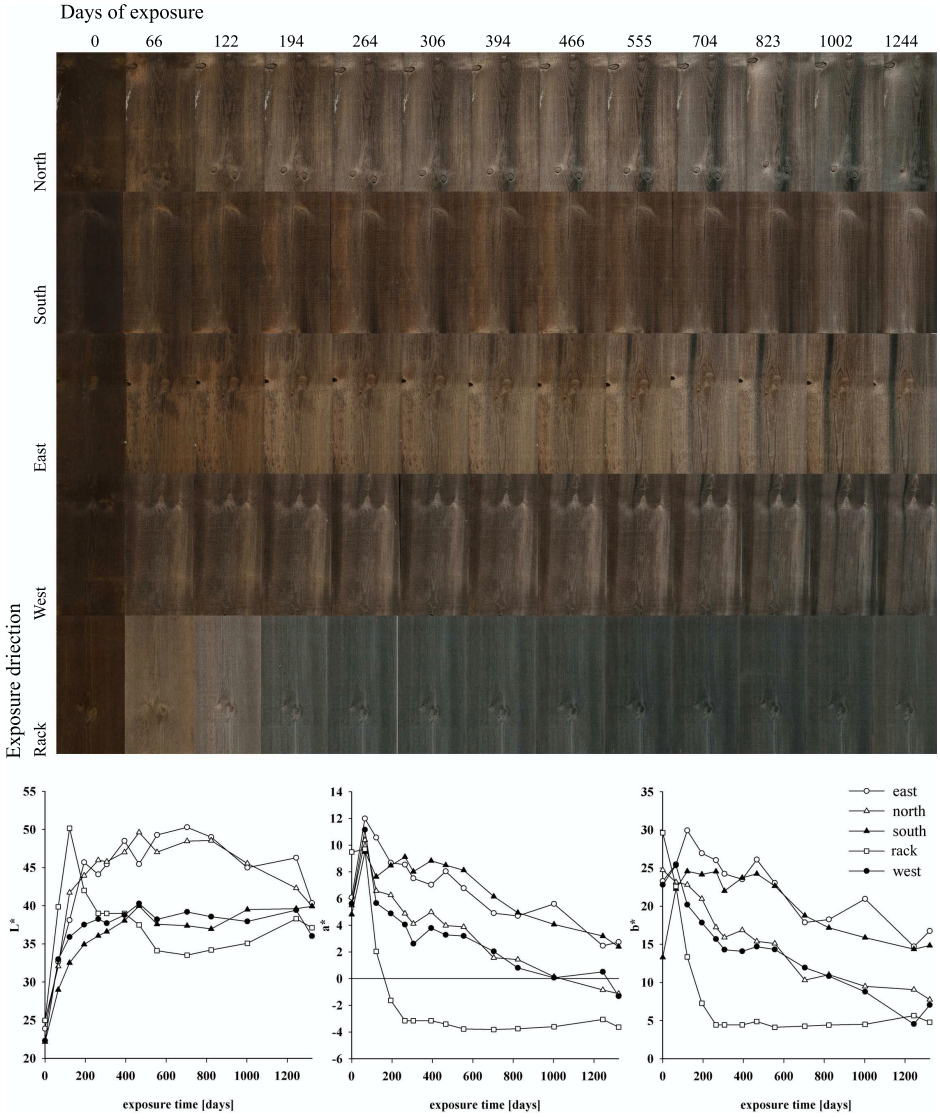


Figure A.6.: Scanned images for Material 6 (Kebony Furu) above and color values L*, a*, b* for outdoor exposure below

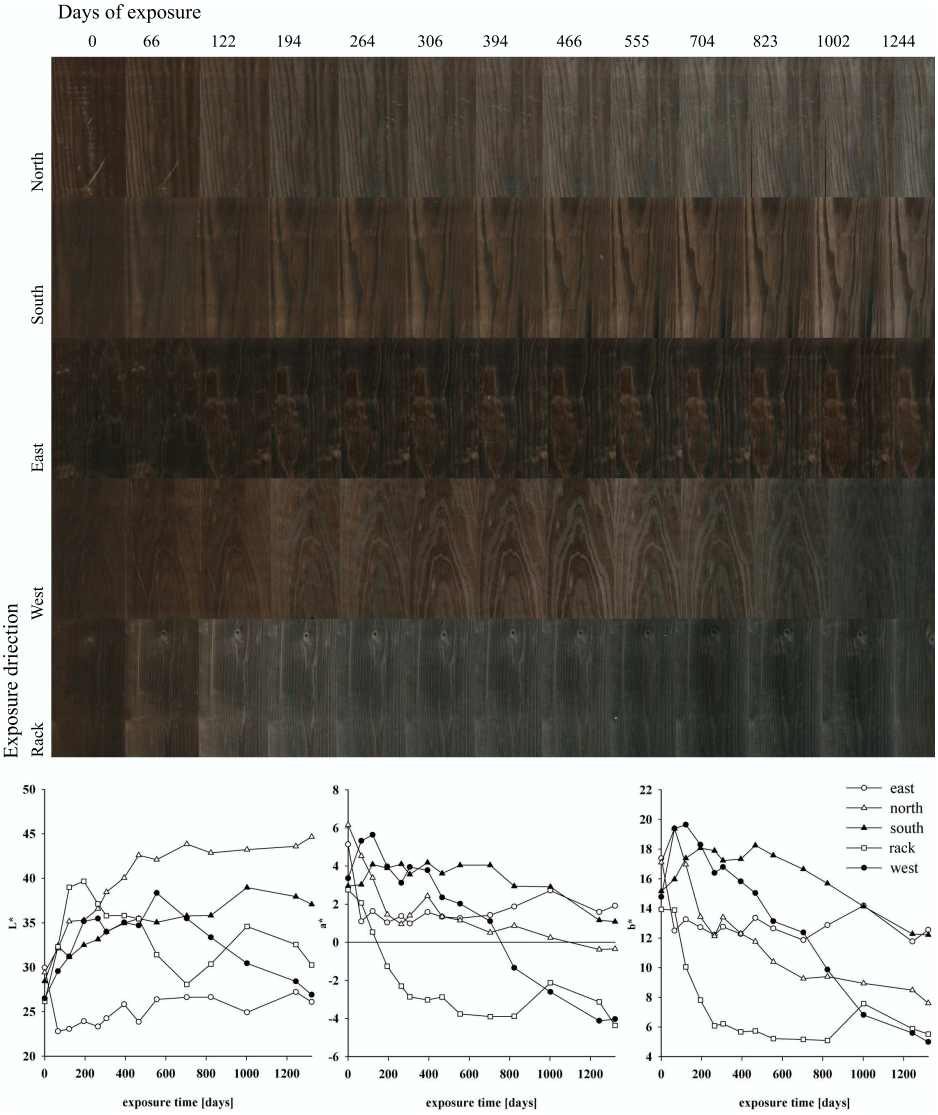


Figure A.7.: Scanned images for Material 7 (Kebony SYP) above and color values L*, a*, b* for outdoor exposure below

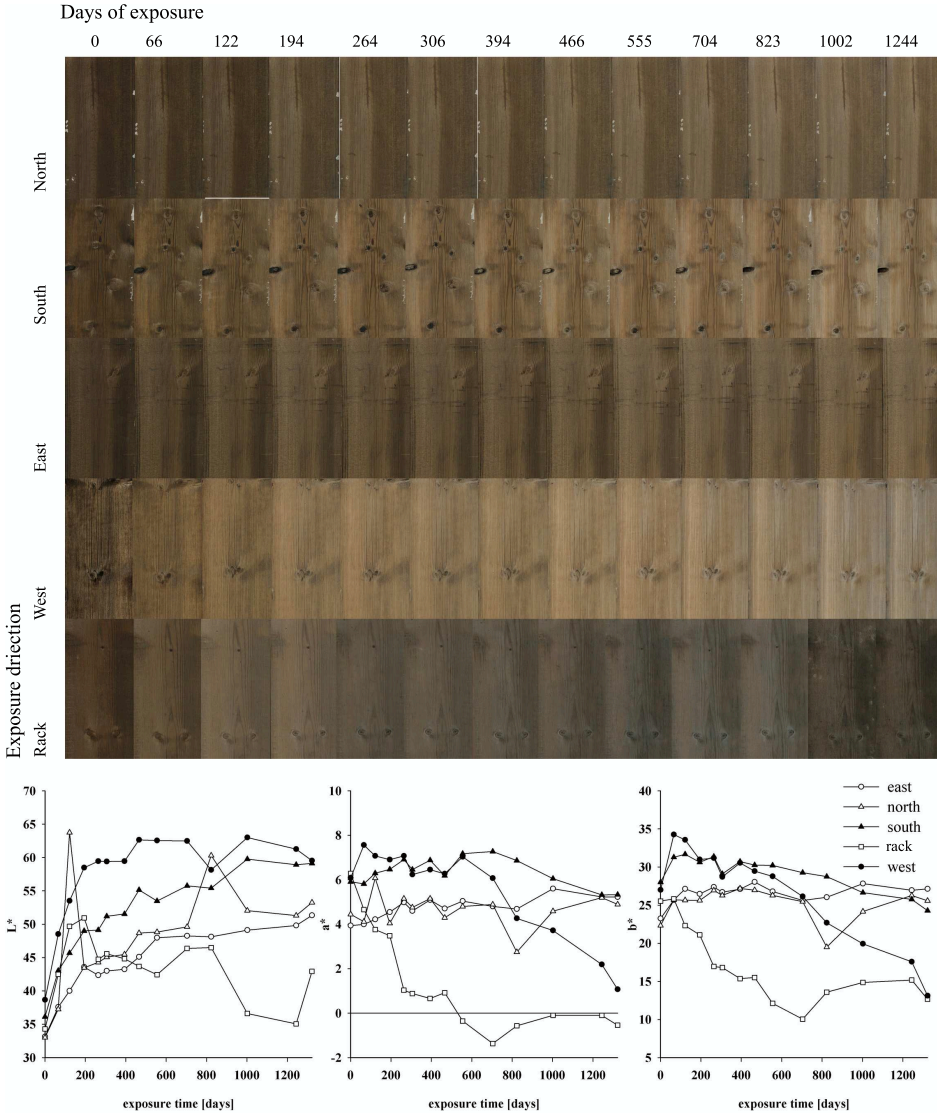


Figure A.8.: Scanned images for Material 8 (Royal impregnation) above and color values L*, a*, b* for outdoor exposure below

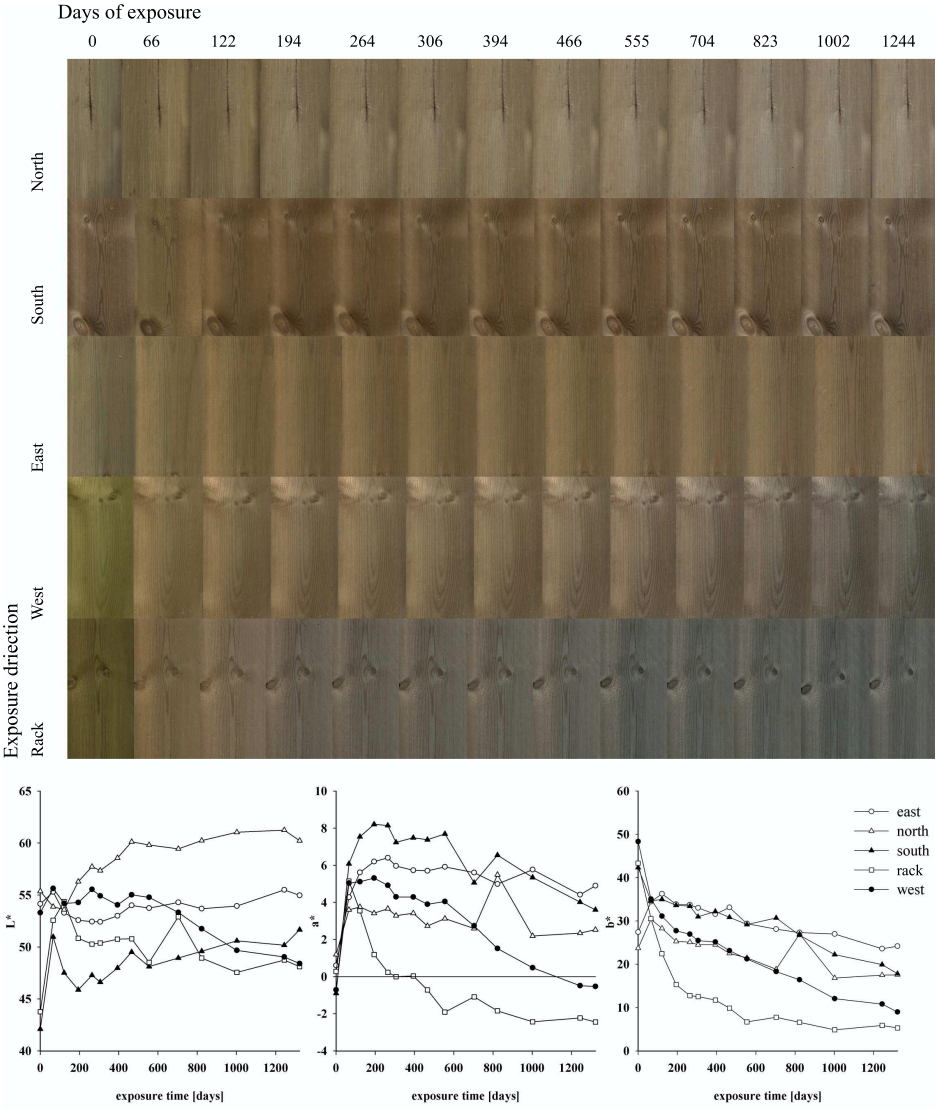


Figure A.9.: Scanned images for Material 9 (Pressure treated) above and color values L*, a*, b* for outdoor exposure below

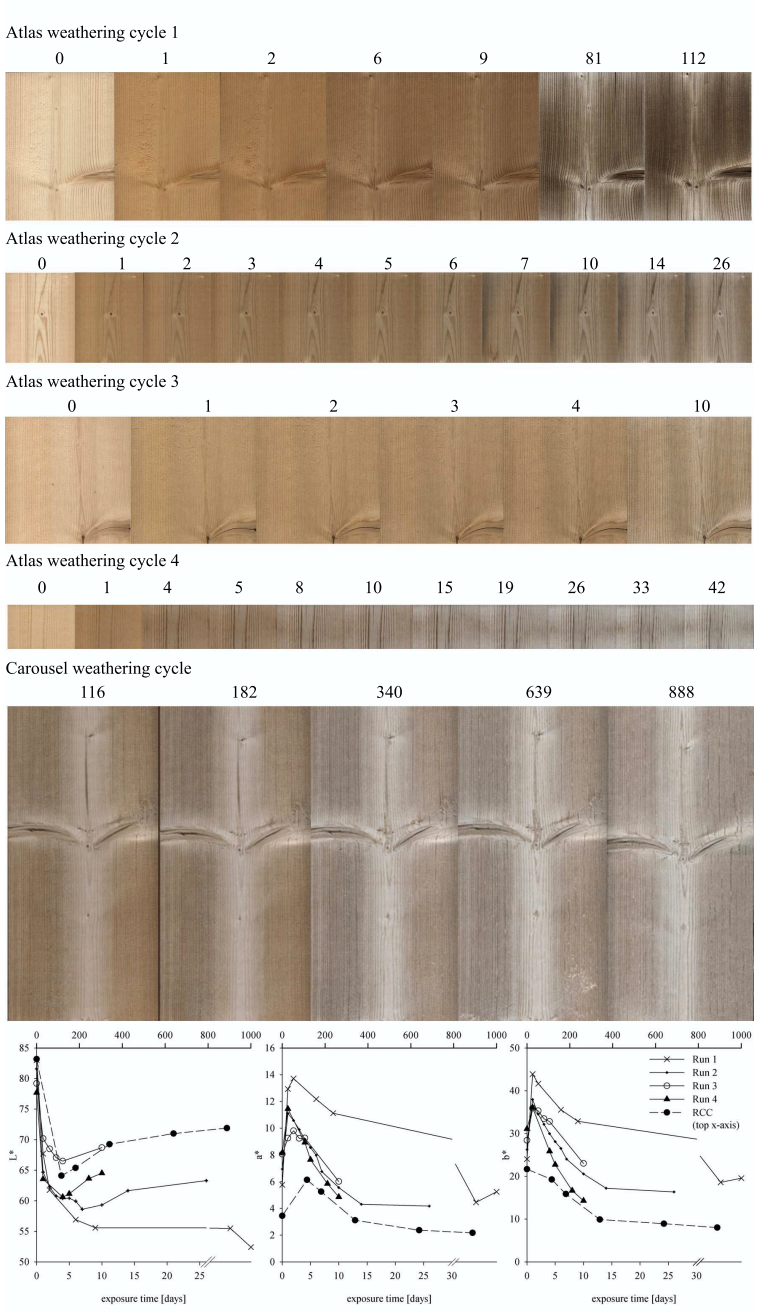


Figure A.10.: Scanned images for Material 1 (Norway spruce, Ruptimal surface) above and color values L*, a*, b* for laboratory exposure below

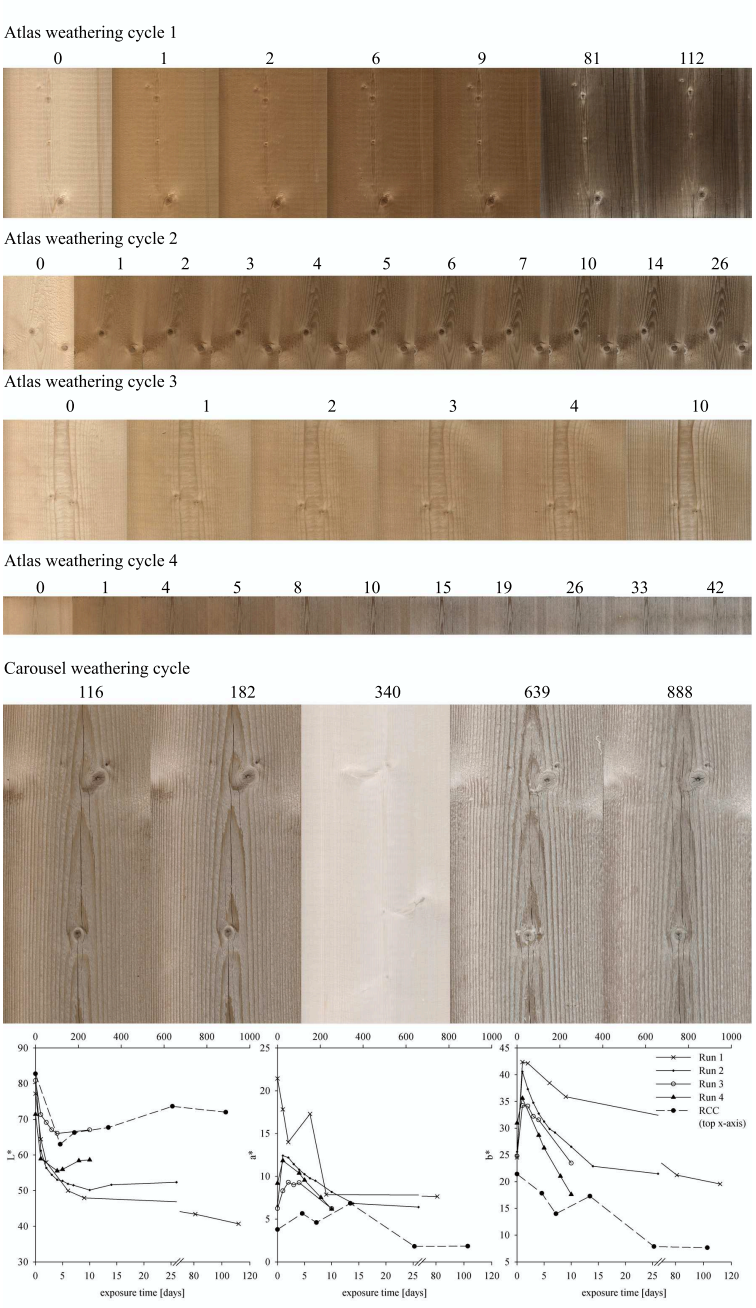


Figure A.11.: Scanned images for Material 2 (Norway spruce) above and color values L*, a*, b* for laboratory exposure below

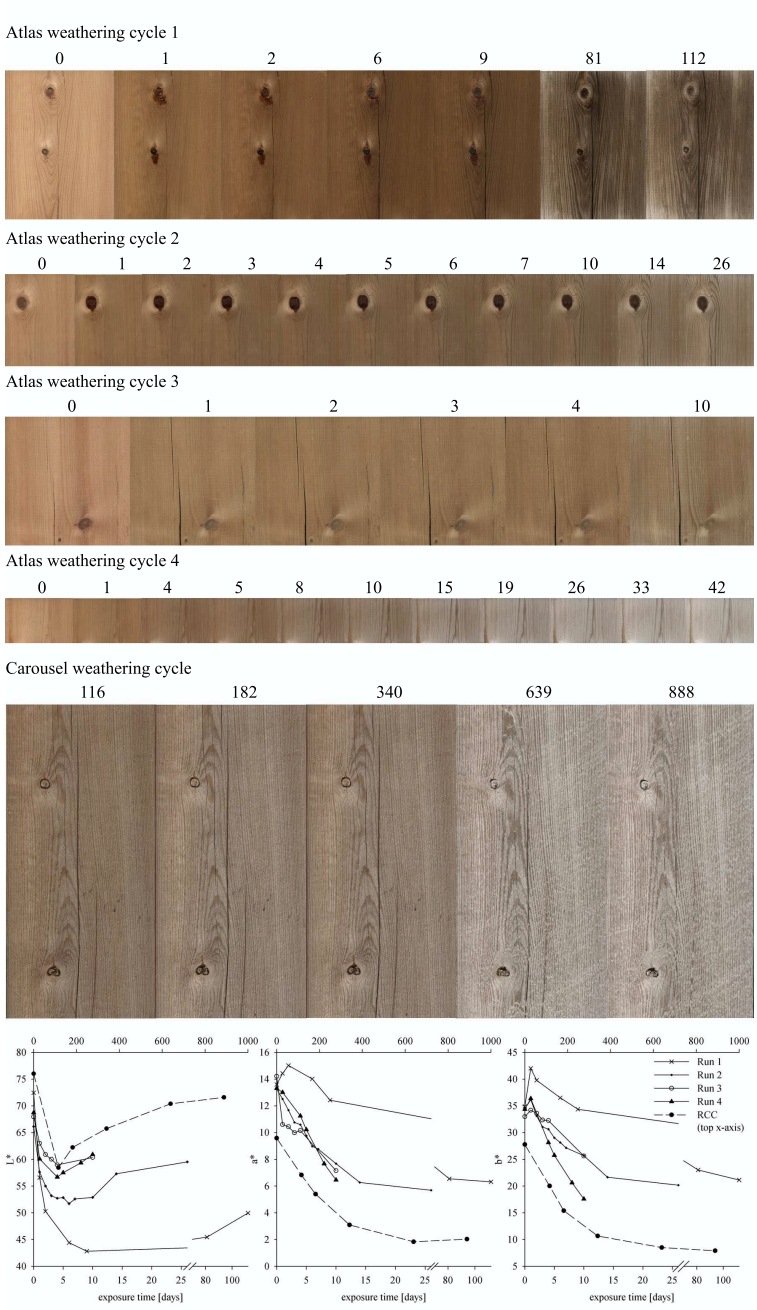


Figure A.12.: Scanned images for Material 3 (Scots Pine) above and color values L*, a*, b* for laboratory exposure below

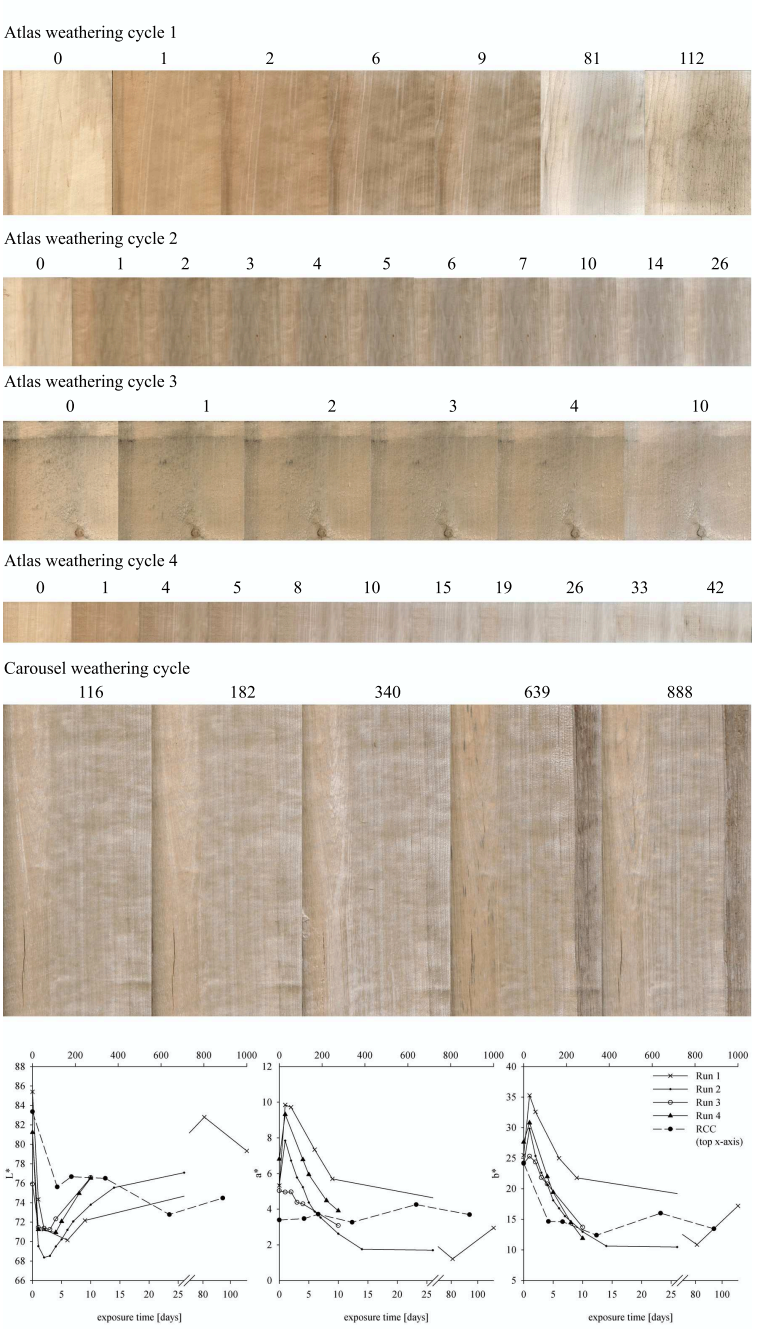


Figure A.13.: Scanned images for Material 4 (Aspen) above and color values L*, a*, b* for laboratory exposure below

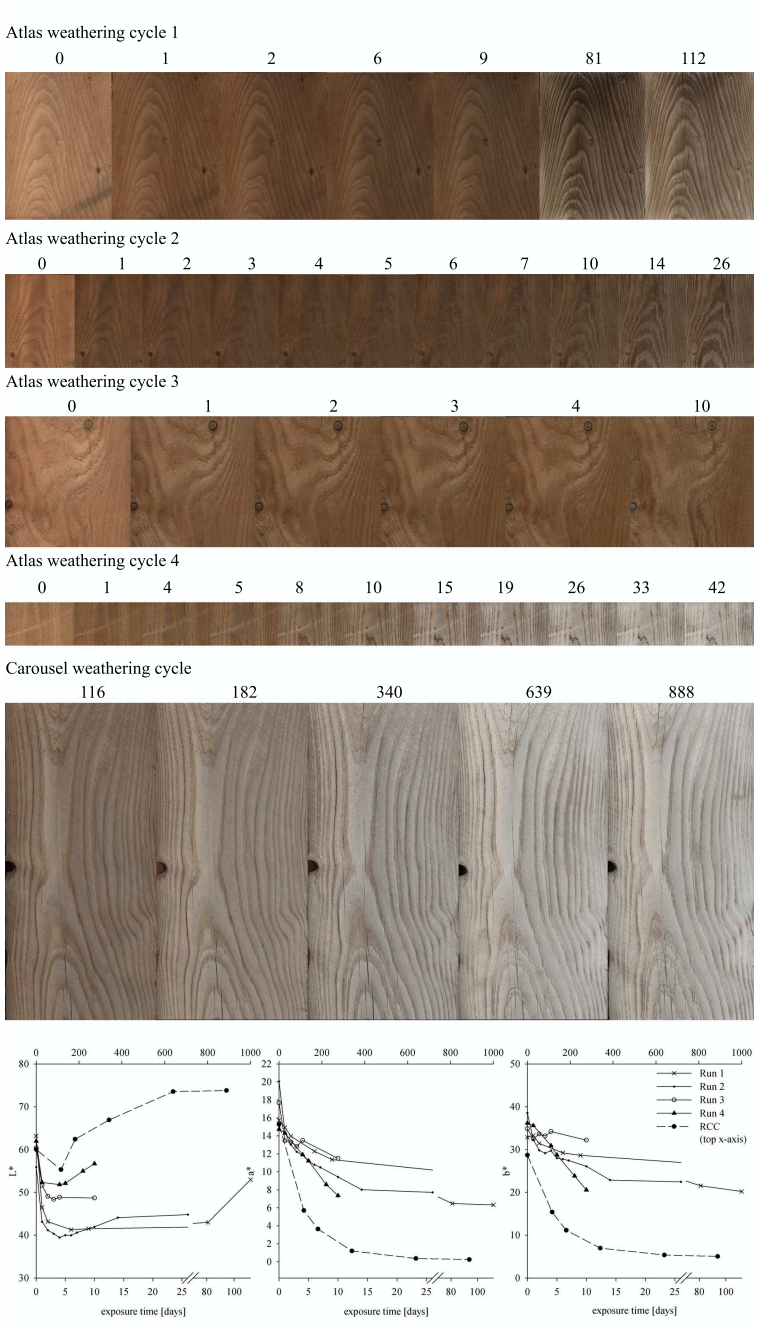


Figure A.14.: Scanned images for Material 5 (Larch) above and color values L*, a*, b* for laboratory exposure below

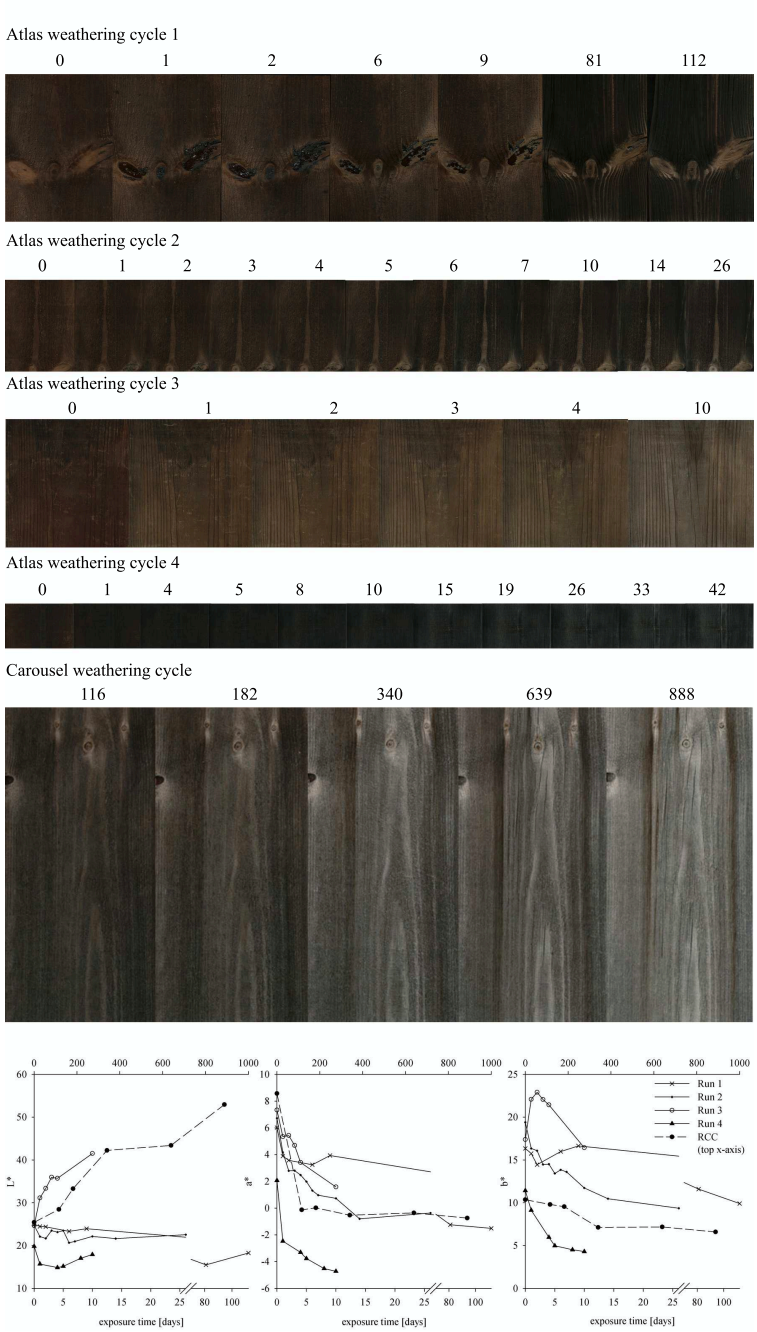


Figure A.15.: Scanned images for Material 6 (Kebony Furu) above and color values L*, a*, b* for laboratory exposure below

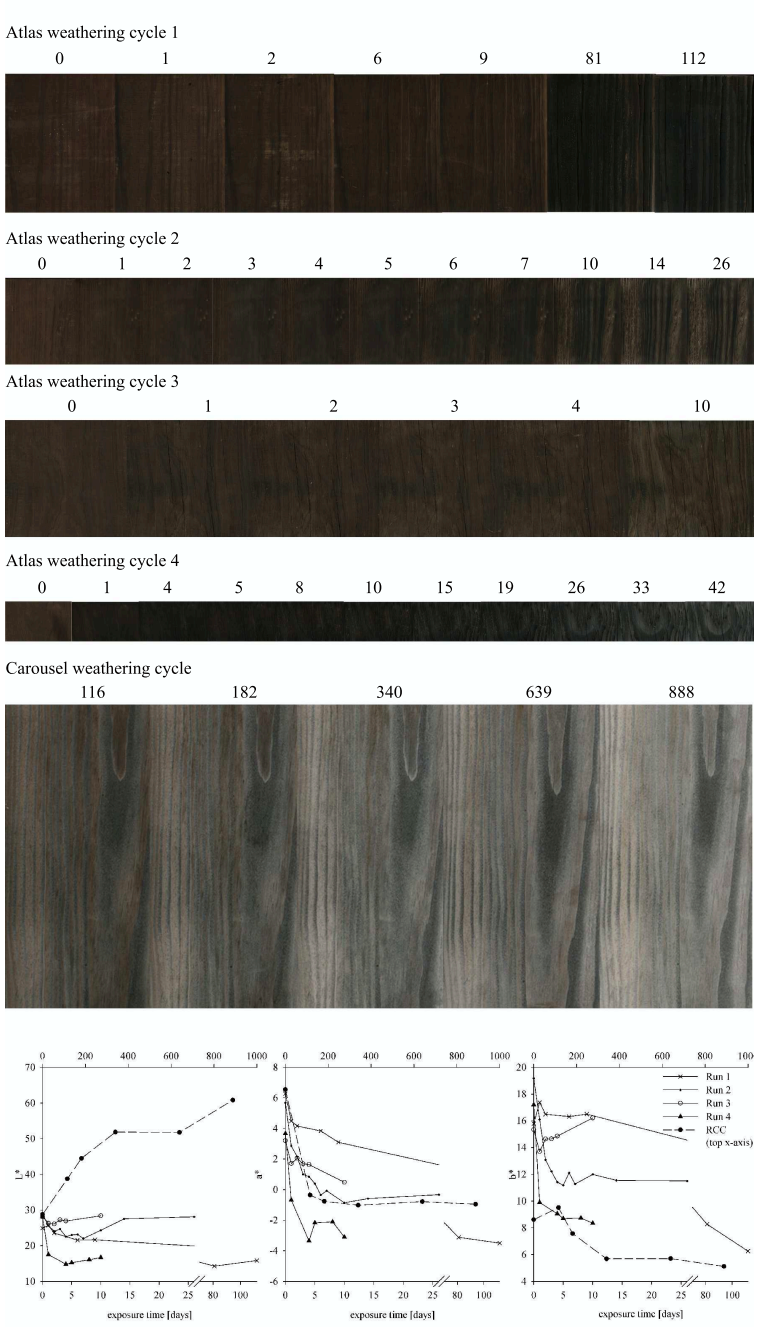


Figure A.16.: Scanned images for Material 7 (Kebony SYP) above and color values L*, a*, b* for laboratory exposure below

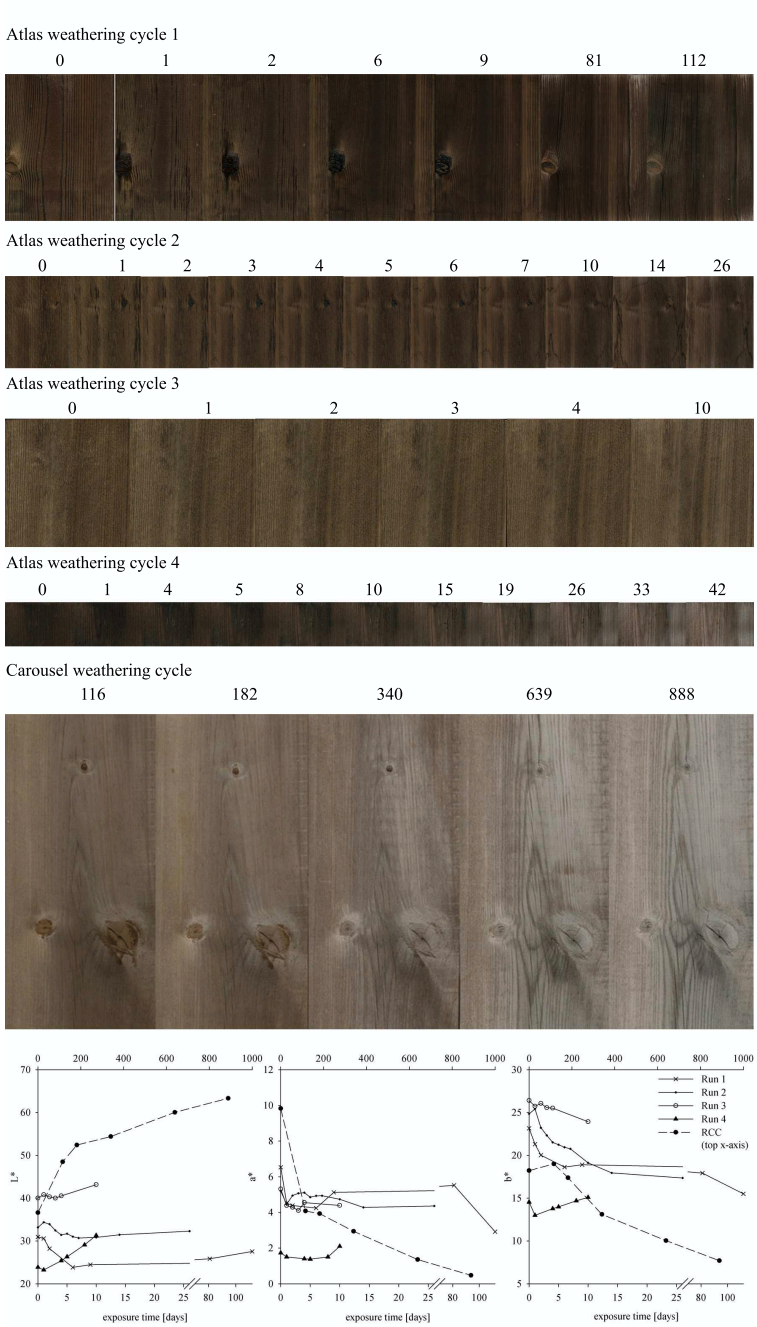


Figure A.17.: Scanned images for Material 8 (Royal impregnation) above and color values L*, a*, b* for laboratory exposure below

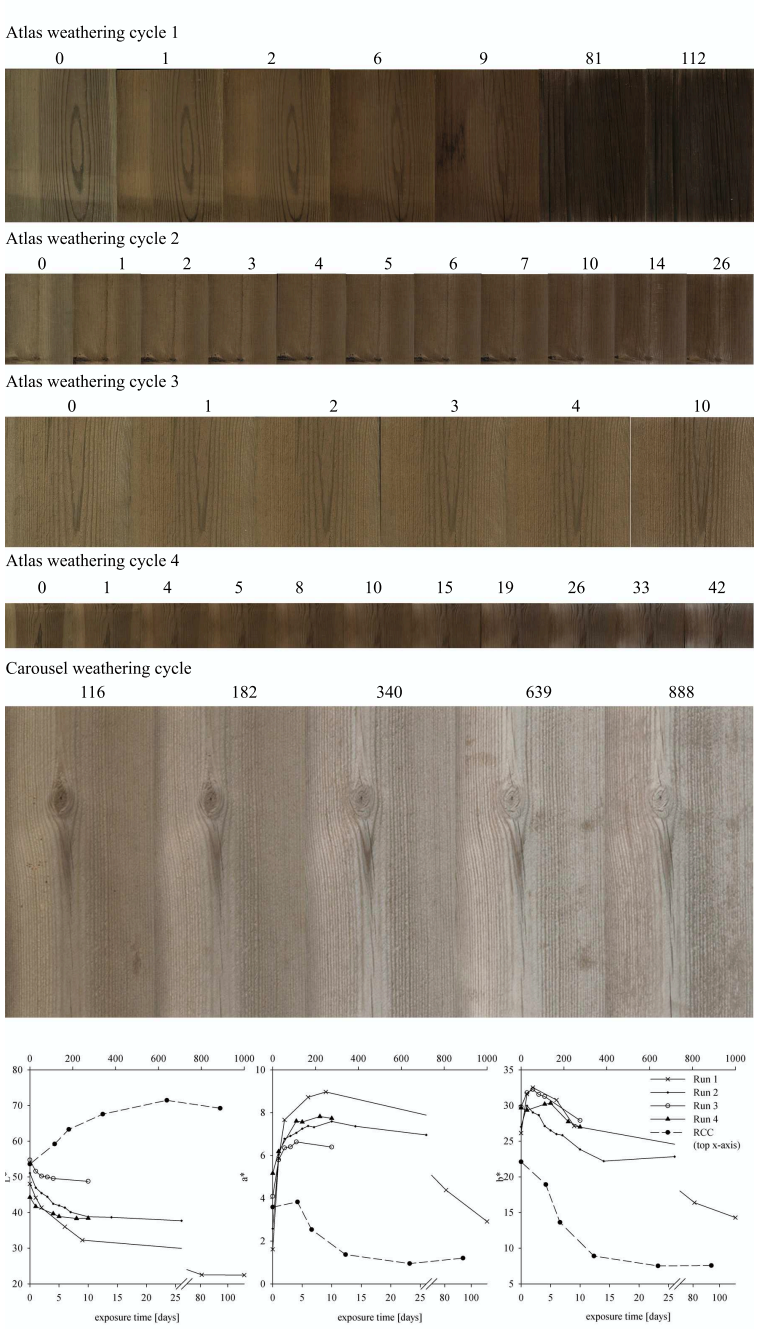


Figure A.18.: Scanned images for Material 9 (Pressure treated) above and color values L*, a*, b* for laboratory exposure below

Table A.1.: Initial and final color values for Norway spruce, Ruptimal surface (Material 1) for outdoor and laboratory exposure.

| | | Outdoor weathering | | | | | | | Laboratory weathering | | | | | | |
|---|---|---|---|---|---|---|---|---|---|---|---|---|---|---|---|
| | | North | South | East | West | Rack | Av. | StDev | Run 1 | Run 2 | Run 3 | Run 4 | RCC | Av. | StDev |
| Initial color values | L* | 80.05 | 81.11 | 80.04 | 81.27 | 80.39 | 80.57 | 0.59 | 83.01 | 81.58 | 79.19 | 77.68 | 83.18 | 80.93 | 2.42 |
| | a* | 5.46 | 5.08 | 5.41 | 5.14 | 4.75 | 5.17 | 0.28 | 5.76 | 6.94 | 8.05 | 8.16 | 3.44 | 6.47 | 1.95 |
| | b* | 23.26 | 22.63 | 22.53 | 21.82 | 21.16 | 22.28 | 0.81 | 24.04 | 26.26 | 28.39 | 31.08 | 21.67 | 26.29 | 3.67 |
| | C* | 23.89 | 23.19 | 23.17 | 22.42 | 21.69 | 22.87 | 0.84 | 24.72 | 27.16 | 29.51 | 32.13 | 21.94 | 27.09 | 3.98 |
| Final color values | L* | 60.47 | 57.82 | 51.03 | 53.43 | 57.45 | 56.04 | 3.77 | 52.43 | 63.30 | 68.69 | 71.21 | 71.88 | 65.50 | 8.05 |
| | a* | 0.42 | 0.72 | -2.18 | -2.16 | -0.95 | -0.83 | 1.38 | 5.25 | 4.18 | 6.01 | 0.75 | 2.17 | 3.67 | 2.18 |
| | b* | 6.86 | 9.50 | 3.95 | 3.43 | 6.89 | 6.13 | 2.47 | 19.57 | 16.35 | 23.01 | 6.58 | 8.01 | 14.71 | 7.18 |
| | C* | 6.87 | 9.53 | 4.52 | 4.05 | 6.96 | 6.38 | 2.20 | 20.27 | 16.87 | 23.78 | 6.63 | 8.30 | 15.17 | 7.47 |
| Color diff. | $\Delta E^*_{tot}$ | 26.03 | 27.09 | 35.28 | 34.15 | 27.61 | 30.03 | 4.33 | 30.91 | 20.97 | 11.97 | 26.39 | 17.77 | 21.60 | 7.37 |
| | $\sum \Delta E^*$ | 60.24 | 65.19 | 48.85 | 99.47 | 79.75 | 70.70 | 19.53 | 62.67 | 47.08 | 27.50 | 52.52 | 35.20 | 44.99 | 13.92 |
| | $\Delta C^*$ | 17.02 | 13.66 | 18.66 | 18.37 | 14.73 | 16.49 | 2.21 | 4.45 | 10.29 | 5.73 | 25.50 | 13.64 | 11.92 | 8.43 |
| | $\Delta L^*$ | 19.58 | 23.29 | 29.01 | 27.84 | 22.94 | 24.53 | -3.18 | 30.58 | 18.28 | 10.50 | 6.47 | 11.30 | 15.42 | -5.63 |
| | $(\sum \Delta E^*) - \Delta E^*$ | 34.21 | 38.10 | 13.58 | 65.31 | 52.13 | 40.67 | 15.21 | 31.76 | 26.11 | 15.53 | 26.12 | 17.43 | 23.39 | 6.55 |

Table A.2.: Initial and final color values for Norway spruce (Material 2) for outdoor and laboratory exposure.

| | | Outdoor weathering | | | | | | | Laboratory weathering | | | | | | |
|---|---|---|---|---|---|---|---|---|---|---|---|---|---|---|---|
| | | North | South | East | West | Rack | Av. | StDev | Run 1 | Run 2 | Run 3 | Run 4 | RCC | Av. | StDev |
| Initial color values | L* | 78.58 | 81.82 | 78.18 | 78.94 | 79.96 | 79.50 | 1.46 | 77.18 | 82.49 | 80.85 | 71.40 | 82.74 | 77.07 | 8.02 |
| | a* | 5.37 | 5.22 | 5.36 | 5.07 | 5.33 | 5.27 | 0.13 | 6.69 | 6.58 | 6.24 | 9.19 | 3.79 | 6.49 | 3.82 |
| | b* | 22.47 | 22.18 | 22.38 | 22.29 | 22.51 | 22.37 | 0.13 | 24.54 | 25.59 | 24.79 | 30.96 | 21.43 | 26.19 | 6.74 |
| | C* | 23.10 | 22.79 | 23.01 | 22.86 | 23.13 | 22.98 | 0.15 | 25.43 | 26.42 | 25.57 | 32.29 | 21.76 | 27.02 | 7.45 |
| Final color values | L* | 65.55 | 63.16 | 63.00 | 51.68 | 56.71 | 60.02 | 5.70 | 40.67 | 52.35 | 67.03 | 65.97 | 71.96 | 68.97 | 4.24 |
| | a* | 2.38 | 2.63 | 3.88 | -2.15 | -1.11 | 1.13 | 2.60 | 5.48 | 6.41 | 6.23 | 1.19 | 1.84 | 1.52 | 0.46 |
| | b* | 8.85 | 12.28 | 13.90 | 3.65 | 6.60 | 9.06 | 4.16 | 19.57 | 21.48 | 23.47 | 7.55 | 7.65 | 7.60 | 0.07 |
| | C* | 9.17 | 12.56 | 14.43 | 4.23 | 6.69 | 9.42 | 4.16 | 20.32 | 22.42 | 24.28 | 7.64 | 7.87 | 7.75 | 0.16 |
| Color diff. | $\Delta E^*_{tot}$ | 19.08 | 21.28 | 17.45 | 33.80 | 28.90 | 24.10 | 6.97 | 36.86 | 30.42 | 13.88 | 25.33 | 17.60 | 21.46 | 5.47 |
| | $\sum \Delta E^*$ | 61.50 | 54.01 | 66.54 | 174.04 | 110.43 | 93.31 | 50.21 | 61.55 | 52.00 | 28.71 | 48.64 | 43.48 | 46.06 | 3.65 |
| | $\Delta C^*$ | 13.94 | 10.23 | 8.58 | 18.63 | 16.44 | 13.56 | 4.18 | 5.11 | 4.00 | 1.28 | 24.65 | 13.89 | 19.27 | 7.61 |
| | $\Delta L^*$ | 13.03 | 18.66 | 15.18 | 27.26 | 23.24 | 19.48 | -4.24 | 36.51 | 30.15 | 13.82 | 5.43 | 10.78 | 8.10 | 3.78 |
| | $(\sum \Delta E^*) - \Delta E^*$ | 42.42 | 32.73 | 49.09 | 140.24 | 81.54 | 69.20 | 43.24 | 24.69 | 21.58 | 14.83 | 23.31 | 25.88 | 24.60 | -1.82 |

Table A.3.: Initial and final color values for Scots Pine (Material 3) for outdoor and laboratory exposure.

| | | Outdoor weathering | | | | | | | Laboratory weathering | | | | | | |
|---|---|---|---|---|---|---|---|---|---|---|---|---|---|---|---|
| | | North | South | East | West | Rack | Av. | StDev | Run 1 | Run 2 | Run 3 | Run 4 | RCC | Av. | StDev |
| Initial color values | L* | 78.41 | 78.20 | 75.93 | 74.94 | 75.60 | 76.62 | 1.58 | 72.44 | 66.12 | 67.93 | 68.72 | 75.99 | 72.36 | 5.14 |
| | a* | 7.99 | 8.12 | 9.92 | 10.98 | 10.22 | 9.45 | 1.33 | 13.59 | 13.26 | 14.20 | 13.31 | 9.58 | 11.45 | 2.64 |
| | b* | 26.16 | 26.70 | 28.62 | 31.67 | 29.07 | 28.44 | 2.19 | 34.90 | 34.42 | 32.96 | 34.36 | 27.77 | 31.06 | 4.66 |
| | C* | 27.35 | 27.90 | 30.29 | 33.52 | 30.81 | 29.98 | 2.48 | 37.45 | 36.89 | 35.89 | 36.85 | 29.37 | 33.11 | 5.29 |
| Final color values | L* | 66.31 | 66.14 | 65.69 | 54.18 | 49.64 | 60.39 | 7.91 | 49.96 | 59.52 | 60.35 | 69.02 | 71.58 | 70.30 | 1.81 |
| | a* | 0.91 | 1.33 | 3.14 | -1.95 | -2.53 | 0.18 | 2.37 | 6.31 | 5.69 | 7.15 | 0.83 | 2.03 | 1.43 | 0.85 |
| | b* | 7.17 | 10.48 | 13.18 | 3.75 | 4.60 | 7.84 | 3.97 | 21.13 | 20.16 | 25.61 | 7.31 | 7.91 | 7.61 | 0.42 |
| | C* | 7.22 | 10.56 | 13.55 | 4.22 | 5.25 | 8.16 | 3.86 | 22.05 | 20.95 | 26.59 | 7.36 | 8.17 | 7.76 | 0.57 |
| Color diff. | $\Delta E^*_{tot}$ | 23.60 | 21.32 | 19.73 | 37.12 | 37.88 | 27.93 | 8.85 | 27.35 | 17.45 | 12.70 | 29.79 | 21.70 | 25.74 | 5.72 |
| | $\sum \Delta E^*$ | 53.48 | 55.26 | 52.44 | 100.55 | 93.28 | 71.00 | 23.82 | 51.96 | 31.87 | 18.49 | 52.40 | 38.50 | 45.45 | 9.83 |
| | $\Delta C^*$ | 20.13 | 17.34 | 16.74 | 29.30 | 25.56 | 21.81 | 5.44 | 15.40 | 15.94 | 9.30 | 29.49 | 21.21 | 25.35 | 5.86 |
| | $\Delta L^*$ | 12.09 | 12.06 | 10.24 | 20.76 | 25.96 | 16.22 | -6.33 | 22.48 | 6.60 | 7.58 | -0.30 | 4.42 | 2.06 | 3.33 |
| | $(\sum \Delta E^*) - \Delta E^*$ | 29.88 | 33.94 | 32.72 | 63.44 | 55.40 | 43.07 | 14.97 | 24.61 | 14.42 | 5.79 | 22.61 | 16.80 | 19.71 | 4.11 |

Table A.4.: Initial and final color values for Aspen (Material 4) for outdoor and laboratory exposure.

| | | Outdoor weathering | | | | | | | Laboratory weathering | | | | | | |
|---|---|---|---|---|---|---|---|---|---|---|---|---|---|---|---|
| | | North | South | East | West | Rack | Av. | StDev | Run 1 | Run 2 | Run 3 | Run 4 | RCC | Av. | StDev |
| Initial color values | L* | 77.90 | 74.80 | 83.21 | 81.35 | 75.72 | 78.60 | 3.61 | 85.39 | 81.29 | 75.91 | 81.22 | 83.36 | 82.29 | 1.51 |
| | a* | 5.01 | 3.55 | 3.79 | 5.31 | 5.96 | 4.72 | 1.02 | 5.33 | 5.37 | 5.04 | 6.81 | 3.39 | 5.10 | 2.42 |
| | b* | 26.20 | 21.22 | 20.87 | 22.12 | 27.47 | 23.58 | 3.04 | 25.50 | 23.98 | 24.15 | 27.65 | 24.21 | 25.93 | 2.43 |
| | C* | 26.68 | 21.52 | 21.21 | 22.75 | 28.11 | 24.05 | 3.14 | 26.05 | 24.57 | 24.67 | 28.47 | 24.44 | 26.46 | 2.85 |
| Final color values | L* | 55.30 | 58.67 | 64.14 | 43.95 | 49.75 | 54.36 | 7.82 | 79.33 | 77.09 | 76.58 | 81.42 | 74.47 | 77.95 | 4.91 |
| | a* | -1.11 | -1.70 | -0.18 | -2.55 | -2.24 | -1.56 | 0.94 | 2.95 | 1.70 | 3.08 | 1.07 | 3.69 | 2.38 | 1.85 |
| | b* | 6.01 | 6.10 | 7.54 | 4.29 | 5.51 | 5.89 | 1.17 | 17.20 | 10.47 | 13.73 | 7.87 | 13.46 | 10.66 | 3.95 |
| | C* | 6.11 | 6.33 | 7.54 | 4.99 | 5.95 | 6.19 | 0.91 | 17.46 | 10.61 | 14.07 | 7.94 | 13.96 | 10.95 | 4.25 |
| Color diff. | $\Delta E^*_{tot}$ | 30.91 | 22.73 | 23.61 | 42.17 | 34.99 | 30.88 | 8.12 | 10.55 | 14.61 | 10.63 | 20.59 | 13.94 | 17.27 | 4.70 |
| | $\sum \Delta E^*$ | 93.40 | 40.55 | 68.31 | 71.63 | 78.22 | 70.42 | 19.28 | 55.02 | 37.15 | 18.02 | 90.20 | 24.00 | 57.10 | 46.81 |
| | $\Delta C^*$ | 20.56 | 15.19 | 13.67 | 17.76 | 22.15 | 17.87 | 3.55 | 8.60 | 13.96 | 10.60 | 20.53 | 10.49 | 15.51 | 7.10 |
| | $\Delta L^*$ | 22.60 | 16.13 | 19.07 | 37.40 | 25.98 | 24.24 | -4.22 | 6.07 | 4.20 | -0.68 | -0.20 | 8.88 | 4.34 | -3.41 |
| | $(\sum \Delta E^*) - \Delta E^*$ | 62.48 | 17.82 | 44.70 | 29.45 | 43.23 | 39.54 | 11.16 | 44.46 | 22.53 | 7.39 | 69.60 | 10.06 | 39.83 | 42.11 |

Table A.5.: Initial and final color values for Larch (Material 5) for outdoor and laboratory exposure.

| | | Outdoor weathering | | | | | | | Laboratory weathering | | | | | | |
|---|---|---|---|---|---|---|---|---|---|---|---|---|---|---|---|
| | | North | South | East | West | Rack | Av. | StDev | Run 1 | Run 2 | Run 3 | Run 4 | RCC | Av. | StDev |
| Initial color values | L* | 60.77 | 64.34 | 67.64 | 67.20 | 60.01 | 63.99 | 3.53 | 63.16 | 55.91 | 60.39 | 62.00 | 60.01 | 61.01 | 1.41 |
| | a* | 12.07 | 14.21 | 10.72 | 13.02 | 12.98 | 12.60 | 1.30 | 15.73 | 20.06 | 17.67 | 14.73 | 15.28 | 15.01 | 0.39 |
| | b* | 31.19 | 33.41 | 32.06 | 34.35 | 33.58 | 32.92 | 1.27 | 32.87 | 38.55 | 34.85 | 36.16 | 28.69 | 32.43 | 5.28 |
| | C* | 33.44 | 36.31 | 33.81 | 36.73 | 36.01 | 35.26 | 1.52 | 36.44 | 43.46 | 39.07 | 39.05 | 32.51 | 35.78 | 4.62 |
| Final color values | L* | 55.20 | 63.57 | 54.53 | 54.82 | 43.05 | 54.23 | 7.31 | 52.98 | 44.80 | 48.68 | 72.14 | 73.78 | 72.96 | 1.16 |
| | a* | 1.67 | 2.80 | 4.11 | -1.14 | -2.84 | 0.92 | 2.86 | 6.32 | 7.72 | 11.50 | 1.60 | 0.24 | 0.92 | 0.96 |
| | b* | 9.54 | 13.50 | 15.98 | 5.38 | 4.90 | 9.86 | 4.89 | 20.20 | 22.46 | 32.19 | 6.91 | 5.03 | 5.97 | 1.33 |
| | C* | 9.69 | 13.79 | 16.50 | 5.50 | 5.67 | 10.23 | 4.89 | 21.16 | 23.75 | 34.18 | 7.09 | 5.04 | 6.06 | 1.45 |
| Color diff. | $\Delta E^*_{tot}$ | 24.65 | 22.96 | 21.77 | 34.54 | 36.89 | 28.16 | 7.02 | 18.78 | 23.12 | 13.50 | 33.63 | 31.23 | 32.43 | 1.69 |
| | $\sum \Delta E^*$ | 98.05 | 79.48 | 110.59 | 64.66 | 80.98 | 86.75 | 17.82 | 43.94 | 32.00 | 17.99 | 51.17 | 39.48 | 45.33 | 8.27 |
| | $\Delta C^*$ | 23.75 | 22.52 | 17.30 | 31.23 | 30.34 | 25.03 | 5.79 | 15.28 | 19.71 | 4.89 | 31.95 | 27.47 | 29.71 | 3.17 |
| | $\Delta L^*$ | 5.57 | 0.78 | 13.10 | 12.38 | 16.96 | 9.76 | -3.77 | 10.18 | 11.10 | 11.71 | -10.14 | -13.77 | -11.96 | 0.25 |
| | $(\sum \Delta E^*) - \Delta E^*$ | 73.40 | 56.52 | 88.82 | 30.12 | 44.10 | 58.59 | 10.80 | 25.15 | 8.88 | 4.49 | 17.54 | 8.25 | 12.89 | 6.57 |

Table A.6.: Initial and final color values for Kebony Furu (Material 6) for outdoor and laboratory exposure.

| | | Outdoor weathering | | | | | | | Laboratory weathering | | | | | | |
|---|---|---|---|---|---|---|---|---|---|---|---|---|---|---|---|
| | | North | South | East | West | Rack | Av. | StDev | Run 1 | Run 2 | Run 3 | Run 4 | RCC | Av. | StDev |
| Initial color values | L* | 24.97 | 22.17 | 23.88 | 22.29 | 24.96 | 23.66 | 1.37 | 24.98 | 24.74 | 24.67 | 19.82 | 25.43 | 22.62 | 3.97 |
| | a* | 5.49 | 4.81 | 6.07 | 5.61 | 9.48 | 6.29 | 1.84 | 6.02 | 6.72 | 7.34 | 2.07 | 8.57 | 5.32 | 4.59 |
| | b* | 24.74 | 13.29 | 23.27 | 22.79 | 29.63 | 22.74 | 5.94 | 16.35 | 19.41 | 17.39 | 11.42 | 10.36 | 10.89 | 0.75 |
| | C* | 25.35 | 14.13 | 24.04 | 23.47 | 31.11 | 23.62 | 6.11 | 17.42 | 20.54 | 18.87 | 11.61 | 13.44 | 12.53 | 1.30 |
| Final color values | L* | 39.93 | 39.93 | 40.33 | 36.00 | 37.11 | 38.66 | 1.97 | 18.27 | 22.53 | 41.51 | 23.76 | 52.94 | 38.35 | 20.63 |
| | a* | -1.13 | 2.39 | 2.74 | -1.32 | -3.63 | -0.19 | 2.70 | -1.51 | -0.37 | 1.58 | -5.20 | -0.75 | -2.98 | 3.15 |
| | b* | 7.76 | 14.84 | 16.74 | 7.05 | 4.80 | 10.24 | 5.23 | 9.92 | 9.36 | 16.44 | 3.05 | 6.59 | 4.82 | 2.51 |
| | C* | 7.84 | 15.04 | 16.97 | 7.17 | 6.01 | 10.61 | 5.01 | 10.03 | 9.37 | 16.51 | 6.03 | 6.63 | 6.33 | 0.43 |
| Color diff. | $\Delta E^*_{tot}$ | 23.59 | 17.98 | 18.01 | 22.00 | 30.60 | 22.44 | 5.19 | 11.96 | 12.49 | 17.82 | 11.77 | 29.28 | 20.53 | 12.38 |
| | $\sum \Delta E^*$ | 51.61 | 43.01 | 68.24 | 79.19 | 59.79 | 60.37 | 14.09 | 21.00 | 19.63 | 22.77 | 29.64 | 34.09 | 31.87 | 3.15 |
| | $\Delta C^*$ | 17.51 | -0.91 | 7.08 | 16.30 | 25.10 | 13.02 | 10.08 | 7.39 | 11.17 | 2.36 | 5.58 | 6.81 | 6.20 | 0.87 |
| | $\Delta L^*$ | -14.97 | -17.75 | -16.45 | -13.71 | -12.15 | -15.01 | -0.59 | 6.71 | 2.21 | -16.84 | -3.95 | -27.51 | -15.73 | -16.66 |
| | $(\sum \Delta E^*) - \Delta E^*$ | 28.02 | 25.03 | 50.23 | 57.19 | 29.19 | 37.93 | 8.91 | 9.03 | 7.14 | 4.95 | 17.87 | 4.81 | 11.34 | -9.23 |

Table A.7.: Initial and final color values for Kebony SYP (Material 7) for outdoor and laboratory exposure.

| | | Outdoor weathering | | | | | | | Laboratory weathering | | | | | | |
|---|---|---|---|---|---|---|---|---|---|---|---|---|---|---|---|
| | | North | South | East | West | Rack | Av. | StDev | Run 1 | Run 2 | Run 3 | Run 4 | RCC | Av. | StDev |
| Initial color values | L* | 29.41 | 28.44 | 29.94 | 26.49 | 26.15 | 28.09 | 1.70 | 24.89 | 28.88 | 28.12 | 28.08 | 28.73 | 28.41 | 0.46 |
| | a* | 6.16 | 2.95 | 5.13 | 3.35 | 2.75 | 4.07 | 1.50 | 6.28 | 5.68 | 3.20 | 3.67 | 6.55 | 5.11 | 2.04 |
| | b* | 17.09 | 15.16 | 17.37 | 14.77 | 13.93 | 15.66 | 1.50 | 15.79 | 19.17 | 15.34 | 17.20 | 8.60 | 12.90 | 6.08 |
| | C* | 18.17 | 15.44 | 18.11 | 15.15 | 14.20 | 16.21 | 1.82 | 16.99 | 19.99 | 15.67 | 17.59 | 10.81 | 14.20 | 4.79 |
| Final color values | L* | 44.55 | 37.07 | 26.10 | 26.90 | 30.24 | 32.97 | 7.78 | 15.84 | 28.10 | 28.37 | 30.47 | 60.79 | 45.63 | 21.44 |
| | a* | -0.35 | 1.08 | 1.91 | -4.03 | -4.37 | -1.15 | 2.90 | -3.50 | -0.33 | 0.48 | -4.62 | -0.96 | -2.79 | 2.59 |
| | b* | 7.61 | 12.21 | 12.55 | 4.98 | 5.52 | 8.57 | 3.61 | 6.25 | 11.50 | 16.22 | 5.24 | 5.11 | 5.18 | 0.09 |
| | C* | 7.62 | 12.26 | 12.69 | 6.41 | 7.04 | 9.20 | 3.02 | 7.16 | 11.50 | 16.23 | 6.99 | 5.20 | 6.09 | 1.26 |
| Color diff. | $\Delta E^*_{tot}$ | 19.01 | 9.31 | 6.95 | 12.27 | 11.75 | 11.86 | 4.53 | 16.39 | 9.78 | 2.87 | 14.75 | 33.11 | 23.93 | 12.99 |
| | $\sum \Delta E^*$ | 63.13 | 22.69 | 29.49 | 39.23 | 61.14 | 43.14 | 18.33 | 22.98 | 22.00 | 7.80 | 41.04 | 35.17 | 38.11 | 4.15 |
| | $\Delta C^*$ | 10.55 | 3.19 | 5.42 | 8.74 | 7.16 | 7.01 | 2.86 | 9.83 | 8.49 | -0.56 | 10.60 | 5.61 | 8.11 | 3.53 |
| | $\Delta L^*$ | -15.14 | -8.63 | 3.84 | -0.41 | -4.09 | -4.89 | -6.08 | 9.05 | 0.78 | -0.25 | -2.39 | -32.06 | -17.23 | -20.98 |
| | $(\sum \Delta E^*) - \Delta E^*$ | 44.12 | 13.38 | 22.54 | 26.96 | 49.39 | 31.28 | 13.80 | 6.59 | 12.22 | 4.93 | 26.29 | 2.06 | 14.18 | -8.84 |

Table A.8.: Initial and final color values for Scots Pine, royal impregnation (Material 8) for outdoor and laboratory exposure.

| | | Outdoor weathering | | | | | | | Laboratory weathering | | | | | | |
|---|---|---|---|---|---|---|---|---|---|---|---|---|---|---|---|
| | | North | South | East | West | Rack | Av. | StDev | Run 1 | Run 2 | Run 3 | Run 4 | RCC | Av. | StDev |
| Initial color values | L* | 33.00 | 36.12 | 33.14 | 38.66 | 34.29 | 35.04 | 2.38 | 30.93 | 33.15 | 40.02 | 22.86 | 36.60 | 29.73 | 9.72 |
| | a* | 4.44 | 5.91 | 3.94 | 6.09 | 6.28 | 5.33 | 1.07 | 6.53 | 5.19 | 5.31 | 1.73 | 9.83 | 5.78 | 5.73 |
| | b* | 22.32 | 28.02 | 23.24 | 27.00 | 25.54 | 25.22 | 2.42 | 23.15 | 24.85 | 26.41 | 14.54 | 18.22 | 16.38 | 2.60 |
| | C* | 22.76 | 28.64 | 23.57 | 27.68 | 26.30 | 25.79 | 2.55 | 24.05 | 25.39 | 26.94 | 14.64 | 20.70 | 17.67 | 4.29 |
| Final color values | L* | 53.26 | 59.12 | 51.33 | 59.52 | 42.93 | 53.23 | 6.78 | 27.54 | 32.29 | 43.16 | 48.74 | 63.33 | 56.04 | 10.32 |
| | a* | 4.89 | 5.33 | 5.22 | 1.07 | -0.54 | 3.19 | 2.74 | 2.93 | 4.36 | 4.39 | 2.93 | 0.47 | 1.70 | 1.74 |
| | b* | 25.58 | 24.29 | 27.13 | 13.11 | 12.65 | 20.55 | 7.08 | 15.51 | 17.36 | 23.93 | 12.27 | 7.69 | 9.98 | 3.24 |
| | C* | 26.04 | 24.87 | 27.63 | 13.15 | 12.66 | 20.87 | 7.34 | 15.78 | 17.90 | 24.33 | 12.61 | 7.70 | 10.16 | 3.47 |
| Color diff. | $\Delta E^*_{tot}$ | 20.53 | 23.31 | 18.65 | 25.56 | 16.95 | 21.00 | 3.47 | 9.10 | 7.58 | 4.11 | 26.01 | 30.22 | 28.11 | 2.98 |
| | $\sum \Delta E^*$ | 132.90 | 36.14 | 26.73 | 55.33 | 61.59 | 62.54 | 41.78 | 16.85 | 13.00 | 6.41 | 113.77 | 89.90 | 101.84 | 16.88 |
| | $\Delta C^*$ | -3.29 | 3.77 | -4.06 | 14.52 | 13.64 | 4.92 | 8.91 | 8.27 | 7.49 | 2.61 | 2.03 | 13.00 | 7.51 | 7.76 |
| | $\Delta L^*$ | -20.26 | -23.00 | -18.19 | -20.86 | -8.64 | -18.19 | -4.40 | 3.39 | 0.86 | -3.14 | -25.88 | -26.73 | -26.31 | -0.60 |
| | $(\sum \Delta E^*) - \Delta E^*$ | 112.37 | 12.83 | 8.09 | 29.77 | 44.64 | 41.54 | 38.31 | 7.75 | 5.42 | 2.30 | 87.76 | 59.68 | 73.72 | 13.90 |

Table A.9.: Initial and final color values for Scots Pine, pressure treated (Material 9) for outdoor and laboratory exposure.

| | | Outdoor weathering | | | | | | | Laboratory weathering | | | | | | |
|---|---|---|---|---|---|---|---|---|---|---|---|---|---|---|---|
| | | North | South | East | West | Rack | Av. | StDev | Run 1 | Run 2 | Run 3 | Run 4 | RCC | Av. | StDev |
| Initial color values | L* | 55.36 | 42.10 | 54.13 | 53.29 | 43.77 | 49.73 | 6.27 | 48.02 | 51.06 | 54.70 | 44.26 | 53.58 | 48.92 | 6.59 |
| | a* | 1.19 | -0.90 | 0.60 | -0.71 | 0.29 | 0.09 | 0.88 | 1.62 | 2.58 | 4.09 | 5.17 | 3.59 | 4.38 | 1.12 |
| | b* | 23.71 | 42.33 | 27.43 | 48.33 | 43.35 | 37.03 | 10.79 | 26.15 | 27.02 | 29.81 | 29.66 | 22.11 | 25.89 | 5.34 |
| | C* | 23.74 | 42.34 | 27.44 | 48.34 | 43.35 | 37.04 | 10.78 | 26.20 | 27.14 | 30.09 | 30.11 | 22.40 | 26.25 | 5.45 |
| Final color values | L* | 60.23 | 51.66 | 54.96 | 48.40 | 48.10 | 52.67 | 5.06 | 22.46 | 37.68 | 48.75 | 41.55 | 69.22 | 55.39 | 19.57 |
| | a* | 2.53 | 3.60 | 4.90 | -0.53 | -2.44 | 1.61 | 3.03 | 2.92 | 6.96 | 6.39 | 4.87 | 1.20 | 3.04 | 2.60 |
| | b* | 17.58 | 17.83 | 24.18 | 8.98 | 5.29 | 14.77 | 7.57 | 14.28 | 22.83 | 27.90 | 15.69 | 7.56 | 11.63 | 5.75 |
| | C* | 17.76 | 18.19 | 24.67 | 9.00 | 5.83 | 15.09 | 7.61 | 3.00 | 23.87 | 28.62 | 16.43 | 7.65 | 12.04 | 6.20 |
| Color diff. | $\Delta E^*_{tot}$ | 7.94 | 26.68 | 5.45 | 39.65 | 38.40 | 23.63 | 16.28 | 28.21 | 14.69 | 6.66 | 14.23 | 21.49 | 17.86 | 5.13 |
| | $\sum \Delta E^*$ | 69.71 | 47.34 | 30.29 | 45.46 | 56.67 | 49.89 | 14.57 | 40.10 | 20.00 | 10.38 | 71.74 | 95.75 | 83.75 | 16.98 |
| | $\Delta C^*$ | 5.98 | 24.15 | 2.77 | 39.34 | 37.53 | 21.95 | 17.12 | 23.20 | 3.28 | 1.47 | 13.68 | 14.74 | 14.21 | 0.75 |
| | $\Delta L^*$ | -4.87 | -9.56 | -0.83 | 4.89 | -4.33 | -2.94 | 1.21 | 25.56 | 13.38 | 5.95 | 2.71 | -15.64 | -6.47 | -12.98 |
| | $(\sum \Delta E^*) - \Delta E^*$ | 61.77 | 20.66 | 24.84 | 5.81 | 18.27 | 26.27 | -1.72 | 11.89 | 5.31 | 3.72 | 57.51 | 74.26 | 65.88 | 11.84 |

Table A.10.: Complete overview over test conditions for laboratory weathering for the ATLAS solar simulator (ASS) (Run 1-4) and the rotating climate chamber (RCC).

| Run | Exp. time [days] | Light [hours] per 24 hrs | Irrad. [W/m$^2$] | Irrad. [kWh/m$^2$] per 24 hrs | Total irrad.[a] [kWh/m$^2$] | Water [hours] per 24 hrs | Water [l/(m$^2$h)] | Water [l/m$^2$] per 24 hrs | Total water[a] [l/m$^2$] | Temp.[b] [°C] | RH[b] [%] | $AF_{tot}$ [e] [-] |
|---|---|---|---|---|---|---|---|---|---|---|---|---|
| 1 | 112 | 20 | 1200 | 24 | 2688 | 4 | 102 | 408 | 45 696 | 63 | 50 | 250 |
| 2 | 26 | 5 x 4h | 1200 | 24 | 624 | 1 x 4h | 102 | 408 | 10 608 | 63 | 50 | 250 |
| 3 | 10 | 5 x 4h | 1200 | 24 | 240 | 1 x 4h | 102 | 408 | 4 080 | 22 | 50 | 9 |
| 4 | 42 | 5 x 4h | 600 | 12 | 504 | 1 x 4h | 102 | 408 | 17 136 | 63 | 50 | 130 |
| RCC | 888 | 6 x 1h | 257 [c] | 1.5 [c] | 1369 [c] | 6 x 50 min | 15 | 75 | 66 600 | 63 | - | 5 |
| | | | 15.4 [d] | 0.0924 [d] | 82 [d] | | | | | | | |

[a] accumulated entire exposure time [b] during solar radiation [c] calculated solar radiation [d] measured UV radiation

# B. Solar radiation basics

Definitions are adapted from Iqbal [66].

**Solar constant $G_{sc} = 1367\ W/m^2$** Energy from the sun, per unit time, received on a unit area of surface perpendicular to the direction of propagation of the radiation, at mean earth-sun distance, outside of the atmosphere (air mass 0). This value is adopted by the World Radiation Centre (WRC), with an uncertainty of the order of 1%.

**Black body temperature 5777 K** By definition a black body is perfect absorber and emitter of radiation. A blackbody is an ideal concept since all real substances will reflect some radiation. The spectral distribution of the sun corresponds to a blackbody with a temperature of 5777 K.

**Variation of extraterrestrial radiation** For engineering purposes, in view of the uncertainties and variability of the atmospheric transmission, the energy emitted by the sun can be considered as constant. Variation of the earth-sun distance, however, does lead to variation of extraterrestrial radiation flux in the range 3%.

**Air mass m** The ratio of the mass of atmosphere through which beam radiation passes to the mass it would pass through if the sun was at the zenith is called air mass. As radiation passes through the atmosphere, it is attenuated by scattering and absorption; the more atmosphere through which it passes, the greater the attenuation. By definition, the sea-level air mass at the zenith is 1. Air mass increases as the angle between the source and the zenith increases, reaching a value of approximately 38 at the horizon. The region above the earth's atmosphere, where there is no atmospheric attenuation of solar radiation, is considered to have air mass zero (AM0).

**Total Solar Radiation** The sum of beam, also called direct, and diffuse

solar radiation on a surface. Total solar radiation is sometimes used to indicate quantities integrated over all wavelengths of the solar spectrum. The most common measurements of solar radiation are total radiation on a horizontal surface, often referred to as global radiation on the surface.

**Beam or direct radiation** The solar radiation received from the sun without having been scattered by the atmosphere. Beam radiation is often referred to as direct radiation; to avoid confusion between subscripts for direct and diffuse, the term beam radiation is preferred.

**Diffuse radiation** The solar radiation received from the sun after its direction has been changed by scattering by the atmosphere. In some meteorological literature diffuse radiation is referred to as sky radiation or solar sky radiation.

**Irradiance [$\mathbf{W/m^2}$]** The rate at which radiant energy is incident on a surface, per unit area of surface. The symbol G is used for solar irradiance, with appropriate subscripts for beam, diffuse, or spectral radiation.

**Irradiation or Radiant Exposure [$\mathbf{J/m^2}$]** The incident energy per unit area on a surface, found by integration of irradiance over a specific time, usually an hour or a day.

**Insolation** is a term specifically to solar irradiation. The symbol H is used for insolation for a day. The symbol I is used for insolation for an hour.

The symbols H and I can represent beam, diffuse, surfaces of any orientation. Subscripts on G, H, and I are as follows:

- o refers to radiation above the earth's atmosphere, referred to as extraterrestrial radiation
- b beam radiation
- d diffuse radiation
- T radiation on a tilted plane
- n radiation on a plane normal to the direction of propagation; if neither T nor n appear, radiation is on a horizontal plane.

**Solar time** is the time based on the apparent angular motion of the sun across the sky, with solar noon the time the sun crossed the meridian of the observer. Solar time does not coincide with local clock time.

**Rb** the ratio of beam radiation on the tilted surface to that on a horizontal surface at any time.

**Solar or short-wave radiation** Radiation originating from the sun in the wavelength range of 0.3 to 3 $\mu m$.

**Long-wave radiation radiation** Radiation originating from sources at temperatures near ordinary ambient temperatures and thus substantially all at wavelengths greater than $3\mu m$. Long-wave radiation is emitted by the atmosphere, by a collector, or by any other body at ordinary temperatures.

**Pyrheliometer** An instrument using a collimated detector for measuring solar radiation from the sun and from a small portion of the sky around the sun at normal incidence.

**Pyranometer** An instrument for measuring total hemispherical solar (beam plus diffuse) radiation, usually on a horizontal surface. If shaded from the beam by a ring or disc, a pyranometer measures diffuse radiation. In addition, the terms solarimeter and actinometer are encountered; a solarimeter can generally be interpreted to mean the same as pyranometer, and an actinometer usually refers to a pyrheliometer.

**Albedo** The albedo of an object is the extent to which it diffusely reflects light from the sun. Albedo is defined as the ratio of diffusely reflected to incident electromagnetic radiation. The range of possible values is from 0 (dark) to 1 (bright).